Cape Peninsula University of Technology

EFFECT OF MICROBIAL CONSORTIUM ON THE BIOKINETIC TEST FOR ASSESSING ACID ROCK DRAINAGE POTENTIAL

Dissertation submitted in fulfillment of the requirements for a

Master of Engineering: Chemical Engineering

Mhlangabezi Tolbert Golela

Supervisors:

Prof S.K.O. Ntwampe and Prof S.T.L. Harrison

Department of Chemical Engineering

Faculty of Engineering

Cape Peninsula University of Technology

Cape Town

2018

DECLARATION

I, Mhlangabezi Tolbert Golela, hereby declare I know the meaning of plagiarism and declare that all of the work in the thesis is properly acknowledged and is my own.

22/01/2018

Signed **Date**

ABSTRACT

Acid rock drainage (ARD) is one of the most severe environmental challenges currently faced by the mining industry worldwide. ARD is formed from the oxidation of sulphide-bearing minerals, particularly pyrite, in the presence of water and oxygen. ARD generation is accelerated by the presence of naturally occurring iron and sulphur-oxidizing micro-organisms, which regenerate leaching agents that facilitate sulphide mineral oxidation. ARD pollution is characterized by a high concentration of metals and sulphates in solution, low pH and a high salt content (salinity) in the environment, contaminating soil and groundwater. In South Africa, ARD is a major challenge in the gold and coal mining industries, where millions of tons of sulphide waste rock and overburden are generated and discarded. Characterization of these waste materials is required to develop an appropriate disposal strategy to minimise the risk of pollution and the generation of ARD.

Potential ARD generation prediction from waste rock depends on the precise characterization of ARD potential using Biokinetic tests. Commonly used ARD prediction methods are static and long-term kinetic tests. Static tests provide data for a worst-case scenario focussing on strong acid chemical leaching potential to give an overall acid forming potential of a sample. Such kinetic tests provide data illustrating the rate of the net acid generation capacity of mine waste. However, these tests are capital intensive and time-consuming and fail to provide adequate information on the effect of micro-organisms on the overall net acid generation capacity of mine waste.

The Biokinetic test reported herein and developed at the University of Cape Town, focusses on addressing a worst case scenario provided by static tests in a cost-effective manner and reduced time frames provided for by conventional kinetic tests. This test primarily provides relative rates of ARD generation in the presence of micro-organisms within 90 days. However, the Biokinetic test is at the developmental stage and thus far, has not been consistently used for different waste ores to determine a standardised approach. Therefore, the aim of this study was to investigate the effects of microbial consortia and to develop a standardisation approach for the test for ARD formation potential using gold-bearing and copper-bearing waste rock. Additionally, to refine the Semi-continuous Biokinetic test simulation, a flow-through system where there is minimal seepage in the waste deposit, was also developed. The sulphur content of the gold and copper-bearing samples used in this study was between 2.3 and 3.15%, respectively. These waste rock samples were found to be potentially acid- forming. In the Biokinetic test, finely milled waste rock samples were slurrified, inoculated with consortia and cultured under standard bioleaching conditions. Leaching and acidification rates were monitored. Data collected allowed for both acid

neutralisation and generation including their relative rates. In the Biokinetic test, a mixed microbial culture dominated by *Leptospirilum ferriphilum* and *Acidthiobacillus caldus* was used at a starting inoculum concentration of 10^7, 10^8, 10^9 and 10^{10} with the tests being performed under three different conditions, namely non-controlled pH, controlled pH, and in Semi-continuous systems.

Findings showed that there was minimal effect of inoculum size on the Biokinetic test for gold-bearing waste rock under non-controlled pH. These results agreed with speciation data performed at the end of experiments, suggesting minimal impact by the quantity of ARD forming micro-organisms added in the inoculum, which culminated in insignificant differentiation between inoculated and non-inoculated samples. This suggested ineffectiveness of inoculated micro-organisms, with their effect being counteracted by the dissolution of minerals with a significant buffering capacity, resulting in a pH exceeding the optimum pH range of the ARD-forming micro-organisms and the precipitation of ferric iron at pH above 3.5. This limited the re-generation of lixiviate (ferric iron) which leaches from the waste rock, causing long microbial lag phases, and thus slowing the mineral leaching process by the microbial community. In contrast, results in the non-controlled pH Biokinetic test for copper-bearing waste rock, with reduced acid neutralisation potential, indicated a significant effect of the inoculum size on leaching, thus on acidification rates. Furthermore, similar experimental work was conducted in pH controlled Biokinetic tests for gold-bearing waste rock to suppress acid generation potential.

Based on Batch Biokinetic Test results, a Semi-continuous system for the removal of readily dissolved neutralising components from the sample was developed, to mitigate against pH increase effects on the inoculum. For these experiments, the Semi-continuous method was determined to be suitable particularly for the mineral composed of high neutralizing capacity for the removal of neutralising minerals; the outcomes indicated that such a method should be used to complement and confirm results from the Batch Biokinetic tests to gain an insight on the relative rates of acid generation and acid neutralisation under microbial mediated ARD conditions.

This research study contributes to the understanding of the behaviour of microbial consortia on the rate of ARD generation. Furthermore, an understanding of influences by the mineral characteristics of the waste rock was found to be the key to gaining insight into the relative rates of acid consuming and acid generating minerals for ARD potential Biokinetic tests. Several recommendations are made, one being to assess the effect of toxic metals which may inhibit the microbial phase in the Biokinetic test system developed.

Keywords: *Acidthiobacillus caldus*; *Leptospirillum ferriphilum*, acid rock drainage, ARD; Biokinetic tests; Mineral leaching; Pyrite; Waste rock.

ACKNOWLEDGEMENTS

I would like to thank:

- God for giving me the courage and will, to undertake and accomplish commendable millstones with regard to my studies thus far,
- My supervisor Prof. Susan T. L. Harrison for giving me an opportunity to undertake experimental work at CeBER (UCT), and her assistance with my personal growth is much appreciated.
- My supervisors Prof. Susan T. L. Harrison and Prof. S.K.O. Ntwampe for their guidance and invaluable input throughout the development of this thesis.
- Mr. Alex Opitz for his continuous input, in writing and reviewing of manuscripts for this project.
- Mr. Emmanuel Ngoma, for assisting me with laboratory work, moral support, motivation and guidance throughout this study.
- A special thank you to Dr. Mariette Smart, who assisted with speciation data for the samples used in this study.
- A special thank you to the UCT Bio-minerals (BM) and acid rock drainage (ARD) discussion groups - your constructive feedback always gave me an opportunity to do more and refine the work reported in this thesis.
- I also express my sincere gratitude to all CeBER members for making me feel at home, Dr. Rob Huddy, Dr. Elaine Govender-Opitz, Dr. Mariette Smart, Catherine Edward and many others.
- I would like to thank my friends Carol Ngwenya, Anna Moyo and Michael Odidi Didi Xhanti Makaula, Qunekani Ngulube, and Lukhanyo Mekuto, for encouragement and positive outlook on life.
- Last but not least, my siblings, Jason Mlungiseleli Golela and Nokulunga Golela, for their continuous support and encouragement and for having faith in my ability to undertake life's difficult challenges.
- The National Research Foundation of South Africa, for financially supporting the thesis through their NRF-DAAD scholarship.

LIST OF PUBLICATIONS AND PRESENTATIONS

1. Golela, M.T., Opitz, A. K. B., Ntwampe, S.K.O., Broadhurst, J.L., & Harrison, S.T.L. (2018). Tailoring the UCT biokinetic test for acid rock drainage potential to characterize stages of acid rock drainage development. (Sustainable minerals '18) conference. Minerals Engineering International. Windhoek Namibia. June 14-15, 2018.

2. Golela, M.T., Opitz, A.K.B, Ntwampe, S.K.O & Harrison S.T.L. (2017) Refinement of the current biokinetic test for characterisation of acid rock drainage potential. Gold case study Processing Conference. Presented in Southern African Institute of Mining & Metallurgy (SAIMM) Western Cape Branch, 4 –5 August 2017, Cape Town.

3. Opitz, A.K.B., Golela, M.T., & Harrison, S.T.L., (2016). The effect of inoculum concentration on the biokinetic test for characterizing acid rock drainage. (Biohydromet '16), Minerals Engineering International, Falmouth, United Kingdom, pp 694. In preparation

4. Itoba-Tombo, E. F., Obed Ntwampe, S. K., Bell, J. J. A., Nzukizi Mudumbi, J. B., & Mhlangabezi Golela, T. (2017). A decade's (2014–2024) perspective on cassava's (Manihot esculenta Crantz) contribution to the global hydrogen cyanide load in the environment. *International Journal of Environmental Studies*, *74*(1), 28-41.

5. Mekuto, L., Ntwampe, S. K. O., Kena, M., Golela, M. T., & Amodu, O. S. (2016). Free cyanide and thiocyanate biodegradation by Pseudomonas aeruginosa STK 03 capable of heterotrophic nitrification Research problem under alkaline conditions. *3 Biotech*, *6*(1), 6.

TABLE OF CONTENTS

LIST OF FIGURES

LIST OF TABLES

ABBREVIATIONS AND NOMENCLATURE

Abbreviation	Description
ABA	Acid base accounting
ABS	Autotrophic basalt salt
ANC	Acid neutralizing capacity
AF	Acid forming
AMD	Acid mine drainage
ARD	Acid rock drainage
CeBER	Centre for Bioprocess Engineering Research
Fe^{2+}	Ferrous iron
Fe^{3+}	Ferric iron
Fe^{Tot}	Total iron
G	Gram
g/t	Gram per ton
Kg/ton	Kilogram per ton
kg H_2SO_4/t	Kilogram of sulfuric acid per ton
HCl	Hydrochloric acid
M	Molarity
mg	Milligram
mL	Millilitre
Mm	Millimolar
MPA	maximum potential acidity
NaCl	sodium hydroxide
NAF	non-acid forming
NAG	Net acid generation
NAPP	Net acid neutralizing potential
PAF	Potentially acid forming
pH	Measure of acid concentration
QEMSCAN	Quantitative evaluation of minerals by scanning electron
SO_4^{2-}	Sulphate
UCT	University of Cape Town
µm	Micron
XRD	X-Ray Diffraction
Wt	Weight

CHAPTER 1

INTRODUCTION

1 INTRODUCTION

1.1 Background

Acid rock drainage (ARD) and acid mine drainage (AMD) are two terminologies used interchangeably to define the acidic leachate generated from the oxidation of sulphide containing minerals such as pyrite (FeS_2) and pyrrhotite ($F_{(1-X)}S$). ARD pollution is a natural process occurring in the presence of water and oxygen. The availability of naturally occurring iron and sulphur-oxidizing microorganisms in the environment promotes the generation of ARD in waste rock deposits and tailing dams. The most common anthropogenic activities with a potential of ARD generation include waste rock piles from mining, tailing dams, heap leaching piles and open pits (Akcil & Koldas, 2006). Other activities such as the building of tunnels and motorways can lead to the immobilisation of sulphide-bearing minerals in the earth's crust, which may subsequently cause ARD development and thus generation in the environment (Akcil & Koldas, 2006). The presence of ARD in the areas surrounding mines is characterised through the development of low pH (pH 2 to 3) turbid water, as a result of the generated drainage which further leads to the leaching of deleterious metals into the environment and the local ecosystem, leading to the mobilisation of heavy metals such as Arsenic (As), Lead (Pb), Copper (Cu), Cobalt, Nickel, Zinc (Zn) and Cadmium (Cd) from the soil and/or waste rock (Hudson-Edwards et al., 2011; Oelofse, 2007).

It has been estimated that mining activities generate nearly 98% of waste from mined ore. According to a survey conducted by Mend (1995), seven billion tons of tailings and six billion tons of waste rocks have the potential of forming ARD in Canada. This ARD formation potential can affect pH of the surrounding soil, increasing its salinity, which will culminate in high concentrations of heavy metals and sulphates. The resulting heavy metals such as Iron (Fe), Copper (Cu), Manganese (Mn) and Silver (Ag), will leach into liquefied matrices, subsequently polluting the environment via mobility mechanisms (Dold, 2010; Lottermoser, 2010). This phenomenon has been observed in South Africa where spillages and accumulation of high volume of ARD forming wastes containing elevated concentrations of toxic heavy metals resulted in the contamination of potable water reserves and the destruction of ecosystems (Yibas et al., 2011; Oelofse, 2007; Neghovela et al., 2006, Mphephu, 2003). To predict and/or mitigate against ARD occurrence, accurate characterisation methods are necessary such that mitigation measures can be developed.

The gold mining industry in South Africa started in 1886 on the Witwatersrand in Gauteng province. South Africa is recognised as a major producer of Gold (Au), contributing nearly 4.4% of the world Au production (Chamber of mines of South Africa, 2016). Due to the high

demand for Au, the grade of the ore processed has decreased with time, with the depth of excavation of mineral increasing from 2.5 to 3.9 km below the earth's crust, for example a mine at Maponeng which recognised as the deepest mine in South Africa. These actions have left a legacy of overburden and gold waste containing sulphide rocks (102-192 Mt/year), which are exposed to conditions suitable for ARD formation (Makgae, 2011).

The prediction of potential ARD generation is commonly achieved using geochemical ARD tests and can be broadly classified into static and long-term kinetic tests. The static tests include acid-base accounting (ABA) and net acid generation (NAG) tests. These tests are used for screening purposes to determine whether waste rock samples have a potential for forming acid or are non-acid forming. The disadvantage of these characterisation tests is that they only measure the balance of acid producing and acid neutralising minerals without accounting for relative rates of ARD generation and provide minimal information regarding the effect of micro-organisms. On the other hand, kinetic tests such as the humidity cell and column leach tests are routinely employed to provide kinetic data. However, these tests are capital intensive and time-consuming, and do not adequately take into consideration the role of micro-organisms, which also promote ARD formation in mine wastes (Hesketh et al., 2010; Stewart et al., 2009). Addressing these constraints in relation to the assessment of ARD formation potential, is important (Hesketh et al., 2010; Herrell et al., 2009; Price 2009). Hence, Biokinetic tests must be developed to provide information of relative rates of ARD generation in the presence of micro-organisms within 90 days.

The challenge related to ARD pollution necessitates the ongoing development of accurate and informative ARD formation characterisation tools. The aim of this study was to explore the impact of Batch and Semi-continuous Biokinetic tests and their standardisation for ARD formation potential assessments, to accurately evaluate ARD formation using gold-bearing and copper-bearing waste rocks.

1.2 Problem statement

An empirical assessment of ARD potential of mined waste rock through characterisation methods is an essential component of sustainable mining practices. The Biokinetic test is in the developmental stage and requires further refinement in terms of standard operating conditions and procedure, to address challenges associated with the use of different waste sources, and to account for the effect of the microbial consortium. Previous studies have investigated parameters such as solids loading and particle size to assess and improve the consistency of this methodology. Therefore, the effect of inoculum size and the nature of the

microbial consortium, coupled with the effect in of varying physicochemical parameters, such as pH and the build-up of dissolved neutralisation potential, must be addressed to elucidate their influence on the ARD Biokinetic test.

1.3 Hypothesis

This research project focussed on the standardisation of the Biokinetic test for ARD characterisation, using gold-bearing and copper-bearing waste rocks as test samples. This research was centred on the following hypotheses:

I. An increase in the initial cell concentration of consortia in the Biokinetic test can enhance or accelerate the onset of the rate of acid generation in the test, until the established microbial community can regenerate the ferric iron and acid more rapidly than it is consumed during mineral leaching. Above this concentration, no further impact of inoculum concentration can be observed.

II. By controlling the pH of the Biokinetic test at pH 2 or below, ferric iron precipitation is minimised, favouring mineral leaching. Furthermore, a favourable environment is maintained for the iron and sulphur oxidising micro-organisms such that the acid generating reactions can proceed in an accelerated manner, allowing for a representative but accelerated test.

III. By using a Semi-continuous Biokinetic test/ draw and fill operational strategy for the Biokinetic test, acid neutralising capacity solubilised does not accumulate in the test, allowing regions of neutralisation and acid generation to be clearly observed, and thus allowing the conditions to be more representative of field conditions.

This study attempted to answer the following questions in order to address the aforementioned hypotheses:

- Will the waste rock samples be potentially acid-forming, non-acid forming, or will the test result in an uncertain classification?
- Will there be any effect of inoculum size on the Biokinetic tests? If so, what will be the effect of different pH conditions under both controlled and non-controlled conditions? Furthermore, will the effect of inoculum size affect the quality of data or ease of data interpretation?

- Does the proliferation distribution of the microbial community inoculated change as the test progresses?

- How do the results of the Biokinetic test and geochemical test contribute to a better characterisation of the potential for future ARD generation in the waste rocks used in this study?

1.4 Research aims and objectives

This research project is organised into three phases to characterise ARD generation potential of two different mine wastes. Phase one consists of the standard ARD characterisation methods. The second phase focuses on the effect of inoculum under non-controlled and controlled pH conditions for standardisation of the Biokinetic test. The third phase aims at refining the Semi-continuous Biokinetic test for better prediction of the behaviour of acid consuming and acid neutralising minerals. The objectives of each phase are outlined below:

Phase 1: Aim: To characterise the ARD potential of gold-bearing and copper-bearing waste rock using geochemical standard methods.

Objective 1: To determine the mineralogical composition of the two waste rocks in order to gain an insight on prevalence of heavy metals present within the samples.

Objective 2: To conduct an acid-base accounting and net acid generation test to classify the ARD potential of the waste rock samples.

Objective 3: To determine the ARD potential of the two waste rocks using the UCT standard Biokinetic test reported herein.

Phase 2. Aim: To determine the effect of inoculum size of a consortium consisting of Fe^{2+} and S oxidising micro-organisms on the Biokinetic test profiles for gold-bearing and copper-bearing waste rocks under different pH regimes, i.e. both non-controlled and controlled.

Objective 1: To perform a test run in pH-controlled experiments similar to non-controlled pH Biokinetic tests and to investigate the effect of inoculum size.

Objective 2: To use molecular techniques to determine the microbial community changes at the mid- and end-point of the experiments.

Phase 3. Aim: Based on the results generated from aim 2, to refine the current Semi-continuous Biokinetic method to test ARD potential of solid waste simulating a Semi-continuous flow disposal scenario.

Objective 1: To determine an instance at which acid consuming and acid generation reactions occur and to determine their impact on the microbial activity. To assess the Biokinetic tests under conditions in which dissolved acid neutralisation capacity is diluted from the test.

1.5 Significance of the study

The results obtained from the sets of tests will contribute to the standardisation of Biokinetic tests and to a thorough understanding of the potential for ARD formation from these sulphide mineral wastes. This will assist with the on-going management of waste rock by mining companies and help to develop mitigation measures for ARD formation potential.

1.6 Scope and limitations of the study

The aim of this study was to determine the effect of inoculum size, under controlled and non-controlled pH conditions, and the influence of pH on controlled Biokinetic tests using gold-bearing and copper-bearing waste rocks. The overarching objective of this investigation was to use ARD geochemical characterisation tests and Biokinetic tests as a tool to aid in the interpretation of the potential for ARD generation from these waste rock samples, obtained from an active gold mining company. The potential for ARD generation from the gold waste rocks was characterised using standard test methods, which involves static ARD characterisation tests, acid-base accounting (ABA) and net acid generation (NAG) as well as in Batch and Semi-continuous Biokinetic tests.

The following were not considered for this study, although they form part of other studies within the research group (CeBER):

- Mathematical modelling of growth kinetics,
- Pilot scale or field prediction tests, were not carried out in this study, and

- Effect of heavy metal deportment on the biokinetic test under the different test conditions.

1.7 Thesis outline

The thesis is divided into six main parts. The introduction in chapter 1 describes the project background, problem statement, hypothesis, research aims and objectives and project scope and limitations as well as a thesis outline. This is followed by the literature review (chapter 2) which describes ARD formation, factors contributing its emergence, and characterisation techniques (and their shortcomings) used to quantify its formation potential. Chapter 3 reports on sample preparation; ARD characterisation tests including ABA tests, NAG test, and Batch Biokinetic tests under non-controlled and controlled pH conditions; as well as a Semi-continuous Biokinetic test. Chapter 4, which contains results and discussion, is divided into three subsections. The first part is based on results from the standard ARD characterisation test and standard Biokinetic test. The second section provides results on the effect of microbial consortia on Biokinetic tests for assessing ARD generation, and the last section focused on the refinement of the semi-batch biokinetic test. Chapter 6 contains conclusions and recommendations for future studies. The detailed procedure for the methods used and raw data of all experimental work conducted are tabulated in the appendices. The schematic outline of this thesis is presented in Figure 1-1.

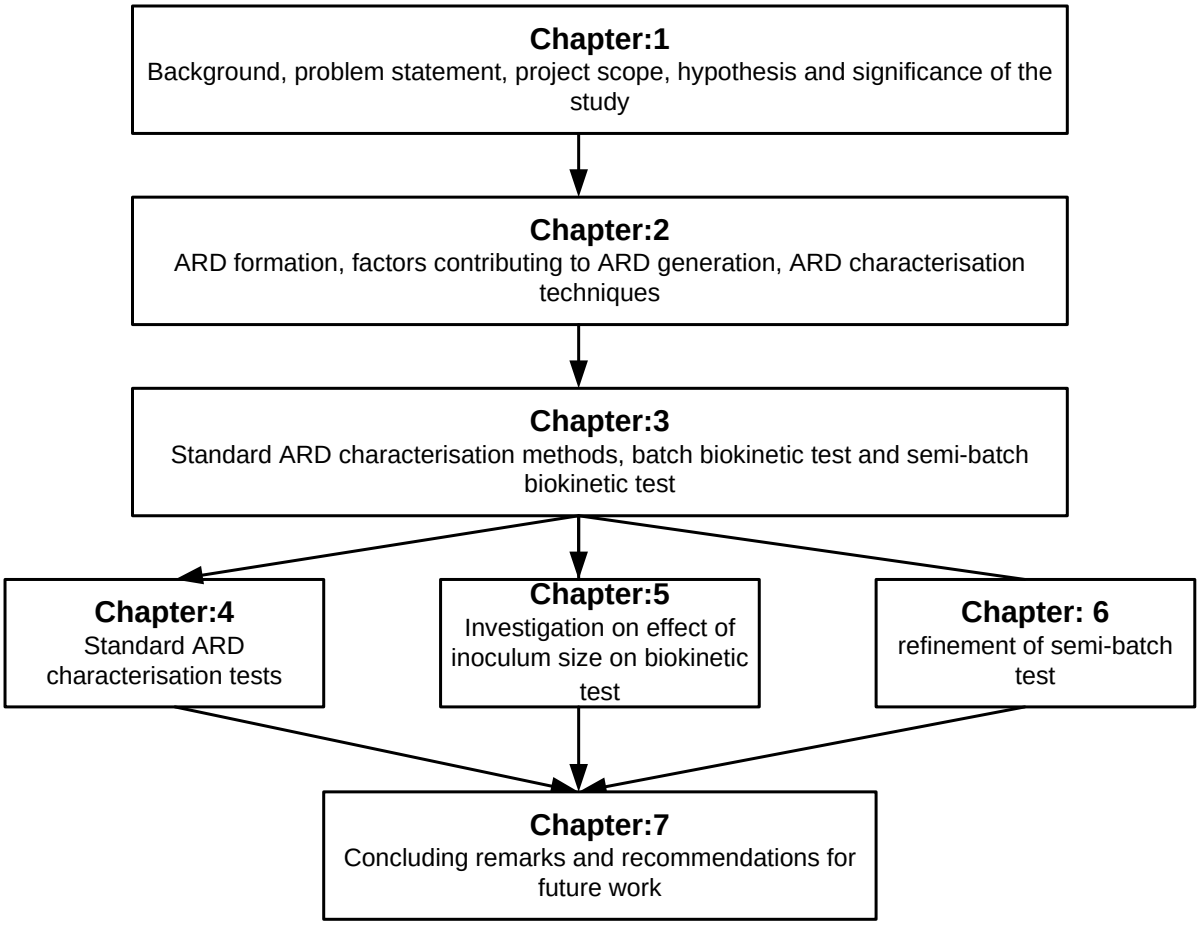

Figure 1-1: Schematic diagram of thesis outline

CHAPTER 2

LITERATURE REVIEW

2 LITERATURE REVIEW

This chapter provides an overview of processes involved in ARD generation, factors which affect its formation, and the environmental challenges associated with ARD formation. Furthermore, the current ARD characterisation and prediction techniques are reviewed.

2.1 ARD formation

Large quantities of waste rock are generated in the extraction of base and precious metals as well as coal; the ratio of waste to a mineral value depends on the product mined and the processes used. When sulphide-bearing minerals such as pyrite, pyrrhotite, marcasite, chalcopyrite, galena, and sphalerite present in a waste rock are exposed to water and air, oxidation reactions occur to produce acidic, sulphate-rich rock drainage. The release of ARD into the environment can occur over centuries, and results in the reduction of the pH of the surrounding soil to as low as 2 to 3. This leads to the leaching of heavy metals such as iron, copper and silver which subsequently pollute the environment (Price 2009; Mphephu, 2003). The most widely distributed sulphide-bearing mineral in gold and copper deposits is pyrite. For this reason, the oxidation mechanisms of pyrite have been studied extensively as it plays a major role in ARD generation in the environment (Gunsinger & Ptacek 2006; Garcia et al., 1996; Evangelou & Zhang, 1995; Davis & Ritchie, 1986). The oxidation of pyrite (FeS_2) occurs in a series of reactions either in the absence or in presence of Fe- and S-oxidising microorganisms (Alpers & Nordstrom, 1999).

The oxidation reaction of pyrite in the presence of water and oxygen occurs at cecum-neutral pH and yields ferrous iron (Fe^{2+}), sulphates ($SO4^{2-}$) and protons (H^+) Equation (2-1). The dissolution of Fe^{2+}, SO_4^{2-} and H^+ decreases the pH of the water (Akcil & Koldas, 2006). In the study conducted by McGuire et al. (2001), ferrous oxidation was observed to occur at a slower rate at a pH above 4.5. However, when the dissolved oxygen is available and water is present in the aqueous form, Fe^{2+} is further oxidised to produce ferric iron according to Equation (2-2). The availability of ferric iron facilitate the rate of pyrite oxidation at pH below 3.5 by a factor of 10 to 100 time faster when compared to oxygen availability (Ritchie, 1994).

$$4FeS_2 + \tfrac{7}{2}O_2 + H_2O \rightarrow Fe^{2+} + 2SO_4^{2-} + 2H^+ \quad (2\text{-}1)$$

$$Fe^{2+} + \tfrac{1}{4}O_2 + H^+ \rightarrow Fe^{3+} + \tfrac{1}{2}H_2O \quad (2\text{-}2)$$

The precipitate of ferric iron in an ARD contaminated site is indicated by an orange-brown colour (Evangelou & Zhang, 1995). The ferric iron generated (see Equation (2-2)) serves as a leaching reagent of pyrite. At pH levels between 2.3 - 3.5, ferric iron is insoluble and forms precipitates such as ferric hydroxide [$Fe(OH)_3$] and secondary minerals including jarosite (jt) and goethite (gt), depending on environmental conditions such a pH, concentration of solute, and temperature (Nordstrom & Southam 1997; Jambor et al., 2000). The formation of $Fe(OH)_3$ also produces acid which lowers the pH, as shown in Equation (2-3). When pH is below 3.5, ferric iron remains in the solution and serves as a leaching agent of pyrite, as in Equation (2-4).

$$Fe^{3+} + 3H_2O \rightarrow Fe(OH)_3 + 3H^+ \quad (2\text{-}3)$$

$$FeS_2 + 14Fe^{3+} + 8\,H_2O \rightarrow 15Fe^{2+} + 2{SO_4}^{2-} + 16H^+ \quad (2\text{-}4)$$

ARD formation is also enhanced by the availability of micro-organisms at low pH conditions and high dissolved metal concentrations (Evangelou & Zhang, 1995). The microbial population under low pH conditions needs a good source of energy in the form of Fe^{2+} and sulphur to proliferate. Microorganisms found in the waste rock and tailing deposits are a combination of autotrophs (which use inorganic carbon sources) and heterotrophs (which use organic carbon sources) (Hallberg, 2010). Some important features of these microorganisms are low pH requirements (1 to 3) and their ability to fix atmospheric carbon dioxide (Rawlings & Johnson 2007). The microbial community is constituted by acidophilic micro-organisms which leach minerals, with the consortia being phylogenetically diverse, and with several prokaryotes making a minute portion of the ARD contaminated sites. Silverman and Ehrlich (1964) discovered that sulphides can be oxidised by bacteria either via a thiosulphate or polysulphide mechanism (see Figure 2-1**Error! Reference source not found.**). This has created a complex biochemical description of the interactions of bacteria with sulphide minerals.

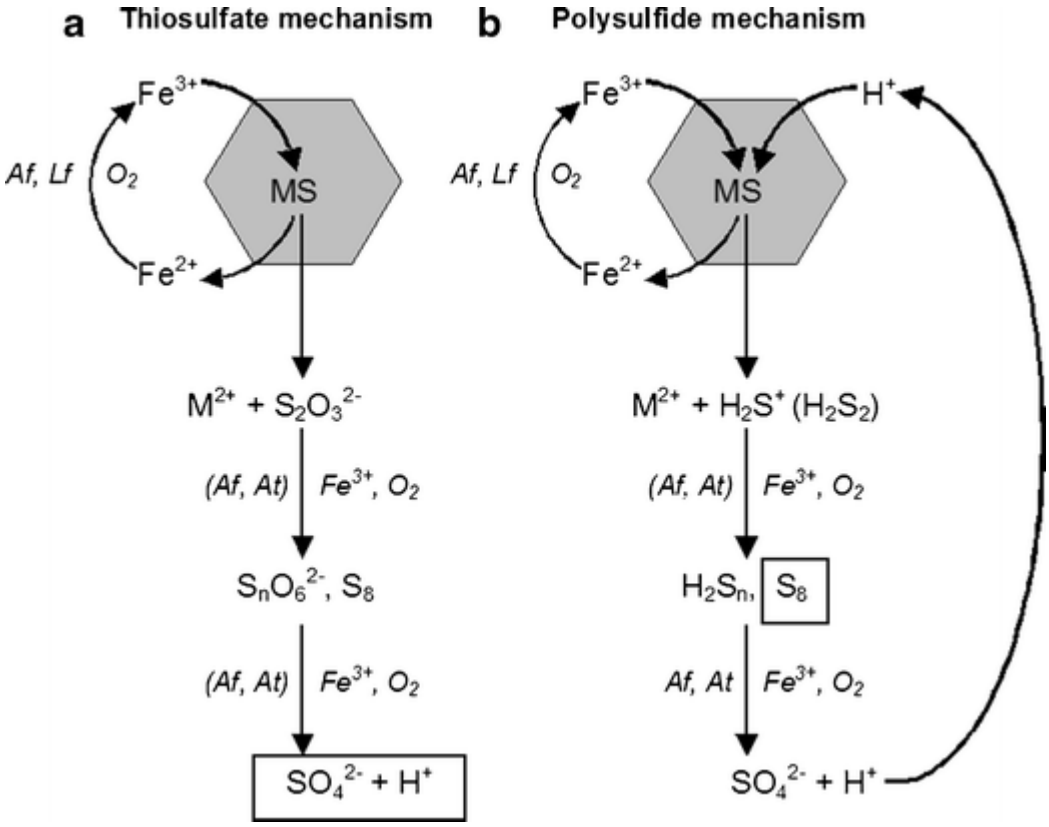

Figure 2-1: Mechanisms of sulphide mineral leaching in the presence of iron and sulphur oxidising micro-organisms (Schipper & Sand, 1999).

There are two proposed mechanisms for microbial-facilitated oxidation of minerals. These are commonly referred to as direct and indirect mechanisms. In the direct oxidation mechanism, Fe-oxidising microbes attach to the surface of sulphide minerals such as pyrite, with the oxidation of the ferrous ion on waste rock surface being facilitated via enzymatic biocatalysts. The indirect mechanisms refer to the oxidisation of ferrous ions in the solution through regeneration of the ferric ion, which serve as a leaching agent with microorganisms, in particular S-oxidisers, converting sulphates to intermediate by-products which are subsequently turned to acid.

For the indirect non-contact mechanism, microorganisms oxidise ferrous to ferric ions in the bulk solution and sulphides or intermediates to sulphate and acid. The sulphide in the waste rock is either oxidised by ferric ions or dissolved in the acidic solution (Tributsch, 2001). Adhesion of microorganisms to the mineral surface is not always required, i.e. oxidation may occur by free floating planktonic microorganisms (Sand & Gehrke, 2006; Tributsch, 2001)

Most recent studies on mineral leaching processes by a microbial community identify the dominance of two pathways depending on the acid solubility of the sulphide, i.e. a thiosulphate pathway for the acid insoluble (such as FeS_2, MoS_2 and WS_2) and a polysulphide pathway for acid soluble (such as ZnS, PbS, FeAsS, $CuFeS_2$).

2.1.1 Thiosulphate pathway

The reactions in Equations (2-5) and (2-6) indicates stoichiometric dissolution of acid-insoluble sulphide (pyrite) resulting in thiosulphate formation and intermediate products.

$$FeS_2 + 6Fe^{3+} + 3H_2O \rightarrow {S_2O_3}^{2-} + 6Fe^{2+} + 6H^+ \quad (2\text{-}5)$$

$${S_2O_3}^{2-} + 8Fe^{3-} + 5H_2O \rightarrow 2{SO_4}^{2-} + 8Fe^{2+} + 10H^+ \quad (2\text{-}6)$$

The net reaction is as demonstrated in Equation (2-7):

$$FeS_2 + 14Fe + 8H_2O \rightarrow 2{SO_4}^{2-} + 15Fe^{2+} + 16H^+ \quad (2\text{-}7)$$

The role of iron oxidising microorganisms such as *Leptospirilum ferriphilum, Scidithiobacillus ferrooxidans, Acidthiobacillus thiooxidans* and *Acidiplasma cupricumulans* is to facilitate Fe^{2+} oxidation to Fe^{3+} (Equation (2-8), in order to regenerate ferric iron which serves as an oxidising agent required for further oxidation of pyritic species. Sulphur oxidising species stimulate the oxidation of sulphur to either thiosulphate or sulphuric acid, depending on the dominant pathway.

$$14Fe^{2+} + 3.5O_2 + 14H^+ \rightarrow 14Fe^{3+} + 7H_2O \quad (2\text{-}8)$$

2.1.2 Polysulphide pathway

The sulphide bearing minerals, such as sphalerite (ZnS), chalcopyrite ($CuFeS_2$), galena (PbS) and arsenopyrite (FeAsS), dissociate via the polysulphide pathway. The dissolution of sphalerite is an example which illustrates the polysulphide pathway. The polysulphide pathway differs from others in that there is an additional proton-facilitated decomposition of the metal sulphide, in addition to that observed for Fe^{3+}, producing free sulphur compounds. These are further oxidised to polysulphides, resulting in elemental sulphur (see Equations (2-9) and (2-10)).

$$8ZnS + 14Fe^{3+} + 2H^{+} \rightarrow 8Zn^{2+} + 14Fe^{2+} + H_2S_8 \quad (2\text{-}9)$$

$$H_2S_8 + 2Fe^{3+} \rightarrow S_8 + 2Fe^{2+} + 2H^{2+} \quad (2\text{-}10)$$

Equation (2-11) describes the dissolution of elemental sulphur to produce sulphates.

$$S_8 + 12O_2 + 12H_2O \rightarrow 8SO_4{}^{2-} + 16H^{+} \quad (2\text{-}11)$$

The end-product of the oxidation of acid soluble minerals in the presence of a microbial community and oxygen is the formation of sulphates; an indication of the initiation of ARD generation in an environment contaminated by waste rock.

$$ZnS + 2O_2 \rightarrow Zn^{2+} + SO_4{}^{2-} \quad (2\text{-}12)$$

The diversity of the microbial community in the ARD and tailing deposits is dependent on several parameters, such as pH, temperature and the ratio of Fe^{2+}: Fe^{3+} concentrations. For the growth and functioning of micro-organisms, an optimum pH range must be achieved. The microorganisms which function at pH below 4.5 are termed acidophilus. The optimum pH range for acidophilic microorganisms is between 0.5-2.5. Singer & Stumm (1970) observed that microorganisms at low pH catalyse the rate of oxidation of sulphide minerals by a factor of 10^6. Therefore, an acidic environment is essential in the leaching, and thus dissolution, of ferric iron. This becomes insoluble and forms a precipitate at pH above 3.5 (Rawlings & Johnson, 2007).

The temperature of waste rock deposits also plays an essential role in selectively promoting the growth of dominant species. The microorganisms are classified into three categories, based on the temperature range for their optimal growth (Rawlings & Johnson, 2007). The three groups of microorganisms isolated in the ARD contaminated site are mesophilic bacteria that live and replicate between 10°C to 45°C, with moderate thermophiles grown at the temperature range of 5°C to 60°C, while thermophilic archaea grow and multiply between 60°C and 90°C. Table 2.1 lists the pH range, including temperature ranges, of different metal sulphide acidophilic microorganisms. To mitigate against acidification, carbonates can be used, as discussed in the subsequent sections.

Table 2-1: pH range and temperature range of metal sulphide acidophilic microorganisms ;(Dew et al., 2011, Schippers et al., 2007)

Microorganisms	pH range	Temperature range (°C)
Acidthiobacillus ferroxodans	1.3-4.5	10-37
Acidthiobacillus thiooxidans	0.5-5.5	10-37
Acidmicrobium ferooxidans	1.0-3.5	20-35
Acidimicrobium species	1.0-3.5	40-55
Acidthiobacillus caldus	1.0-3.5	32-52
Leptospirilum ferriphilum	1.4-4.0	30-45
Acidoplasma cupricumulans	0.4-1.8	22-63
Salfobacillus thermosulfooxidans	1.7-2.4	45-58
Leptospirilum nitrospira	1.5-4.0	30-45

2.2 Acid neutralisation by carbonates

During mineral processing, valuable minerals are normally found embedded in large portions of sulphide-containing minerals and gangue material. When sulphide bearing minerals are oxidised under chemical and biological conditions, acid is produced and minerals with neutralising potential are formed. Acid neutralisation is described as the reaction that increases the drainage pH to neutrality as a result of dissolved acid-consuming minerals. The presence of neutralising minerals in significant concentrations may reduce the acid generation potential of an ARD forming environment.

Calcite ($CaCO_3$) is reported to be the fastest reacting carbonate mineral which begins the neutralisation of acidic solution, and generation of ARD at pH values between 6.5-7.5 (Lapakko, 2002; Lottermoser, 2010, White et al., 1999). Equation 2-13 indicates the role of pH in the presence of protons (H^+) to dissolve calcite, forming calcium and bicarbonate at pH 7. However, at pH values below 6.3, neutralisation by calcite becomes exhausted and thus the calcite in the solution may provide buffering for reactions whereby a single mole of calcium yields 2 moles of carbonic acid (Equation 2-14). It is therefore assumed that one mole of pyrite is neutralised by 1 mole of calcite (Dold, 2017). A study conducted by Gunsinger & Ptacek (2006) observed a significant increase in the solution pH correlating with the depletion of carbonate minerals, which suggests a contribution of calcite to the neutralisation of ARD generation. The reactivity of some of the carbonate minerals is one

magnitude slower relative to that observed for calcite, dolomite [Mg, Ca (CO_3)] and siderite ($FeCO_3$), respectively.

$$CaCO_3 + H^+ \rightarrow Ca^{2+} + HCO_3^- \quad (2\text{-}13)$$

$$CaCO_3 + 2H^+ \rightarrow Ca^{2+} + H_2CO_3^- \quad (2\text{-}14)$$

The dissolution of dolomite is giving by Equation (2-15):

$$CaMg(CO_3)2 + 4H^+ \rightarrow Ca^{2+} + Mg^{2+} + 2HCO_3^- \quad (2\text{-}15)$$

With the dissolution of siderite being described by Equation (2-16):

$$FeCO_3 + H^+ \rightarrow Fe^{2+} + HCO_3^-$$

$$4Fe(CO_3) + O_2 + 10H_2O \rightarrow 4Fe(HO)_3 + 4HCO_3^- + 4H^+ \quad (2\text{-}16)$$

Siderite can provide neutralisation under defined pH conditions and buffer the acid to pH between 5.0 to 5.5. Under the oxidising conditions related to sulphide mine waste, siderite may serve as an acid producer. This is caused by ferrous oxidation, which in turn produces ferric hydroxide depending on the pH according to the reaction (2-16).

A study conducted by Brantly (2008) reported that minerals present in mine waste react at different rates. These neutralising minerals are classified on the basis of their reactivity into fast weathering (carbonates), intermediate weathering (hydroxides) and slow weathering minerals (silicate).The potential of neutralising acid relies on the reactivity and availability of acid-consuming minerals in significant quantities. Table 2-2 illustrates the relative pH range at which different minerals react to neutralise the acid generated in ARD. Other neutralising constituents include aluminosilicate minerals.

Table 2-2 classifications of minerals based on their relative rates of weathering at pH 5 (Lawrance & Wang, 1996,).

Mineral	Composition	Relative reactivity at pH 5
Dissolving	Calcite, dolomite, magnesite and aragonite	1.00
Fast weathering	Anorthite, olivine, forsterite, garnet, jadeite, nepheline, leucite, spodumene, diopside and wollastonite	
Intermediate weathering	Sorosilicates, (zoisite, epidote), pyroxenes, augite, enstatite, amphiboles (glaucophane, hornblende and actinolite), phyllosilicates (talc, biotite chlorite).	0.02
Slow weathering	Plagioclase feldspars (albite, oligoclase, labradorite), clays (vermiculite, montmorillonite)	0.01
Very slow weathering	K-feldspars, muscovite	0.01
Inert	Quartz, rutile, zircon	0.004

2.3 Neutralization by aluminosilicate minerals

During the dissolution of carbonate minerals in the solution, basic metals such as calcium (Ca), iron (Fe), magnesium (Mg) and manganese (Mn) are released into the solution. When carbonate minerals are exhausted in the system, the basic metals produced contribute to the formation of iron and aluminium hydroxides ions which dissolve and ultimately contribute towards acid neutralisation. Gibbsite $(AlOH)_3$ and Ferrihydrite (FeOH) neutralisation reactions occur as a result of aluminium and hydroxide precipitation at pH 3.5 and 4.3, according to Equations (2-17) and (2-18) respectively (Dold, 2017; Blowes et al., 2003).

$$Fe(OH)_3 + 3H^+ \rightarrow Fe^{3+} + 3H_2O \quad (2\text{-}17)$$

$$Al(OH)_3 + 3H^+ \rightarrow Al^{3+} + 3H_2 \quad (2\text{-}18)$$

Generally, some neutralisation potential of ARD from mine waste is offered by fast weathering minerals such as olivine, plagioclase, diopside and wollastonite in an acidic pH,

but at a slower rate compared to that of calcite (Jambor et al., 2010; Nordstrom & Southam, 1997). Overall, the weathering of silicate and aluminosilicates provides some neutralization due to the dissolution of calcium (Ca), Fe^{2+} and the availability of alkaline metals. Including potassium (K) and sodium, which leach aluminium together with silicon, resulting in ARD neutralisation. This reaction is mostly governed by the pH and availability of sufficient concentration of neutralisation species such as potassium, sodium, calcium and silica. This neutralisation potential of the aforementioned species results from feldspars ($KAlSi_3O_8$ – $NaAlSi_3O_8$ – $CaAl_2Si_2O_8$), as illustrated in Equations (2-19) and (2-21). When H^+ is consumed, Ca and K enter the solution, which further promotes dissolution of the feldspars. Such neutralisations are highly dependent on environmental factors, which also contribute to ARD formation.

$$CaAl_2Si_2O_8(S) + 2H^+(aq) + H_2O(aq) \rightarrow Ca^{2+}(aq) + Al_2Si_2O_5(OH)_4(S) \quad (2\text{-}19)$$

$$2KAlSiO_3O_8 + 9H_2O + 2H^{2+} \rightarrow Al_2Si0_5(OH)_4 + 2K + 4H_4SiO_4 \quad (2\text{-}20)$$

2.4 Factors contributing to ARD formation

There are several factors that accelerate the oxidation reaction of sulphide minerals in mine waste dumps. These include the presence of air and water, the presence of sulphur and iron oxidising microbes which regenerate reactants in the sulphide oxidation reaction, mineral composition, and the physical characteristics of the mine waste. These factors are discussed in detail in subsequent sections.

2.4.1 Availability of water and air

Dissolved oxygen is one of the most crucial factors for the oxidation of mineral ore waste to occur through both chemically and biologically facilitated reactions. Micro-organisms, i.e chemolithoautotrophy, present in ARD sites require oxygen and carbon dioxide for their survival. Under such conditions, the pyrite is oxidised and so produces indicators of ARD generation, as indicated in Equations (2-1) and (2-2). The penetration of oxygen into the grain size of sulphide minerals at cecum-neutral pH accelerates the rate of ARD generation in the environment. The availability of water during ARD formation is required, as it serves as both a reactant and medium in which transportation mechanisms are facilitated, culminating

in leached metal species mobility to uncontaminated areas. This process is also dependent on temperature.

2.4.2 Effect of temperature and weather conditions

Weather conditions existing in the locality of waste rock deposits may play an essential role in ARD generation. The main contributing factors include a warm temperature, humidity, precipitation and sustained availability of groundwater (Plumlee,1999). The oxidation of sulphide minerals is an exothermic reaction, which therefore can raise the temperature above 40-60°C, temperatures which facilitate rapid microbial proliferation. On the other hand, a decrease in temperature increases the solubility of carbon dioxide (CO_2), which reduces the pH such that dissolution of carbonate minerals may occur at a faster rate to neutralize the acid generated under low pH conditions. The heat generated from sulphide oxidation may increase the temperature and the rate of mineral leaching under low pH catalysed by ferric ions.

This illustrates that the temperature of a waste rock deposit also plays an essential role in the growth of dominant species, which are classified into three categories according to the temperature range suitable for their optimal growth (Rawlings & Johnson, 2007). The three groups of micro-organisms normally isolated from ARD contaminated sites are mesophilic bacteria that live and replicate between 10°C to 45°C, moderate thermophiles which function at the temperature range of 5°C to 60°C, and thermophilic archaea growing at 60°C to 90°C. These temperatures can be sustained by the exothermic oxidation of sulphide minerals such as pyrite. The most active microbial species in the mesophilic range are *L. ferrooxidans*, *A. ferroxidans* and *L. ferriphilum*.

L. ferrooxidans are gram-negative bacteria that can grow at temperatures ranging from 15°C to 45°C with an optimum of 30°C. These Fe-oxidising micro-organisms function best at pH 1.5 to 4.0. Similarly, *A. ferroxidans* are the most abundant naturally occurring micro-organisms that were first isolated in an ARD contaminated site (Colmer et al., 1950). This species is able to oxidise Fe^{2+} to Fe^{3+} at an optimum pH of 2.0 to 2.5, provided that it is at an optimum temperature of 40°C (Dopson et al., 2005); however, *L. ferriphilum, which* is an obligate chemo lithotrophic micro-organism which uses pyrite/Fe^{2+} as a source of energy, grows at an optimal pH range of 1.4 to 1.8 and a temperature between 30 to 35°C. The latter was first isolated in South Africa, and it is currently used in gold-bearing plants to treat arsenopyrite concentrates (Rawling et al., 2002).

Some acidophilus, including *A. caldus*, do grow in the presence of sulphur compounds such as sulphates, elemental sulphur, sulphide and thiosulphates, which are by-products of ARD. This species is a gram-negative autotrophic proteobacteria that optimally functions at pH 2.0 to 2.5 and at 45°C. *A. caldus* has been observed to be the best active acidophilic sulphur oxidising micro-organisms in the ARD environment (Norris et al., 2011). For persistent ARD formation, the availability of these organisms is crucial.

2.4.3 Availability of micro-organisms

Micro-organisms play an extensive role in ARD generation as they are capable of oxidising ferrous to ferric iron which becomes available to dissolve minerals (Moon, 1995). At neutral pH, the oxidation of pyrite is sluggish. However, this reaction is catalysed by acidophilic sulphur oxidising microbes such as *A. thiooxidans, A. caldus*, and iron-oxidising microbes such as *A. ferrooxidans* and *L. ferriphilum* (Swaine & Goodazi, 1995*).* In the presence of these microbes, the dissolution of pyrite results in the formation of ferrous iron which is converted to ferric iron, and the intermediate sulphur compounds produced are converted to sulphates (Shippers & Sand, 2006), with *A. thiooxidans* and *A. caldus* facilitating the formation of sulphuric acid through the oxidation of sulphur components (Loos et al., 2002; Parker & Robertson, 1999). Generally, these micro-organisms survive best at optimum temperatures of 25°C to 30°C and at a pH of 0.5 to 4.0 (Johnson & Hallberg, 2003), with the mineralogical characteristics of the mine waste and its constituents playing a limiting reactant role without which ARD formation will be limited.

2.4.4 Mineralogy and physical characteristics of mine waste

Acid formation from waste rocks is mostly dependent on the abundance of acid generating minerals found in a particular waste dump. The physical properties of oxidisable species in the waste, and physical characteristics such as the size of the particles, texture and permeability, play a crucial role in ARD formation (Lapakko et al., 2006).

During the extraction of valuable minerals in mineral processing industries, waste rock size is reduced by milling. A deleterious consequence of this process is that particles of different sizes composed of sulphide and gangue material are produced with reactive sulphide species being exposed. For ARD formation potential, the surface area of the milled sulphide species-containing ore, in relation to non-sulphide species, becomes an important characteristic to assess (Enviromine, 2012). In fine grains with a high surface area, sulphide species exposure, thus availability under oxidation conditions, is high, which will promote a

higher rate of ARD generation., Large grains possess a smaller surface area, which reduces the penetration of oxygen, and therefore a delay in the onset of ARD generation (Abiddin & Kalyoncu, 2015). The formation of ARD generation in waste rocks is therefore directly proportional to grain size and exposed surface area under oxidising conditions (Ferguson & Erickson, 1988). The four different scenarios of non-sulphide and metallic sulphide species exposure is indicated in

Figure 2-2.

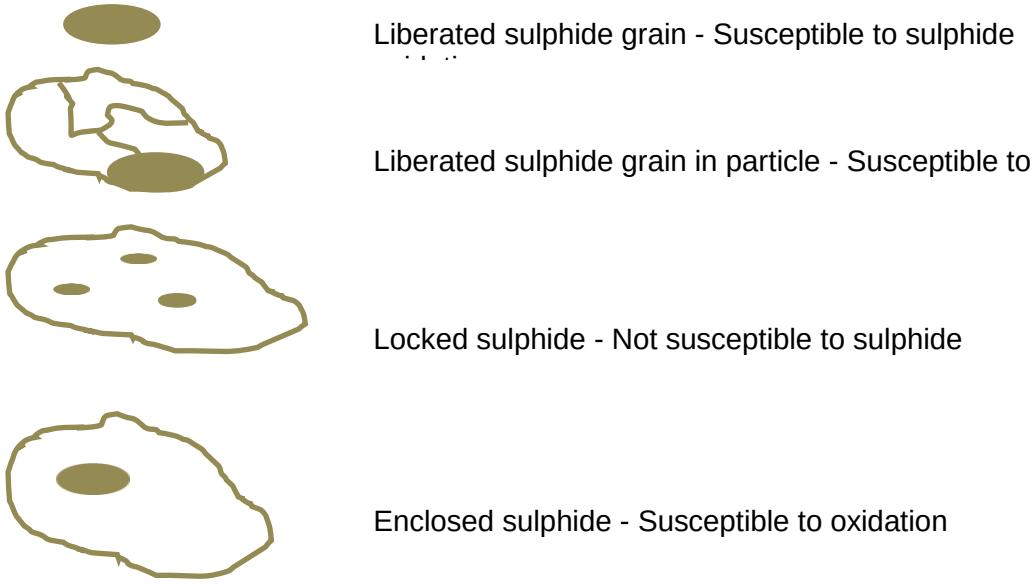

Figure 2-2: Four possible scenarios of ARD generation due to liberation sulphide minerals (Erguler & Erguler, 2015; Lapakko et al., 2006).

In order to elucidate the ARD formation potential including characterisation, suitable tests and/or methods must be developed, some of which can be used to account for the influence of microbial activity on the ARD generation potential of the different size of waste rock particles containing sulphide species.

2.5 ARD characterisation methods

The ability to characterise waste rocks prior to disposal of waste deposits enables mining companies to consider informed waste management strategies to prevent imminent risks of ARD generation, and to develop effective mitigation measures. The characterisation of mine waste material is achieved through the use of static tests, lab-based kinetic techniques and

predictive models (see Figure 2-3) (Morin & Hutt, 1998; Akcil & Koldas, 2006). ARD rapid screening tools such as acid-base accounting and NAG tests are used to determine the acid generating and acid neutralising potential of mine waste, without an indication of the relative rate of ARD generation. Samples classified as uncertain and potential acid generating are further investigated under laboratory conditions using kinetic tests such as the column leach test and humidity cell test, to gain an insight into the relative rates of ARD generation. The results generated from the characterisation methods are combined to complement the data from the ARD prediction tests, which account for the climate conditions of a particular mining site. Morin & Hutt (1997) proposed a wheel approach to fully characterise and predict future drainage. However, the wheel is has the disadvantages of the long time frames and excessive cost of some of the listed methods required to complete such an assessment. Hence there is a need for the development of rapid and reproducible ARD characterisation test for mine waste.

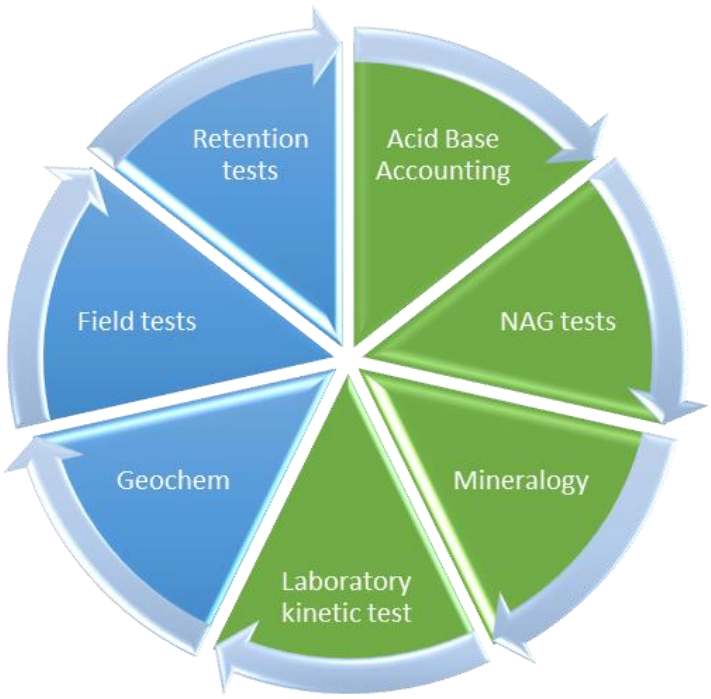

Figure 2-3: The wheel approach for ARD prediction (re-drawn from Morin & Hutt, 1998)

The ability accurately to predict the acid potential of a waste rock sample is essential for reducing and preventing ARD formation. Static tests, kinetic tests and mineralogical assessment are well-established methods for the characterization of mine waste (Price, 2009). The most widely used static test protocols are categorised into acid-base accounting (ABA) and Net Acid Generation (NAG) tests. Mineralogical assessments are also used to gain an insight of the different groups of minerals in waste rock. The biokinetic test, a subject

of this thesis, is one of a few newly developed and emerging techniques; it is currently being researched to establish its suitability in predicting ARD formation of waste material from mining activities.

2.5.1 Acid-Base Accounting

Acid-base accounting is used to estimate the overall net acid producing potential of waste rock samples. This estimation is represented by a net acid producing potential (NAPP) value which is a balance between the maximum potential acid generated (MPA) and acid neutralizing capability (ANC) (Stewart et al., 2006b) – see Equation (2-21).

$$\mathrm{NAPP} = \mathrm{MPA} - \mathrm{ANC} \tag{2-21}$$

2.5.2 Acid neutralising capacity

Acid neutralising capacity (ANC) is a quantitative method used to assess the neutralising ability of mine waste. ANC is used as a rapid screening tool due to its cost-effectiveness and short timelines (days to weeks) to determine ARD potential of samples (Sobek et al., 1978; Morin & Hutt, 1997). The neutralisation abilities of mine waste are assessed by adding standardised hydrochloric acid and titrating using a standard base (sodium hydroxide). The appropriate concentration of acid to be used for the determination of ANC is done by performing a Fizz rating. The Fizz rate enables the determination of the volume and concentration of acid that is necessary to leach the mine waste. After selecting a suitable concentration, the sample is heated to temperatures between 80°C and 90°C until minimal effervescence is observed. The sample is titrated to pH 4.5 to assess the buffering capacity resulting from weathering of fast dissolving minerals such as calcite, dolomite and magnetite, and precipitation of silicate mineral, iron hydroxide, calcium hydroxide, and other low reactive minerals, including feldspar and plagioclase. The sample is further titrated to pH 7 to determine unreacted acid residue (Dold, 2017; Parbhakar-Fox & Lottermose, 2015a).

Sobek et al., (1978) note that the most widely used method for acid-base accounting is the static test because of its cost-effectiveness and the ease at which it is conducted. However, this method has some drawbacks, such as overestimation of acid neutralising potential of samples, because it does not consider the acidity occurring as a result of ferric oxidation and sulphate (Dold, 2017; Price, 2009). The ANC value can also be underestimated by the

influence of metal hydroxides formed during the titration process with a strong base such as NaOH (Stewart et al., 2009). The ANC value does not provide an indication of the reactivity of the acid neutralizing capacity of the sample, nor its availability to completely neutralize the acids produced within the sample. Again, the use of hydrochloric acid and heating of the sample promote the dissolution of mine waste that would not dissolve under normal environmental conditions. The fizz rating test is only limited to assess carbonate concentration, and does not consider the other buffering minerals such as siderite and non-carbonate minerals such as silicate that has neutralising capabilities in the form of chlorite and biotite mica. The fizz rating is used to determine the amount of HCl concentration required; however, the test lacks reproducibility (Bouzahzah et al., 2015).

In order to address the above-mentioned shortcomings, the ABA static test was further developed by Stewart et al., (2006) to improve the accuracy of the ARD formation potential. The modification of ANC determination disregards the boiling step and involves the addition of hydrogen peroxide at pH 4.5. Also prior to back titration, samples must be filtered due to the dissolved metal hydroxide resulting in an underestimation of the ANC (Steward et al., 2009). In addition, this test does not provide an indication of the relative rates of ANC.

2.5.3 Maximum Acid Potential

The maximum potential acidity (MPA) estimates the total potential for acid generation and is determined by measuring the total sulphur content (wt%) in relation to increments equivalent to a stoichiometric factor of 30.6, to convert the measured sulphur content to kg H_2SO_4/ton as highlighted in Equation (2-23) (Weber et al., 2005). The technique is based on the assumption that all the sulphur exists as pyrite and that sulphides are completely oxidised to form sulphuric acid. This assumption is described by Equation (2-7) whereby each mole of pyrite yields two moles of sulphuric acid (Stewart et al., 2006; Smart et al., 2002). The application of MPA is limited because it doesn't account for any other sulphide species within the waste material. The existence of acid generating minerals that are non-sulphide such as gypsum and organic sulphur may cause inaccuracies in MPA measurements of samples (Stewart et al., 2006; Lapakko 2002). The NAG test and mineralogical assessment are therefore often used together with the ABA test to give an accurate description of the acid producing potential of mine waste (Becker et al., 2015; Parbhakar-Fox et al., 2013).

$$\text{MPA Kg H2SO4 /ton} = (\text{total S \%}) \times 30.6 \qquad (2\text{-}22)$$

2.5.4 Net Acid Generation tests

The Net Acid Generation (NAG) test is also used to classify the acid generating potential of a sample by directly assessing the sulphuric acid produced by the sulphide waste (Lottermoser, 2010; Weber et al., 2005; Smart et al., 2002). This test involves the use of hydrogen peroxide which acts as a strong oxidising agent to hasten sulphide oxidation within the mine waste (Equation. (2-23) (Plante et al., 2012; Smith et al., 2002). The advantage of using the NAG test is that both acid-forming and acid-neutralising minerals react simultaneously to provide a net acid generating potential of a sample. The resultant liquid is back titrated to pH 4.5 to account for acid (H_2SO_4) produced from the oxidation of sulphide and iron-bearing minerals including siderite.

$$FeS_2 + \frac{15}{2} H_2O_2 \rightarrow Fe(OH)_3 + 2SO_4^{2-} + 4H^+ + 4H_2O \quad (2\text{-}23)$$

There are three types of NAG test procedures used to assess the geochemical characteristic of different mine waste: single addition NAG, multi-NAG, and kinetic NAG tests (Smith et al., 2002; Stewart et al., 2006). A single addition NAG uses hydrogen peroxide to assess the potential of acid generation of overburden samples. This method involves the addition of standardised (15%) hydrogen peroxide solution to a pulverised sample for 24 hours. This promotes the oxidation of sulphide minerals within the waste rock sample. The solution and the sample are heated at 90°C to decompose residual hydrogen peroxide and allow the release of residual ANC. The mixture is allowed to cool to ambient temperature with the NAG_{pH} recorded for waste classification. When the pH is below 4.5, the material has the potential to generate ARD. The leachate is then titrated to pH 4.5 considering the acid and aluminium liberated, including other dissolved ions. Further titration to pH 7 takes into consideration the availability of other sulphide-bearing minerals such as siderite, which forms a precipitate at pH between 4.5 to pH 7 (Parbhakar-Fox & Lottermoser 2015; Smart et al., 2002).

The single addition NAG was refined and further developed to a Multi-NAG test due to the inadequate oxidation of sulphide greater than 1% wt (Stewart et al., 2006a). This method uses similar conditions to the single NAG test; however, the only difference is that the single NAG requires the addition of acid only once while in the multi-NAG test acid it is added several times to enhance the completion of the reaction facilitated by hydrogen peroxide (Stewart et al., 2006a). Additionally, kinetic NAG tests are designed to assess the rate of acid formation and further validate the classification of NAG_{pH} against pH (Smart et al., 2002). The kinetic NAG test procedure is similar to the single addition NAG, with

differentiation being on measuring parameter monitoring, i.e. the monitoring of temperature, pH and electrical conductivity (Chotpantarat, 2011; Stewart et al., 2006a; Smart et al., 2002).

2.5.5 Interpretation of static tests

The data generated from the aforementioned tests is used to categorise the samples according to their status of generating acid potential drainage that may arise in the long-term. Mine waste samples can be classified as potential acid forming (PAF), non-acid forming (NAF), or uncertain ARD formers (UC). From the ABA static tests, samples with a NAPP value above 20 Kg H_2SO_4/ton are classified as potential acid-forming, while samples below -20 are classified as having non-ARD forming abilities, which suggests high neutralising capabilities as a result of low sulphur content (Smart et al., 2002). Samples falling in the range of -20 to 20 Kg H_2SO_4/ton are classified as uncertain as indicated in Table 2-3.

Table 2-3: Ore sample classification using NAPP and NAG pH values [After Stewart et. al. 2006]

ARD characterisation tests	Results Kg H_2SO_4/tonne	Classification
Acid-base accounting	NAPP > 20	Potentially acid forming
	NAPP < -20	Non-acid forming
Net acid generation	NAG pH < 4 &NAGpH7 > 10	Acid forming
	NAG pH > 4.5 & 5 < NAGpH7 < 10	Non-acid forming
Combined static tests	NAG pH < 4.5 & NAPP > 0	Potentially acid forming
	NAG pH > 4.5 & NAPP < 20	Non-acid forming

A graphical comparison between the Net acid producing potential (NAPP) to Net acid generation NAG_{pH} in a 2-D plot, is used to classify a waste sample as either PAF, NAF, or UC. Some of the limitations associated with this classification is based on the NAG_{pH} used. For instance, the preferred pH used by Broadhurst, (2009), Moon et al., (2008) and Stewart et al., (2006a) was 4.5 while Weber et al., (2005) used a pH of 4 due to the consideration acidity of assessed samples (see Figure 2-4). However, this classification plot is essential as

it combines the results obtained from ABA and NAG tests to assess the potential of acid generation and the acid neutralising ability of mine waste concurrently, and a sample is classified using guidelines presented in Table 2-3.

Table 2-3.

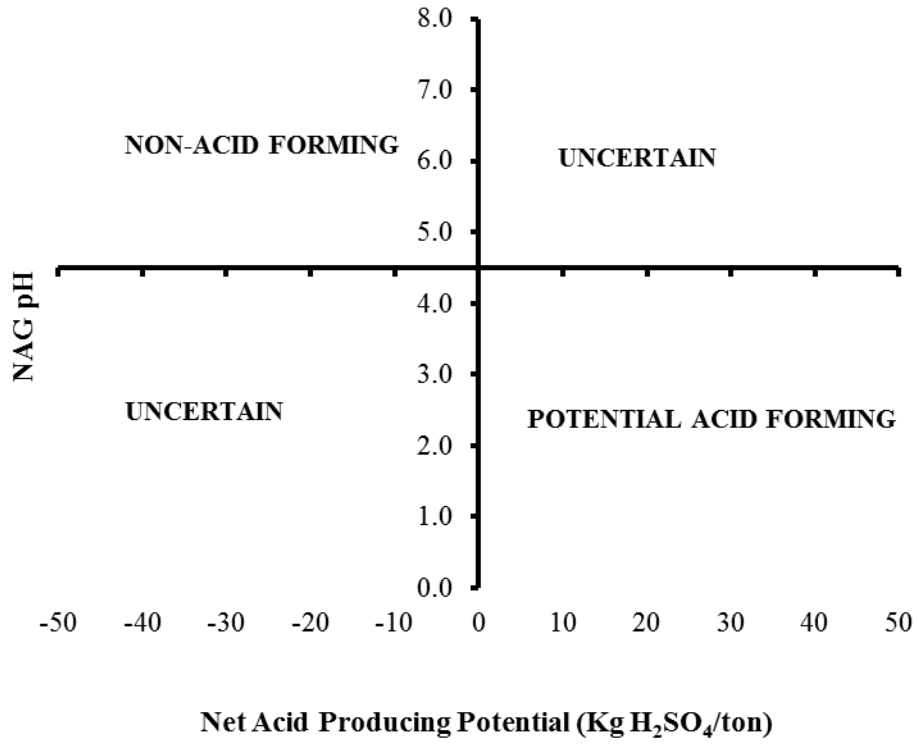

Figure 2-4: Classification plot showing ARD regions as proposed by Steward et al., (2006)

The limitations of the static tests include lack of information on the rate of ARD formation or neutralisation (Lapakko 2002), and particularly their relative rates (Harrison et al., 2010; Hesketh et al., 2010); overestimations, including inaccuracies due to the use of strong oxidants not found in waste heap environments; and failing to account for microbial activity. Biokinetic tests were therefore developed at UCT (Opitz, 2013, Mbamba et al., 2012; Hesketh et al., 2010). These tests give information on the relative kinetics of acid neutralizing and generating potential based on microbial activities, as would be the case in an environment containing waste rock.

2.5.6 Standard kinetic tests

Long-term kinetic tests such as humidity cell and column leach tests were established to provide information concerning the rate of ARD generation over time and confirm static test results (Smart et al., 2002). Furthermore, these kinetic tests offer a better understanding of samples classified as uncertain under static tests. These tests are also essential to assess the quality of potential mine water through progressive analysis of solution pH and conductivity changes as a result of mineral leaching. They are also useful for providing the rates at which acid generating and acid neutralising minerals leached can be tailored for specific conditions. However, these tests are unfavourable due to the cost intensiveness and long time frames necessary to provide quality data. The estimated cost to sustain one sample is approximately 1000 USD, while the prescribed duration for running these test is about 20 to 22 weeks (Berry et al., 2015; Parbhakar-Fox & Lottermoser 2015a; Lapakko, et al., 2006; White et al., 1999).

2.5.7 Humidity tests

Humidity cell kinetic tests are performed to assess rates of weathering and oxidation of mine waste contributing to ARD generation. This is achieved by subjecting 1kg of less than 2 mm crushed mine waste to a humidity cell test. The humidity cell test is run on a weekly basis whereby there is a constant supply of dry air into the cell, followed by another three days of moist air, and rinsing with deionised water for one day. This test is conducted with the purpose of assessing drainage quality of the mine waste as a result of weathered minerals. After flushing the cells, the resultant solution pH is measured and metal iron released is determined (Sapsford et al., 2009). This test is essential in providing an indication of relative rates for weathering of different minerals. The disadvantage is the once-off flushing cycle per week needed throughout the experimental run. Further, this condition of once off-flushing may not present precipitation occurring during the wet and dry seasons which occurs in field conditions (Parbhakar-Fox & Lottermoser 2015a; James & Philip 2009). Furthermore, a large volume of water added for flushing may wash away oxidants/reaction products and this is contrary to field conditions where less water comes into contact with the waste rock. This test is also not designed to consider the role played by the microbial community in the ARD sites.

To address some of these short-coming, ASTM (2000) designed the accelerated humidity cell test in which acid digestion is performed prior to the performance of any experimental

work. The acid digestion is done in order to minimise the neutralisation potential of the mine waste and ultimately reduce the lag period.

2.5.8 Column test

Column leach tests involve loading a crushed sample of 2-3 kg into a column, with a supply of water and purged air to promote oxidation reaction (Smart et al., 2002). The rates of acid production, leaching of elements, and depletion of carbonates and other minerals with neutralising abilities from sulphide oxidation can be estimated directly to determine the acidification of the drainage (Bradham & Caruccio, 1995). The most important parameters that are measured include redox potential and pH. Some of the benefits of this test include the use of particle size and mass of waste rock necessary for a specific study, and time intervals for sample collection. Integration of the mineralogical micro textural analysis was highlighted as one of the shortcomings in the method (Parbhakar-Fox et al., 2013). To address this issue Parbhakar-Fox et al. (2013) integrated the mineralogical assessment of leached samples from bulk mineralogy and other geochemical characterisation tests in order to ascertain weathering of the waste rock to produce heavy metals under different test conditions. Research conducted by Smart et al. (2002) suggested that the experiments should be run over six months. Refinements have been suggested such as microbial inoculation to better understand the effect of microorganisms during leaching of minerals (Brady & Hornberger 1998; Blowes et al., 2003).

2.5.9 Biokinetic Accelerated Weathering Tests

Due to the lack of information of microbial activity in the ARD, a Biokinetic test was developed by Hesketh et al. (2010). This method offers an innovative and cost-effective alternative compared to the normal kinetic tests. The advantages of using Biokinetic tests is that they are easy to conduct and provide relative rates of ARD generation over a shortened time-frame. Furthermore, they are used to complement the results obtained from the static test for a quicker characterisation of different waste rock. In addition, meaningful data on the relative rates of potential ARD generation is obtained within a period of ninety days (Opitz & Harrison, 2016; Hesketh et al., 2010). This test provides a valuable insight into the rate of acid-consuming and acid-forming reactions in the presence of microbial facilitated conditions.

A mixed culture of sulphur and iron oxidising micro-organisms such as *L. ferriphilum, A. ferrooxidans* and *At. caldus* were inoculated into shake flasks containing waste rock and incubated in a 37ºC shaking incubator for a minimum of ninety days (Hesketh et al., 2010). The important parameters monitored during this period were redox potential, pH and iron and sulphate concentrations. The leachate of the biokinetic tests might be further used for chemical analysis to gain knowledge of oxidation of sulphide minerals and dissolved acid neutralising minerals within a reasonable timeline.

This method is used to characterise the acid generating ability of a waste rock from different mine wastes such as gold, copper and coal processing in the presence of a microbial consortium. The application of the Biokinetic test for characterisation of ARD generation has focussed on solid loading, and particle size using different minerals copper tailings (Karl & Opitz, 2013; Hlongwane 2015; Hesketh et al., 2010), fine coal waste (Kotelo, 2013; Mbamba et al., 2012), and gold tailings (Opitz & Harrison, 2016). However, the Biokinetic test is still in its initial stages of development and certain parameters are not sufficiently well-defined to obtain a standard approach that can be applied to different waste ores. It is therefore necessary to determine standard operating conditions for the Biokinetic test and confirm its relevance across different waste ores. Furthermore, the Biokinetic test should be used in conjunction with static test and mineralogical assessment to better characterise ARD generation from different mine wastes.

2.6 Summary

The literature reviewed has shown the influence of different mechanisms on the chemical and biological processes which accelerate the lixiviate contributing to ARD generation. The rate of ARD formation in the presence of air and water occurs at cecum-neutral pH and the reactions are slow. However, a consortium of iron and sulphur micro-organisms capable of oxidising the ferrous iron to produce ferric iron, which leaches minerals, is unaccounted for in the ARD formation potential test. Several studies indicated that the rate of ARD generation by iron and sulphur oxidising micro-organisms is faster than that occurring as a result of oxygen availability. The different weathering of waste rock with neutralising abilities, due to constituents such as carbonates, silicates and aluminosilicate minerals which dissolve at different rates due to differentiation in pH, can contribute towards neutralisation. Several studies observed that carbonate in the form of calcite dissolves faster and neutralises the acid generated. Similarly, ores that contain silicate and aluminosilicate also contribute to neutralisation, albeit at a reduced rate compared to calcite. The literature reviewed has also

highlighted the limitations of the static test characterisation approach usually employed to characterise ARD generation. Static tests methods such as ABA and NAG can only provide information on acid generating and acid neutralising minerals under aggressive chemical oxidation. Hence, there is a need for determining the bulk mineralogical composition of mine waste in order to identify minerals in different waste rock. However, this is not well established in the industry but rather at the research level. It is also highlighted in the literature reviewed that kinetic tests including humidity cells are unfavourable due to the elongated test runs required to provide quantitative data; hence, they are only applied when a waste rock is known to be acid forming or uncertain, and additional data on it is sought for prediction purposes.

CHAPTER 3

MATERIAL AND METHODS

3 MATERIALS AND METHODS

The aim of this study was to investigate the effect of inoculum size on an ARD Biokinetic Test profile for standardisation of the protocol; furthermore, to refine the current Semi-continuous Biokinetic test in order to complement the Batch Biokinetic Test, in comparison with static ARD characterisation tests. The effect of the microbial consortia was determined through the measurement of redox potential, pH, Fe^{2+}, Fe^{Tot}, SO_4^{2+} and microbial speciation.

This chapter presents a brief description of the experimental work conducted in order to accomplish the aforementioned aims. Mineral composition, ARD characterisation tests and Biokinetic tests were conducted to characterise the ARD potential of gold-bearing and copper-bearing waste rocks as schematically illustrated in

Figure 3-1. Preliminary work entailed preparation of waste rock samples by splitting, determination of particle size distribution, quantification of total sulphur content, and inoculum preparation. The effect of inoculum size was investigated for both waste rock samples with different acid neutralising capacities to gain insight into the impact of pH.

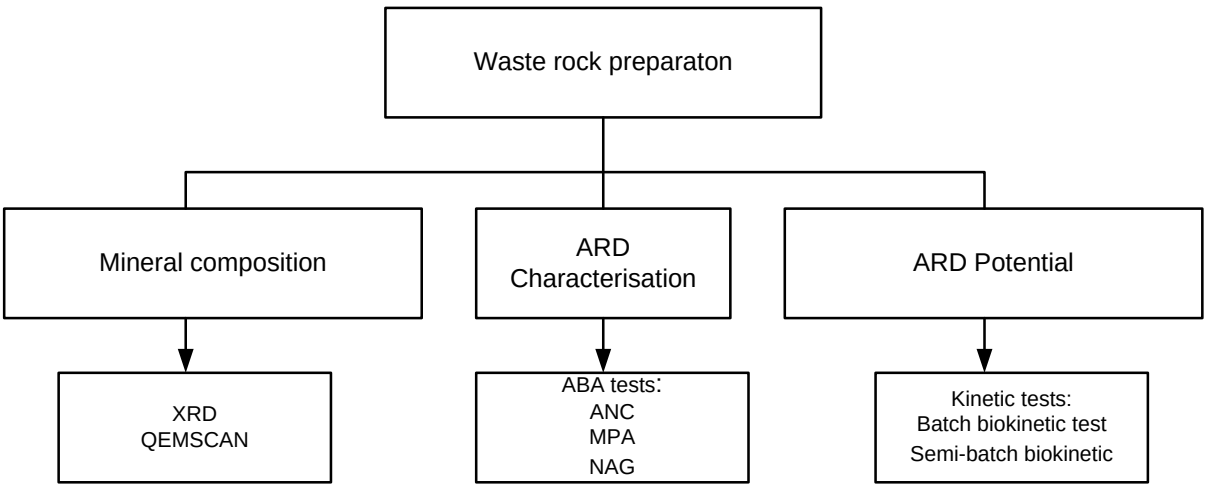

Figure 3-1: Schematic outline of the methods used to conduct the study

3.1 Description: waste rock samples

Two waste rock samples used in this study, namely gold-bearing (sample 1) and copper-bearing (sample 2) waste rocks, were obtained from active mines in Tanzania and Chile respectively. An amount of 125 kg, of sample 1 was divided into 3.5 kg portions using a 2-

way riffle splitter. Sample 2 was received already crushed to a particle size such that 80% (w/w) passed through a 12.5 mm screening sieve.

3.2 Waste rock preparation

Sample 1 was milled using high pressure grinding rolls at a pressure of 120 bar with further milling for 20 minutes using a rod mill (290 × 25 mm stainless steel rods) with a working volume of ~3 L. After the milling process, the fine material was dried and sieved to pass through a 150 µm sieve to suit the ARD characterisation tests. The fine ore was then split using a 10-Dickie & Stockler rotary splitter to obtain representative samples ranging between 100 to 500 g. The samples of approximately 50 grams were further split down to between 7.5 to 8 g using an 8-way Fischer rotary sample divider.

3.3 Particle size distribution

Milled waste rock with a particle size passing through a 150 µm sieve was chosen to represent conditions of waste rock deposits. The particle size distribution (PSD) is an essential component for the liberation of sulphide constituents from waste rock. The PSD of the two processed samples was determined using a Malvern multi-sizer 1000 nm in the analytical laboratory at the University of Cape Town, with a particle size distribution as shown in Figure 3-2.

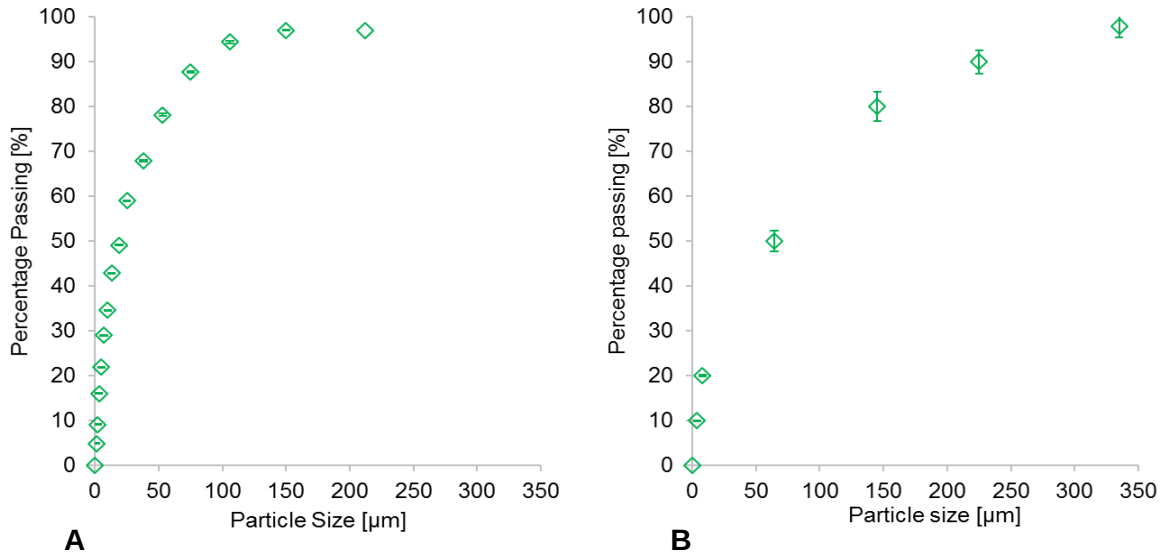

Figure 3-2: Particle distribution of gold-bearing (A) and copper-bearing (B) waste rocks were used in this study

3.4 Analysis of mineral composition

A representative fraction of the waste rock samples was sent for analysis to determine the mineral composition of the waste rocks. This was conducted in the Department of Geology at UCT, and results are presented in chapter 4, section 4.1.

3.4.1 Total sulphur determinations

Total sulphur content was conducted using LECO 632 sulphur analysis equipment, which employs thermal decomposition and combustion infrared spectrophotometry. Sulphur analysis was performed by the analytical laboratory in the Department of Chemical Engineering at UCT.

3.4.2 Determination of mineral composition

X-ray diffraction was performed to determine the waste rock species composition. The analysis was also done in the Analytical Chemistry laboratory in the Department of Chemical Engineering at the University of Cape Town.

3.5 ARD characterisation techniques

3.5.1 Fizz rating tests

Fizz rating was employed to determine the quantity of acid required to dissolve the carbonates, whose presence is indicated by fizzing or effervescence, when reacted with HCl or H_2O_2, using 0.5 g of the pulverised samples (Sobek et al., 1978). The sample was placed in a ceramic plate and one or two drops of eight percent of hydrogen peroxide (H_2O_2) were added. The fizz rating was evaluated according to the conditions outlined in Table A.1 in appendix A. Fizz rating associated acid quantities and concentrations were used in the ANC determinations.

3.5.2 Acid-Base Accounting tests

Acid-base accounting (ABA) was used to estimate the acid-forming and acid neutralising abilities of the waste rock samples. This estimation was represented by net acid producing

potential (NAPP) value which is quantified by determining the maximum potential acid generated (MPA) and acid neutralizing capability (ANC). This estimated value was expressed as kg H_2SO_4 /ton of solid waste. A negative NAPP indicates that the sample had sufficient ANC to counterbalance acid production. Similarly, when the MPA is greater than the ANC value and the NAPP was positive, this means that the sample is acid generating.

3.5.3 Acid Neutralizing Capacity tests

It was assumed that acid generated from the oxidation of pyrite to some degree reacts with acid neutralizing minerals present in the waste rock samples. The ANC aided in quantifying the acid neutralising capacity of the samples. The ANC method employed in this research was the hydrogen peroxide (H_2O_2) siderite correction test, adapted from Skousen et al. (1997). ANC is affected by iron carbonates such as siderite, which reacts with the acid produced and may contribute to the alkaline-producing potential of the samples, thereby, causing an overestimation of the ANC (Stewart et al., 2006; Skousen et al., 2002).

ANC was determined by adding a known volume of hydrochloric acid (HCl) to a precisely weighed pulverised sample, which was allowed to react by heating the mixture for a maximum of 2 hours in an electronic plate set at 90°C. The mixture was cooled and back-titrated with a standardised solution of sodium hydroxide (NaOH). This was done to determine the quantity of HCl reacted, as per the procedure listed in Smart et al. (2002). The detailed procedure followed for each test is listed in appendix A.1.

3.5.4 Maximum Potential Acidity tests

The maximum potential acidity (MPA) (see Equation 3-1) estimates the total potential for acid generation which is determined by measuring the total sulphur content of the sample, assuming that all sulphur exists as pyrite and that sulphides completely oxidize to form sulphuric acid.

$$MPA\ kg\ H2SO4\ /t = (total\ S\ \%) \times 30.6 \quad (3\text{-}1)$$

NAPP, MPA, and ANC are expressed in terms of kg H_2SO_4/ton waste rock. MPA is determined from the total S content of the sample in (wt %) in increments associated with a stoichiometric factor of 30.6 to convert to kg H_2SO_4/ton, whereby the entire sulphur content is present as pyrite (Weber et al., 2005). The stoichiometric factor used is based on the

assumption that H_2SO_4 is the sole and primary acidity product of the sulphide oxidation reactions occurring. The % S was determined using a LECO analysis.

3.5.5 Net Acid Generation tests

In this test, hydrogen peroxide was reacted with a sample to promote the oxidation of sulphide constituents in the waste rock. Unlike the ANC test, the NAG test involves simultaneous acid generation and neutralisation, with outcomes being the net acid generated by the sample (Stewart et al., 2006).

An amount (~2.5g) of the milled sample was weighed in an electronic balance and transferred into a 500 mL Erlenmeyer flask. To this, 250 mL of a 15% H_2O_2 solution was added. This solution was corrected to a pH between 4.5 and 5.0 using a 2M NaOH solution. The mass of the flask was recorded and allowed to react overnight. After 24 hours, the flasks were boiled for a minimum of two hours and/or until minimal effervescence was observed. Once effervescence ceased, distilled water was used to correct the mass of the flask to its original weight, with the pH being measured. The sample was cooled and allowed to settle for one hour. Prior to filtering, the mass of the filter paper was recorded. Both the filtrate and the filter cake were recovered from the filtering process. The filtrate was titrated against a 0.1M NaOH solution to a pH of, firstly, 4.5 and, secondly, 7.0, with the volumes of NaOH used being recorded when both pH values were reached. The filter cake was recovered and once again reacted with a 15% H_2O_2 solution, with the mass of sample lost, i.e. as unrecoverable from the filter paper, being recorded. This was repeated until the pH of the filtrate had a value of 4.5 or greater. The NAG values for each titration were calculated using the following Equation (3-2):

$$NAG = \frac{49 \times VNaOH \times M}{W} \qquad (3\text{-}2)$$

Where *V* is the total volume of NaOH used in each titration step (mL), *M* is the molarity of the NaOH solution used, and W is the mass (g) of ore samples used in each reaction step.

3.6 Biokinetic tests: Effect of inoculum size

Biokinetic tests were conducted under two different conditions, namely Batch, and Semi-continuous/draw and fill conditions. This was done to simulate long-term weathering of waste rocks in environmental waste heaps. Shake flasks simulating long-term weathering in a

disposal environment were inoculated with various inoculum sizes of mixed cultures of iron and sulphur-oxidizing micro-organisms. The Batch Biokinetic test was carried out under three different conditions: non-controlled and non-inoculated, pH controlled and non-inoculated, and pH controlled and inoculated.

3.6.1 Micro-organisms for Biokinetic tests

The bacterial culture used in this study was mainly dominated by *Leptospirilum ferriphilum* (Iron-oxidising micro-organism) previously isolated from a bioleaching stock bioreactor used to treat pyrite concentrate at Gamsberg mine (SA). These cultures were maintained at 35 °C in a 1L amplicon reactor and fed on a weekly basis with 3% pyrite (w/v) with a particle size of 55 µm and a Norris medium having (g/L): $MgSO_4$ (0.5), $(NH4)_2$ SO_4 (0.4), KH_2PO_4 (0.2) and KCl (0.1). The *Acidthiobacillus caldus* (sulphur oxidising organism) was obtained from the Centre for Bioprocess Engineering Research (CeBER) laboratories at the University of Cape Town. The enriched sulphur oxidisers were maintained in 500 mL shake flasks containing 250 mL of autotrophic basal salt (ABS) media with trace elements and 1% (w/v) sulphur. The trace element solution contained (g/L) $ZnSO_4$. $7H_20$ (10), $CuSO_4$ $5H_2O$ (1), $MnSO_4.4H_2O$ (1) $Cr(SO_4)_3.15H_2O$ (0.5), H_3BO_3 (0.6), $Na_2MoO_4.2H_2O$ (0.5), $NiSO_4.6H_2O$ (1), $NaSeO_4.10H_2O$ (1), and $Na_2WO_4.2H_2O$ (0.1). This culture was agitated in a rotary shaking (120 rpm) incubator at 30ºC.

3.6.2 Inoculum preparation

The inoculum was prepared by mixing the cultures dominated by *L. ferriphilum* and the enrichment culture of *At. caldus* in a 1:1 ratio. The combined cultures were grown in 0K media that contained (g/L): $(NH_4)_2PO_4$ (30), $MgSO_4.7H_2O$ (5), KH_2PO_4 (5), KCl, (1) and Ca $(NO_3)_2.10H_2O$, (0.14) in 500 mL shake flasks (Bryan et al., 2006). This was supplemented with 0.6% w/v (6 g/L) of pyrite and maintained for a period of approximately four weeks on a shaking platform (120 rpm) at 37 ºC. At 72 hour intervals, 10% of the inoculum volume was decanted from the cultures and replaced with an equivalent volume of fresh 0K media, to sustain microbial activity and growth.

3.6.3 Bacterial counts

The cultures were monitored by performing cell counts (Equation 3-3) using the Thomas counting chamber and a phase contrast microscope at 100X magnification in an oil immersion. The maximum cell concentration obtained was 6.379×10^8 cells/mL. The inoculum was further concentrated to achieve the maximum cell concentration of 1.67×10^9 cells/mL by filtering 300 mL of the co-cultured cells using a 0.22 µm cellulose filter membrane. Cells in the filter discs were washed with 10 mM of citrate buffer to remove the soluble iron prior to inoculation. The filter discs were re-suspended in falcon tubes containing 10 mL of 50X ABS media at pH 2 and this served as an inoculum.

$$Cell\ concentration\left[\frac{cells}{ml}\right] = \frac{cells\ counted\left(\frac{total\ no.of\ big\ squares(16)}{no.of\ squares\ counted\ (4)}\right)}{vol\ of\ 1\ small\ square \times total\ no.of\ small\ squares} \qquad (3\text{-}3)$$

3.6.4 Inoculum quality characteristics

Prior the commencement of an experiment, the inoculum was assessed for cell counts, pH, redox potential and DNA copy numbers via a quantitative real-time polymerase chain reaction (qRT-PCR). Prior to the initiation of a new experiment, the inoculum composition was analysed using qRT-PCR.

The effect of inoculum size on Biokinetic tests for assessing ARD was investigated using the inoculum with a bacterial community profile as presented in Figure 3-3. The inoculum preparation procedure is described in Appendix B. The culture was maintained throughout the experimental runs and subcultured on a weekly basis by 10%, replacing it with an equal volume of fresh 0K media at pH 2 and 0.5 g of pyrite concentrate. As shown in Figure 3-3, the inoculum composition for the first and second experiment contained 15% of *At. Caldus*, 36% *L. ferriphilum*, a small proportion (4%) of *archea* and 45% of unknown bacteria, assumed to be dominated by sulphur oxidisers.

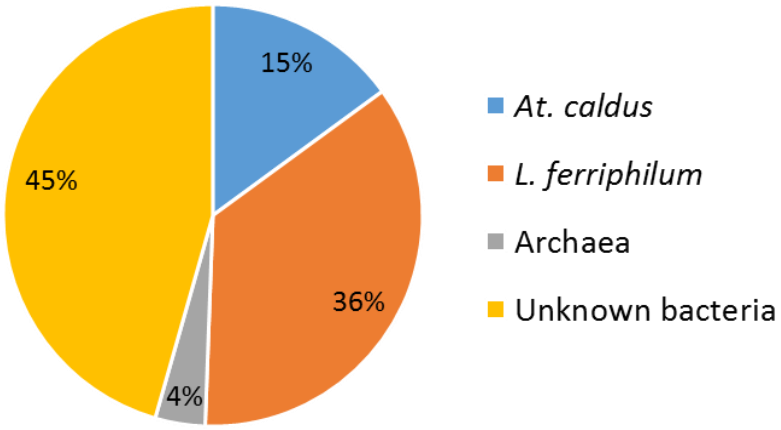

Figure 3-3: Microbial consortium profile of the inoculum as determined by qPCR at CeBER

3.6.5 Non-controlled pH experimental conditions

Initial inoculum concentrations of 10^7, 10^8, 10^9 and 10^{10} cells in 150 mL were prepared in triplicate and non-inoculated flasks were used as a control. To remove the initial soluble iron from the inoculum, approximately 300 mL of culture was filtered through a 0.22 µm filter.

After filtration, the soluble iron was removed from the filter paper through successive washes using an excess 10 mM citrate buffer solution. The micro-organisms retained on the filter paper were re-suspended in 10 mL ABS solution at a pH of 2.0. Thereafter, microbial counts were performed to quantify the total microbial concentration.

3.6.6 Controlled pH experimental conditions

The pH controlled Biokinetic test was conducted similarly to the non-controlled pH tests described in section 3.6.5. The pH controlled samples were inoculated with a known inoculum cell concentration calculated from the filtered inoculum procedure, developed to an initial cell concentration of 10^7, 10^8, 10^9 and 10^{10}. Appropriate inoculum sizes were introduced into respective shake flasks to make a final volume of 150 mL, for which the pH was controlled at pH 2 by adding 0.5M of standardised sulphuric acid using a burette, with acid consumption being recorded. Sulphuric acid was added until pH 2 was maintained. The shake flasks were closed with sterile cotton buds covered externally with aluminium foil and incubated on an orbital shaker (150 rpm) at 37 ºC for 90 days. On day 45, one sample from each of the flasks was used for microbial speciation to determine microbial composition using qPCR.

3.6.7 Semi-continuous/Draw and fill experimental conditions

The Semi-continuous/draw and fill method was developed to simulate a disposal scenario where there is minimal leachate containment and/or leachate seeps into the environment (Kotelo, 2013). The setup of the draw and fill method was similar to Batch Biokinetic tests as defined in section 3.6.5 One set of shake flasks was inoculated with the standard inoculum size (10^9) in 150 mL of ABS media containing 7.5 g of the waste rock, while the other set of flasks was non-inoculated. During sampling, 10%, i.e. 15 mL of the supernatant was removed and replaced with an equal volume of fresh ABS medium at pH 2. The planktonic micro-organisms present in the 15 mL supernatant were processed for the microbial speciation on days 5, 15 and 30.

3.6.8 pH and redox potential determinations

The pH of the leachate was measured using a 713 Metrohm pH meter with silver/silver chloride reference probe. The probe was calibrated on a daily basis to remain between 95% and 100% for accuracy using pH buffer solutions 1.00 and 4.00. The redox potential was measured using a 703 Metrohm Eh meter against a saturated AgCl/AgCl reference electrode. This electrode was tested for precision using a Crison redox standard of 650 mV daily prior to redox readings for each sample.

3.6.9 Ferrous and total iron quantification

The concentration of ferrous iron and total iron were quantified calorimetrically using a 1-10 phenanthroline method defined by Komadel & Stuck (1998). In this test, 2 mL of an ammonium acetate buffer and 2 mL of a 1-10 phenanthroline solution served as an indicator, with dilutions being accounted for during the determinations.

The 1-10 phenanthroline reacts with ferrous iron and results in the formation of an orange-red colour absorbing between 400-600 nm. The contents in the test tube were then mixed thoroughly by vertexing, with absorbance readings conducted using a Helios UV-Vis spectrophotometer at a wavelength of 510 nm. Blank samples composed of ammonium acetate and 1-10 phenanthroline were also prepared, to calibrate the spectrophotometer. Total iron was quantified using the same methods, with the addition of hydroxyl ammonium chloride to reduce ferrous iron to ferric iron. This mixture was allowed to react for five minutes prior to absorbance readings. A standardised calibration curve was used to determine the concentrations of the ferrous and total iron, as presented in Appendix C

3.6.10 Sulphates quantification

The concentration of sulphates was determined using a turbidity method for the non-controlled pH Biokinetic test following the method defined in the American Public Health Association (Gilcreas, 1966). Then a Helios UV-Vis spectrophotometer at a wavelength of 420 nm was used to measure the absorbance's, which were further used to calculate the concentrations of oxidised sulphides from a standard curve. The detailed procedure followed is outlined in Appendix C.

3.7 Analysis of microbial composition using quantitative real-time polymerase chain reaction

3.7.1 Preparation of samples for gDNA extraction

The composition of microbial consortia was analysed using qPCR prior to inoculation, and periodically during experimentation. Shake flasks were allowed to rest for a few hours and the supernatant containing planktonic micro-organisms was removed and aliquoted into Eppendorf tubes. The tubes were then centrifuged at 13000 rpm for 10 minutes, a procedure repeated several times to obtain a pellet of sufficient quantity for DNA extraction. After filtering, a citrate buffer was added to the 20 mL of the supernatant obtained from each sample, until the yellow colour was unobservable, indicating the complete removal of soluble iron. The formed pellet was recovered through the removal of the supernatant in the Eppendorf tubes. The pellet was washed using 10 mM TE buffer to dissolve and preserve the DNA The pellets recovered were re-suspended in 200 µL of a TE buffer and kept at -20 °C prior to analyses.

3.7.2 Extraction of Genomic DNA

The DNA extraction of microbial consortium used in this study was performed in-house, using the High Pure PCR preparation kit following manufacturer's guideline (Roche, South Africa).

3.7.3 Lysis and DNA binding

The microbial cells from preserved samples (-20 °C) were re-suspended in a 200 µL of tissue lysis buffer, 10 µL lysozyme and 5 µL RNAse, and vortexed for 60 seconds.

The mixtures were placed in a heating block set at 37 °C for 30 minutes. A volume of 40 µL of proteinase K was added to the mixtures and incubated at 55°C for 30 minutes. After incubation, 200 µL of the binding buffer was added and the samples were placed at 70°C for 10 minutes. A volume (100 µL) of isopropanol was added and the mixtures were centrifuged at 8000 x *g* for 60 seconds. The solutions were transferred into separate high filter tubes with a collection tube and centrifuged at 8000 x *g* for a further 60 seconds.

3.7.4 Washing and elution

The collection tubes were discarded and the filter tubes were transferred into new collection tubes; 500 µL of the inhibitor buffer was added to the filter tubes and centrifuged at 8000 x *g* for 60 seconds. The filtrate in the collection tube was discarded and the filter tubes were transferred into clean collection tubes, where 500 µL of the wash buffer was added to the filter tubes with subsequent filtration via centrifugation at 8000 x *g* for 60 seconds. The filter tubes were then transferred to new collection tubes and centrifuged for an additional 10 seconds to remove any residual wash from the filter tubes. The filter tubes were then placed in sterile 1.5 mL microfuge tubes. A volume of 200 µL of a pre-warmed elution buffer was added to the upper reservoir of the filter tubes and centrifuged further at 8000 x *g* for 60 seconds. The concentration of gDNA was measured using a Nanodrop at 260 nm to determine the concentration of DNA. Raw data obtained is presented in Appendix F, Table F.7 and Table F.12. The eluted DNA was run on PCR following the method described below.

The gDNA extracted was further analysed using qRT-PCR to gain an insight into the microbial composition. The universal bacterial primers and primers of specific species (Table 3-1) were used according to the method described in the unpublished CeBER manual.

Table 3-1: Primers used to determine the microbial species present from the extracted gDNA determined using PCR adapted from (Tupikina et al., 2013)

Microorganisms	Primer	Sequence (5'-3')
Universal bacteria	UniBact	GAC TCC TAC GGG AGG CAG CA
Acidthiobacillus caldus (At. c)	Atc	CGG ATC CGA ATA CGG TCT G
Acidthiobacillus ferrooxidans	Atf	AGG TGG GTT CTA ATA CAA TCT GCT
Leptospirilum ferriphilum strain	LH	GGG GGC CTG AAT AAG GTC A
Acidthiobacillus thiooxidans	Att	GGG TGC TAA TAN CGC CTG C
Leptospirilum ferrooxidans	LT	AAG GGA TAT CGA ACA AAT ATC CCC
Universal archaea	UniArch	TGC TCC CCC GCC AAT TCC
Acidiplasma cupricumulans	JTC/3	AAG CCT AAC TTC AGA AGG CCT G
archaea	JTC1/2	AAG CCT AAC TTC AGA AGG CCT G

CHAPTER 4

RESULTS AND DISCUSSION: ARD CHARACTERISATION

4 RESULTS AND DISCUSSION: ARD CHARACTERISATION

4.1 Introduction

Characterisation of the ARD formation potential of rock wastes centres primarily on the potential for acid generation under extreme chemical and environmental conditions (Price, 1997). The standard static acid-base accounting tests measure both acid neutralising capacity (ANC) and maximum potential to form acidity (MPA) based on mineral sulphide oxidation, with the difference between these values giving an estimate of the net acid producing potential (NAPP) (Plante et al., 2012). In addition, the net acid generation (NAG) test investigates the *in-situ* generation of acidity through the reaction of the rock wastes with H_2O_2. Measurement of the resulting solution pH is used an as an overall indication of ARD potential (Miller, 1997). The standard tests, however, fail to account for the relative rates of acid consumption and acid generating reactions. Furthermore, the action of Fe and S-oxidising micro-organisms on the ARD generation rate is not accounted for in the standard chemical characterisation tests (Hesketh et al., 2010). These may be determined by kinetic tests, such as humidity cell tests. These tests are essential to assess the quality of generated acidic water through progressive analysis of solution pH and conductivity changes as a result of mineral leaching. The test are also useful for providing the rates at which acid generating and acid neutralising minerals are leached form the waste materials. However, these tests are unfavourable due to the long timelines necessary to provide sufficient and quality data (Berry et al., 2015; Parbhakar-Fox & Lottermoser, 2015a).

To address the aforementioned limitations, the Biokinetic test was developed (Hesketh et al., 2010). In the Biokinetic test, the finely divided milled waste rock samples are prepared with the addition of autotrophic basal salt (ABS) solution and inoculated with a standard inoculum (10^9 cell per 150 mL of media) of microbial consortium dominated by iron and sulphur oxidisers such as *Leptospirilum ferriphilum* and *Acidthiobacillus caldus*. Leaching rates and formation of acidity are monitored over the duration of the experiment. The nature of the data collected provides a better understanding of relative rates on both acid neutralisation and generation. Integration of the Biokinetic test results with those obtained from other standardised static ABA characterisation tests, have been the focus of a number of studies (Hesketh, 2010; Opitz et al., 2015) with Biokinetic tests providing for the generation of kinetic data over a shortened time-frame. However, research is still required to ascertain the applicability of the Biokinetic test across a number of different and compositionally differentiated mine waste.

The results reported in this sections highlight mineralogical analysis for the waste rock obtained from XRD analyses. This was followed by static ARD characterisation tests, from which acid neutralising capacity, maximum acid potential, and net acid producing potential results were obtained. The drainage potential of the samples was thereafter classified using NAPP and NAG results. The UCT standard Batch Biokinetic tests results are also presented for both samples studied.

4.2 Aims and objectives

Objectives for this chapter were to use ARD geochemical characterisation tests and UCT standard Biokinetic tests as a tool to aid the interpretation of the potential for ARD generation. This was achieved by:

- Determining the mineralogical composition of the two waste rocks in order to gain an insight into acid consuming and acid generating constituents present in each of the samples;
- Conducting acid-base accounting and net acid generating quantifications in order to estimate the drainage potential under chemical oxidising conditions;
- Predicting the ARD potential of the two waste rocks using a UCT standardised biokinetic test.

4.3 Estimating the ARD potential from the sample mineralogy profile

The mineralogical assessment of the waste rocks provides information of different minerals present within the samples. This information is used to estimate the ARD potential and understand observed results from static and Biokinetic tests. The availability of a significant amount of acid-consuming minerals within the mine waste would mean that a progression of ARD may be neutralised to a certain extent. Alternatively, the presence of a high proportion of sulphide-containing minerals would indicate rapid ARD generation. The mineral compositions of the two samples used in the study were determined by XRD and the results are presented in Table 4-1.The acid generating minerals identified in sample one are pyrite, pyrrhotite and other sulphides, while in sample 2, chalcopyrite, pyrite, galena, and other sulphides, were observed. The common acid neutralising minerals present in high quantities in sample 1 and sample 2 were classified as magnetite, which may also be termed iron oxide/hydroxide and hornblende. Some of the acid-consuming minerals included chlorite, biotite mica and plagioclase.

Carbonate as a rapidly dissolvable mineral in acidic water and this was observed in sample 1. The inert minerals were identified as quartz and kaolinite in both samples.

Table 4-1: Mineralogical composition (%) of the waste rock samples used in the completion of this study following QEMSCAN® analysis

Mineral Sample 1	Composition	Mineral Sample 2	Composition
Pyrrhotite	5.77	Chalcopyrite	1.27
Pyrite	1.20	Pyrite	2.62
Other Sulphides	0.06	Galena	1.70
Carbonates	0.92	Other sulphides	<1.35
Chlorite	1.37	Magnetite	16.45
Fe oxides/hydroxides	33.37	Quartz	39.80
Hornblende	9.63	Hornblende	1.31
Plagioclase – Albite	13.56	Kaolinite	4.84
Biotite	1.67	Mica	21.45
Quartz	26.01	Albite	3.73
Sulphates	0.85	Plagioclase	1.11

Minerals identified from the waste rocks were further classified into acid generating, acid consuming, and inert minerals following the criteria described in Table 2-3.

Table 2-3. According to the results illustrated in Figure 4-1 and Figure 4-2, both samples comprised a similar proportion of acid generating minerals. However, the acid-consuming mineral profile was different between the two samples, with sample 1 presenting a 35.66% acid-consuming mineral profile. This suggests high neutralisation potential, as does the high proportion (51.77%) of gangue material which also contributes to neutralisation due to slow weathering minerals. Sample 2 was found to be dominated by slow weathering minerals (76.17%), with a lower proportion (16.55%) of acid-consuming minerals. These results suggest that sample 1 had a significant amount of acid-consuming minerals which would reduce the rate of ARD generation by increasing the pH. The opposite was observed for sample 2 with a low ANC profile, suggesting minimal increases in the solution pH, which would facilitate a rapid formation of ARD in the environment.

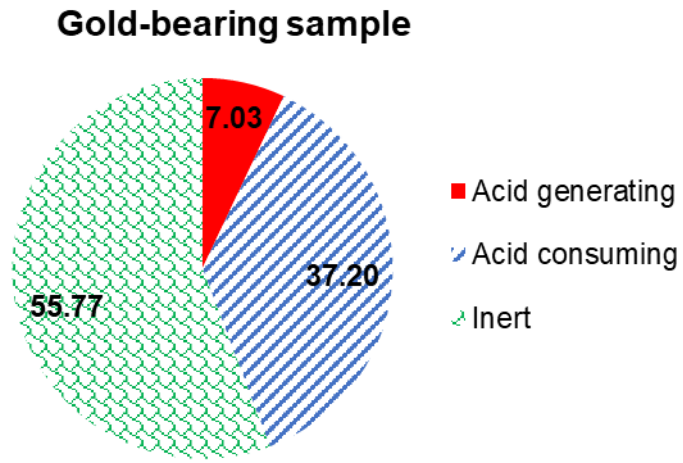

Figure 4-1: Mineral composition of gold-bearing (sample 1) relating to acid generation

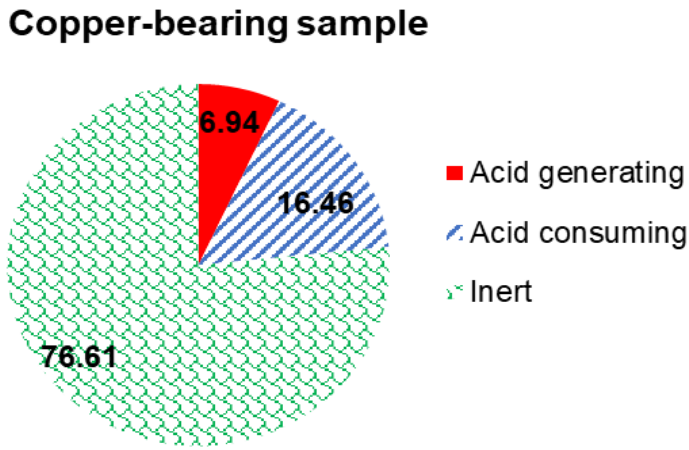

Figure 4-2: Mineral composition of copper-bearing (sample 2) relating to acid generation

4.4 Results of static ARD tests

The ABA characterisation results performed on the gold-bearing and copper-bearing waste rocks are shown in Table 2-2. Both samples had significant NAPP values of 17.0 and 92.9 Kg H_2SO_4/ ton, suggesting the potential of ARD generation. This was expected owing to the high sulphur content of 2.3% and 3.15% for sample 1 and 2 respectively. However, the ANC value obtained for gold-bearing waste rock sample was relatively high (53.2 kg H_2SO_4/ ton), and this was due to the reaction of fast weathering minerals such as calcite and slow dissolving minerals including magnetite which contribute to neutralisation. In contrast, opper-bearing waste rock 2 had less ANC of 3.39 kg H_2SO_4/ton suggesting lack of acid consuming minerals to counteract the acid generated as observed from the mineralogy data**.** To achieve a realistic assessment of the overall acid generating potential of the samples, single NAG test was also conducted. In this test the acid consuming and acid generating minerals reacts

concurrently and provide the overall classification of the mine waste. The net acid producing potential (NAPP) against NAG_{pH} plots were used to classify waste rock samples as shown in Figure 4-3. The NAG_{pH} was found to be pH 2.50 and pH 2.63, for sample 1 and 2, respectively, suggesting the potential of ARD generation. The NAG pH of the two samples was found to be similar due to similarities in the acid generating minerals Figure 4-1 and Figure 4-2, although the NAPP values were determined to be dissimilar due to the high ANC content in the gold-bearing waste rock, which would consume the acid generated.

Table 4-2: Static results for ARD characterisation of waste rocks

Waste Sample	Sulphur Grade [%]	MPA [kg H_2SO_4/ton]	ANC [kg H_2SO_4/ton]	NAPP [kg H_2SO_4/ton]	NAG pH	ARD Classification
Sample 1	2.3 ± 0.0	70.2 ± 0.7	53.2 ± 1.8	17.0 ± 1.9	2.50 ± 0.0	Potentially acid forming
Sample 2	3.15 ± 0.1	96.3 ± 1.7	3.39 ± 0.2	92.9 ± 1.7	2.63 ± 0.0	Potentially acid forming

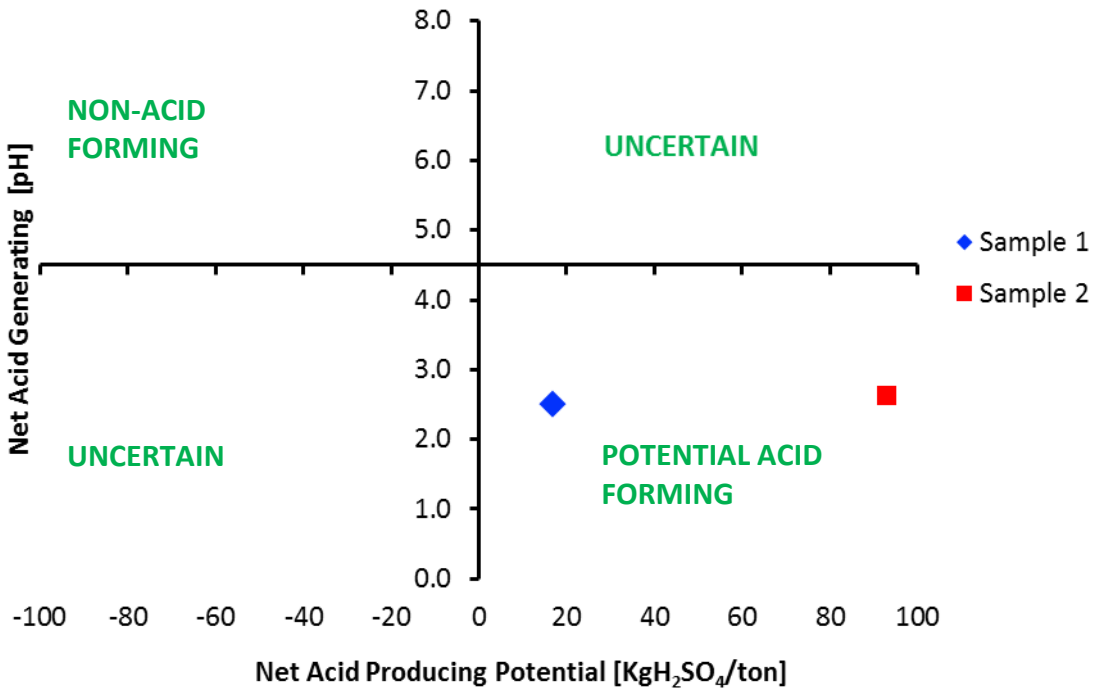

Figure 4-3: Classification of ARD potential for sample 1 (gold-bearing) and sample 2 (copper-bearing) based on NAG and NAPP pH values

The static tests provide a rapid and easy classification tool for the characterisation of ARD potential of each sample; (Parbhakar-Fox & Lottermosesr, 2015. Stewart et al., 2006). However, the limitations of the static tests include the lack of information on the rate of acid formation or neutralisation, as previously highlighted (Harrison et al., 2010; Hesketh et al., 2010) with overestimation being the primary challenge, as the use of synthetic chemicals is not a representation of conditions found in waste heap environments. These tests also do not take into consideration the impact of microbial activity in regenerating the reactants which facilitate the rate of ARD generation in the environment. Static tests also do not distinguish between the various acid consuming minerals and their neutralizing potentials (Coastech Research, 1991). Such limitations can be addressed using the UCT standard Biokinetic test for classification validation of rates associated with ARD generation under microbial mediated conditions.

4.5 ARD characterisation of samples using the standard biokinetic test

ARD generation from the two waste rocks was further evaluated under standard Biokinetic test conditions, which determine relative rates of acid-consuming and acid generation reactions in the presence Fe^{2+} and S oxidising micro-organisms. The potential for ARD generation was investigated under inoculated and abiotic conditions. The acid formation and acid neutralising potential produced were monitored over the experimental run determined through pH, Eh, Fe^{2+}, Fe^{Tot} and sulphates measurements of the leachates from experiments conducted separately using the waste rock samples.

The pH and redox potential profile for sample 1 is presented as a function of leaching time in Figure 4-4 (A) and (B). The pH of the leachate increased slowly during the first 6 days from 2.5 to 4.5 and to pH 5.5 for inoculated and no-inoculated flasks respectively. The pH increases suggested the dissolution of calcite with neutralizing potential from day 1 to day 5, as presented in Table 3.1. This was followed by a subsequent decrease in pH until day 20, indicating reactions associated with acid generating minerals such as pyrite, and thus the precipitation of ferric iron which leached the mineral into solution. Redox potential as shown in Figure 4-4 (B) decreased due to the dissolution of acid-consuming minerals. This was supported by an increase in solution pH from day 0 to day 3 and 7 for inoculated and non-inoculated experiments respectively. A long lag period of 20 days in redox potential with minimal significant difference between inoculated and non-inoculated samples suggested a lack of oxidation of ferrous to ferric iron. After 20 days of the experiments, the redox potential

increased to an exponential degree by day 30, suggesting conversion of ferrous iron to ferric iron. These observations indicated activity of the mineral-associated microbial activity. This corresponds with a slow decrease in pH until it stabilizes around pH 2 by day 30, and a redox potential which was unchanged at 650 mV.

The rates of change in ferrous concentrations and total iron concentration were assessed to gain an insight into the activity of Fe-oxidising micro-organisms between inoculated and non-inoculated samples, as highlighted in Figure 4-5 (A) and (B). The ferrous iron concentration increased over the first 20 days for both inoculated and non-inoculated experiments, reaching the highest concentration of 456 and 250 mg/L respectively. These results are supported by an increase in the total iron concentration in the leachate (Figure 4-5(B)). This was attributed to mineral oxidation, which culminated in a drastic decline of ferrous iron prevalence as observed on day 21, which suggested that the rate of ferrous oxidation is determined by the leaching of Fe^{2+} from the mineral.

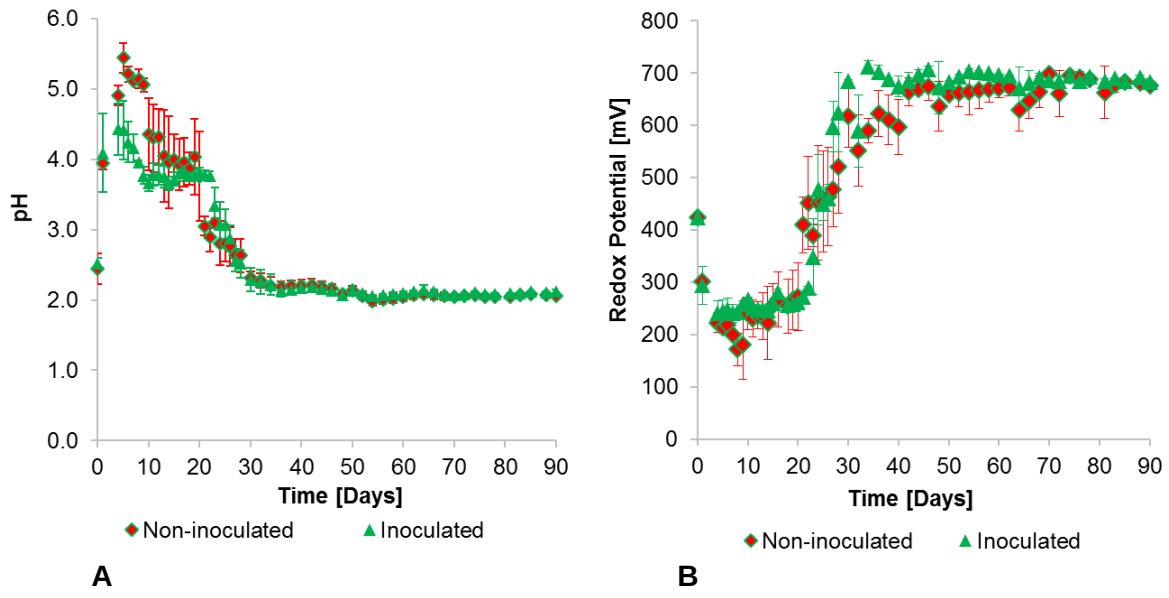

Figure 4-4: Leachate pH (A) and redox potential (B) for inoculated and non-inoculated Biokinetic tests performed on sample 1

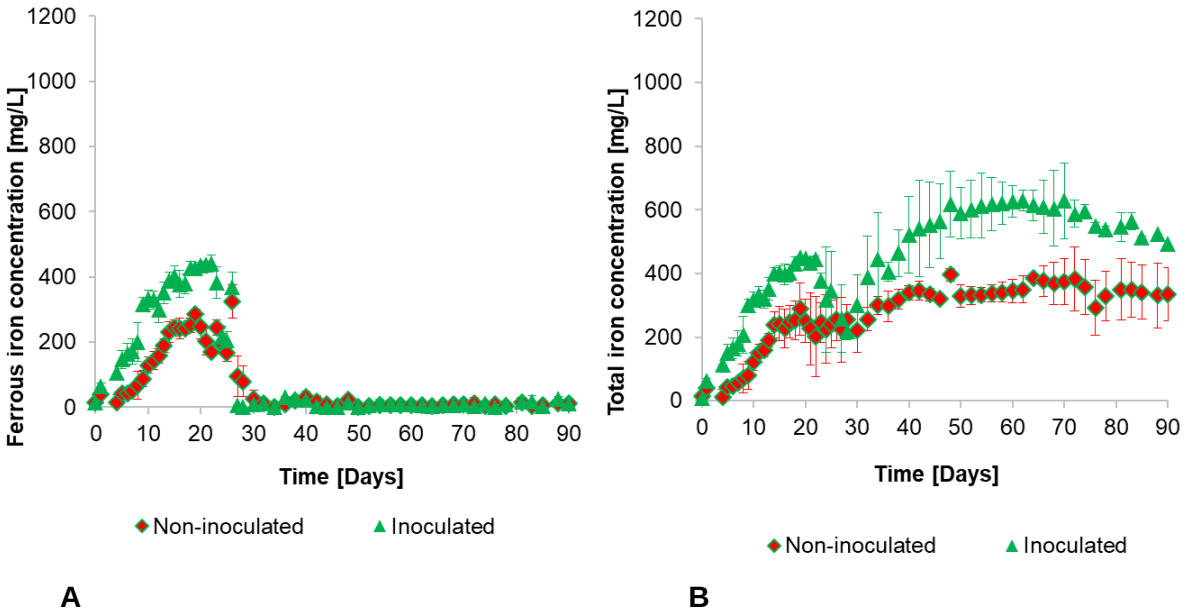

A B

Figure 4-5: Cumulative ferrous iron concentration of (A) and total iron concentration (B) for standard Biokinetic test on sample 1

There was minimal significant differentiation between the inoculated and non-inoculated samples. This showed that the microbial community used as an inoculum could not strongly influence the high ANC, which increased the pH above the optimum pH of Fe and S-oxidising micro-organisms. As the redox potential increased above 650 mV, it was plausible to hypothesise that the oxidation of ferrous iron to ferric during leaching was due to the high ANC in sample 1, which had a negative impact on the inoculum. Sample 2, with a low ANC, was used to compare the effectiveness of Fe and S oxidising micro-organisms for standardisation of the Biokinetic test and the data is presented in the subsequent section. A different mineral (copper-bearing waste rock) with a low ANC was used on the Biokinetic test in order to verify the aforementioned results for standardisation purposes of the Biokinetic test.

4.6 ARD characterisation of copper-bearing sample using the UCT standard Biokinetic test

The pH curve of the feed sample and redox potential for sample 2 are presented in Figure 4-6 (A) and (B). An initial increase in pH of the feed sample was observed in all flasks from day 1 to 14 due to the easily leachable components of the minerals with a neutralising capacity of the mineral, namely chlorite. The non-inoculated samples increased up to a pH of 2.63 while the pH of the inoculated flasks increased to 2.50. There is an insignificant difference between the two conditions studied due to the lack of acid neutralising capacity of

the samples. The pH remained stable between 1.8 and 2.10 from day 50 to 90, indicating that acid generating minerals (sulphide-containing minerals) dissolved at a faster rate than acid neutralising minerals within the feed sample. Furthermore, the redox potential for both inoculated and non-inoculated tests was initially at ~400 mV, and subsequently reduced to 340 mV as results of the readily leachable mineral component with buffering abilities, as indicated by a rising of the leachate pH. The reduction in redox potential correlated with the initial increase in solution pH. After day 4, a gradual increase in redox was observed. This was attributed to biological leaching since an ideal pH was maintained in the flasks. A microbial lag period of 12 days was observed in non-inoculated tests with redox potential reaching 650 mV thereafter, suggesting biological leaching as result of native microbial community associated with the samples.

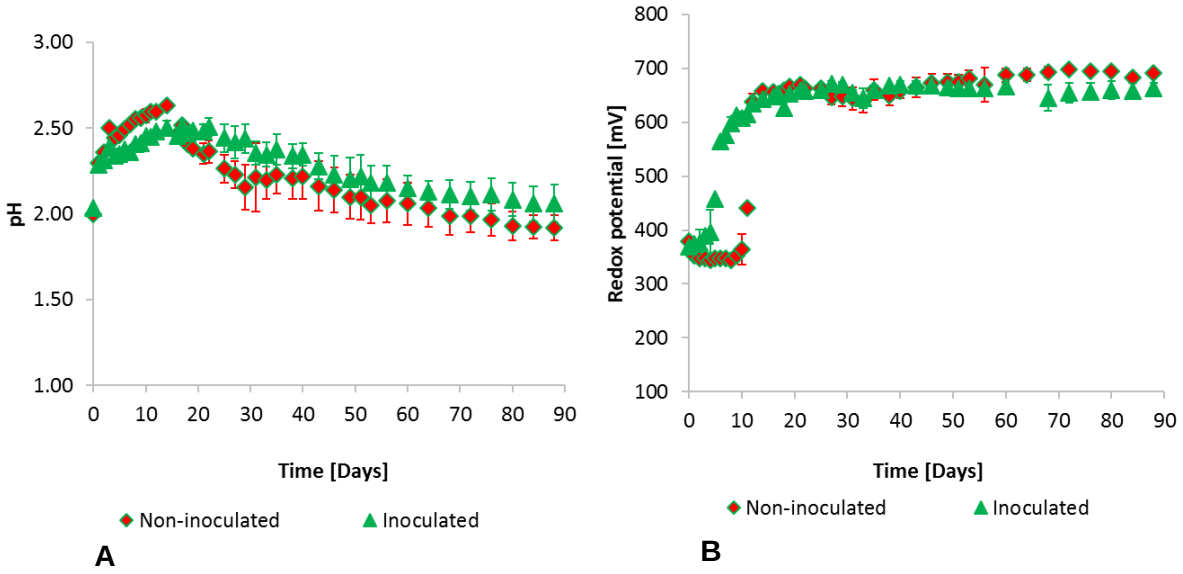

Figure 4-6: pH (A) as a function of time and redox potential (B) on the Biokinetic test for sample 2

The ferrous iron concentration profiles provided information on the leached Fe-bearing minerals, including pyrite. The concentration of ferrous iron increased from 0 to 60 and 100 mg/L, determined to be a maximum, on day 2 and day 7, for inoculated and non-inoculated samples respectively. Subsequent decreases in ferrous iron concentration below 20 mg/L were observed after day 3 and 7 for both inoculated and non-inoculated tests respectively. The low ferrous oxidation in the non-inoculated samples was solely attributed to the absence of an inoculum; however, on day 9, ferrous concentration declined, coinciding with an increase in redox potential. This suggested activity of the inherent microbial community when the waste material was not sterilised.

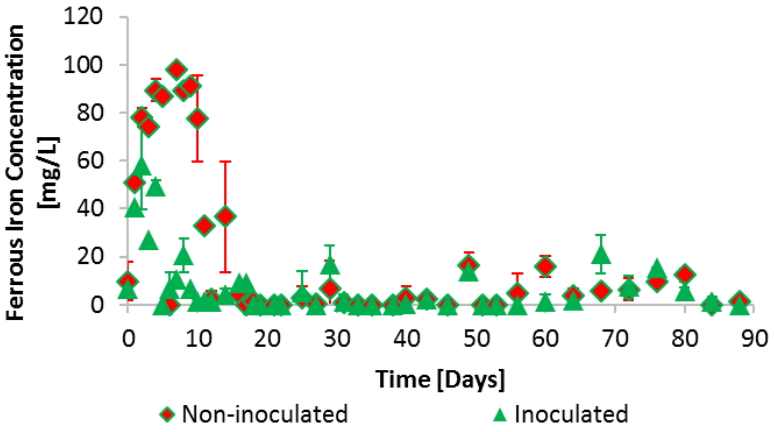

Figure 4-7: Accumulated ferrous iron concentration on standard biokinetic test for sample 2

4.7 Summary

The acid consuming and acid generating minerals identified from the waste rocks were investigated using different ARD characterisation tests. The ABA tests indicated that sample 1 with, net acid producing a potential of 17.20 Kg H_2SO_4/ton, was classified as potential acid forming, while sample 2 was found to be acid forming with a NAPP of 92.3 Kg H_2SO_4/ton. However, these tests may overestimate the ARD potential due to the use of synthetic and inorganic chemicals such as hydrochloric acid, while providing minimal information on the microbial activity as well as relative rates of ARD generation, conditions which are not a representation of environmental conditions. To address the aforementioned challenges, Biokinetic tests were performed to complement static test results under the influence of microbial consortia for better characterisation of the waste rocks.

Comparison of the two samples provided an illustration of the effect of the neutralising capacity on the results of the Biokinetic test. The neutralising potential of the samples differed in amount and composition between the two samples. Whereas sample 1 contained fast- (calcite), intermediate- (chlorite) and slow-weathering minerals (magnetite), the neutralising potential of sample 2 was governed predominately by slow-weathering magnetite. The presence of acid-soluble sulphide minerals, such as chalcopyrite and galena, within sample 2, however, also contributed to the neutralisation of the acidity within the Biokinetic tests. Both waste samples classified as potentially acid-forming (PAF) following standard acid-base accounting classification tests, with the potential for acid formation greater than the capacity for its neutralisation for both samples. The differences in the overall neutralising potential, may be observed from the pH profiles of the tests performed on the two samples. The greater neutralising potential, specifically the fast-weathering carbonate minerals, resulted in a greater initial increase in solution pH for the tests performed on

sample 1. This initial dominance of the acid neutralising mineralogy on solution pH over the initial 15 days is further illustrated by the lack of substantial difference between the pH profiles for the inoculated and non-inoculated tests for both samples. This is in contrast to the differences observed in the concentrations of the sulphide oxidation products, the iron and sulphate concentrations over the same time period.

According to the results obtained from the standard Batch Biokinetic test for sample 1, there was minimal effect of inoculum size on the Biokinetic test except for samples inoculated with 10^{10} cells. However, the effectiveness of the microbial community used as an inoculum was observed for sample 2 with low ANC. The difference observed between the samples under Biokinetic test conditions was predominantly influenced by the composition of the mineral profiles in the samples, as suggested by the complimentary static test results.

To validate these observed results between inoculated and non-inoculated samples using the Biokinetic test, further research was necessary to investigate whether the inoculum size affected the ANC determined in sample 1. This can be achieved by suppressing the ANC of the mineral in a sample through the addition of a dilute sulphuric acid solution to sustain and the control the pH to under 2.0.

CHAPTER 5

RESULTS AND DISCUSSION: BIOKINETIC TESTS

5 RESULTS AND DISCUSSION: BIOKINETIC TESTS

5.1 Introduction

The Biokinetic test developed by Hesketh (2010) offers an innovative and cost-effective alternative compared to the standard kinetic tests. This new emerging method gives a valuable insight into the rate of acid consuming and acid-forming reactions in the presence of microbial population within ninety days (Broadhurst et al., 2015; Opitz et al., 2015; Hesketh et al., 2010). However, the Biokinetic test is still in its initial stages of development and certain parameters are not sufficiently well-defined to obtain a standard approach that can be applied to different waste ores. Hence, the objective of this part of the study was to use Batch Biokinetic Tests to investigate the required inoculum size of Fe and S oxidising microorganisms for effective and reproducible performance.

The effect of inoculum size for standardisation of the Biokinetic Test, experiments were conducted under two different scenarios, namely in non-controlled pH and pH controlled tests. The detailed methodologies are described in Appendix B. For pH-controlled experiments, the pH of the experimental flasks was adjusted using a 0.5M sulphuric acid solution until the pH remains close to pH 2. The volume of sulphuric acid consumed was recorded while the other set of experiments, the pH was not controlled. To ensure reproducibility and consistency of the results, a triplicate set of shake flasks were ran simultaneously with the pH, redox potential, Fe^{2+}, Fe^{3+} and SO_4^{2-} being measured to understand the impact of the initial cell concentration on the test. The microbial species present at the mid-leach and end of the experiment, were determined using qPCR as described in section 3.7 and in appendix E.

This chapter reports on the influence of inoculum size on the Biokinetic tests under non-controlled pH and non-controlled pH conditions. Microbial speciation data for sample 1 was analysed on day 90 under non-controlled pH, and on day 45 and day 90 for controlled pH experiments as presented in this chapter.

5.2 Aims and objectives

Objectives for this chapter were to assess the influence of inoculum size on the UCT standard Biokinetic test as a tool to aid the interpretation of the potential for ARD generation. This was achieved by:

- Determining the effect of inoculum size of Fe^{2+} and S oxidising micro-organisms on the Biokinetic test profiles for gold and copper waste rocks;
- Determining the effect of non-controlled pH and controlled pH;
- Using molecular techniques to determine the microbial community changes at mid-leach and at the end of the experiments.

5.3 Effect of inoculum size on the Biokinetic test using sample 1

Since a high neutralising capacity of the minerals in sample 1 was observed to cause a negative impact on the inoculum, by controlling the pH in the Biokinetic test, variations in pH could perhaps be minimised, with a positive outcome being stabilisation, and thus accurate characterisation of ARD formation potential. Batch Biokinetic tests simulating long-term weathering in a mine waste rock disposal environment were inoculated with inoculum sizes ranging from 10^7 to 10^{10} of mixed cultures containing iron and sulphur-oxidizing micro-organisms, primarily *L. ferriphilum* and *At. caldus* in 150 mL of ABS solution at pH 2. These experiments were carried out under three different conditions: pH controlled/non-inoculated, pH controlled/inoculated and non-controlled pH/non-inoculated. The tests were carried out at 37 °C in an orbital shaker (150 rpm) for 90 days. For pH controlled tests, the solution pH was controlled by the addition of 0.5M H_2SO_4 to pH 2 with the volume of acid added being recorded. The redox potential, pH, and Fe assay were used to quantitatively assess the effect of initial cell concentrations and determine the microbial speciation, and thus changes at different times during the experiments.

Under non-controlled pH Biokinetic tests (see

Figure 5-1 (A)), the results showed that there was an insignificant effect attributable to inoculum on the starting solution pH as a result of the order of magnitude differences in inoculum concentrations used. An initial increase in pH was observed across all flasks after three days of the test. The pH increased from pH 2.4 to approximately pH 5, with an associated decrease in redox potential to below 300 mV (

Figure 5-1(A)), attributed to ferric iron precipitation. For the non-inoculated flasks, a similar increase in solution pH was observed, with a higher pH value of 5.4 being reached. The bulk mineralogical assessment as reported for sample 1 was dominated by 35.66% of acid-consuming minerals such as calcite, magnetite and biotite, culminating in an increase in the leachate pH, which was attributed to the acid neutralising capacity of the waste rock. Thereafter, a gradual decrease in the pH in all flasks was observed to plateau at pH ~4.0 until day 20, suggesting the dominance of the acid generating reactions over acid neutralizing reactions. The solution pH of the highest inoculum concentration (10^{10}) decreased from pH 4 to pH 2 on day 15. This indicated microbial influences at this inoculum concentration, corresponding to an increase in redox potential (Figure 5-4(A)) sooner than the other flasks with a lower inoculum size.

For the pH controlled Biokinetic test, minimal differences in the pH profiles for the inoculated and non-inoculated flasks was observed (

Figure 5-1(B)). This was attributed to the minimal microbial concentration influencing the oxidation process rather than the chemical leaching of the waste material. The constant increase in pH was observed in all flasks, prior to a decrease over the initial 15 days before reaching a plateau at a pH of 1.6 for the duration of the experiments. The plateau in the solution pH, in conjunction with the oxidising environment within the test flasks, suggested high sulphide oxidation due to biological reactions. These results indicated that there was no effect of the acid neutralizing mineral profile of the samples under pH controlled test conditions,. Therefore, the rapid calcite dissolution on initiation of the experiments was counter balanced through drop-wise addition of the standardized H_2SO_4 acid, and subsequent acid generating minerals preceded at a faster rate to' reduction of the solution pH.

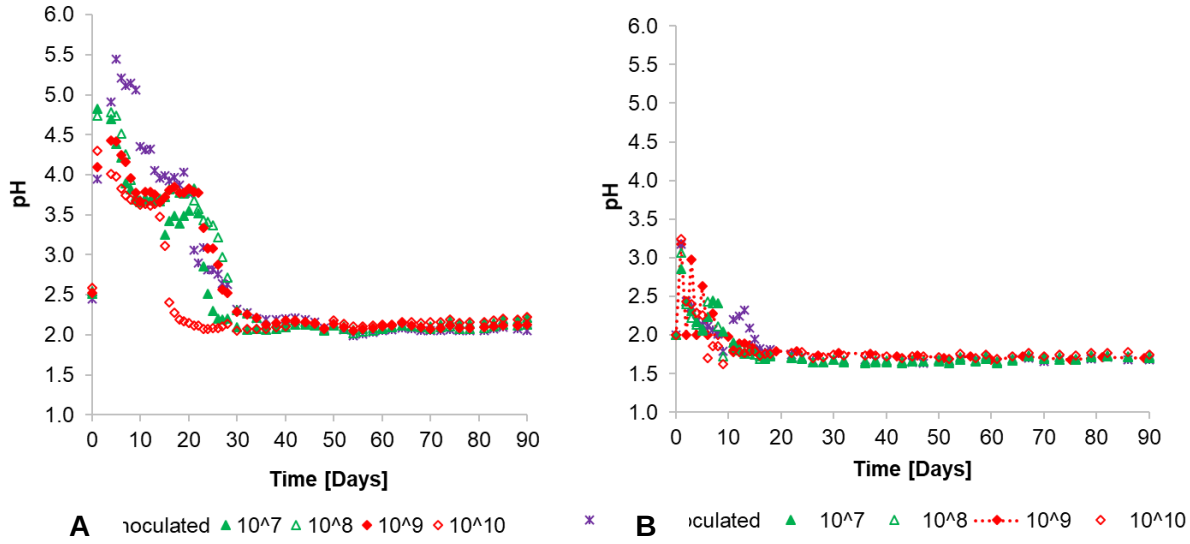

Figure 5-1: Solution pH profile of non-controlled pH (A) and controlled pH (B) under Biokinetic test conditions

The net accumulated hydrogen ion concentration corresponding to the above pH values as observed in

Figure 5-2 (A) and (B) for non-controlled pH and controlled pH Biokinetic tests, respectively, confirmed the accumulation of hydroxide ion and hydrogen ions for each inoculum size used. Hydrogen ion concentrations declined on day 1 and remained constant until day 15 to 20, suggesting an accumulation of hydroxide ions during the period in which minimal pH decreases were observed. This was attributed to the dissolution of fast weathering minerals with acid consuming abilities. Thereafter, an increase in the hydrogen ions was observed, indicating an accumulation of hydrogen ions. Under pH controlled Biokinetic test conditions, the concentration of hydrogen ions increased exponentially for all different inoculum size test experiments, and stabilised between day 20 and day 45. This was due to the suppression of ANC by addition of a standardised sulphuric acid solution. From day 45, the concentration of hydrogen ions decreased significantly from above 0.060 to 0.04 mole/L. The net accumulation of H^+ for pH controlled Biokinetic tests increased the concentration of H^+ when compared to non-controlled pH Biokinetic tests. This was due to accelerated leaching of sulphide minerals.

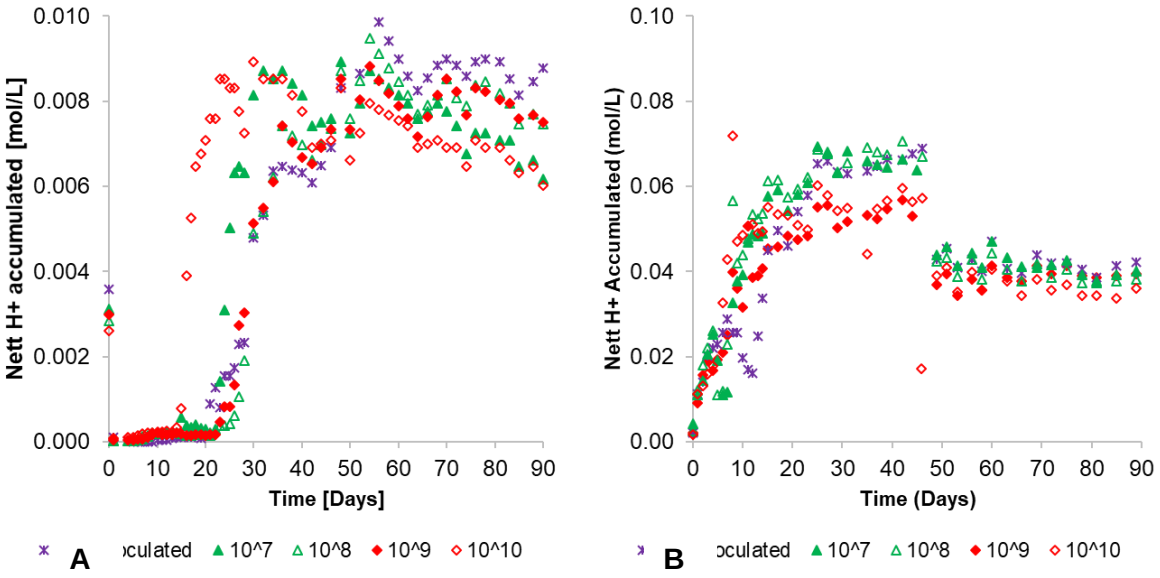

Figure 5-2: Net accumulated H^+ ions as measured in solution in the non-controlled pH (A) and pH-controlled Biokinetic tests (B)

The addition of 0.5M sulphuric acid maintained a lower pH environment such that the microbial community might facilitate the regeneration of ferric iron which leaches the waste rock at a faster rate. As a result of this, pH controlled conditions, even when using differentiated inoculum sizes, were found to have an effect on the mineral leaching in the Biokinetic test profile. There was a significant difference in terms of acid consumption between inoculated and non-inoculated shake flasks, with non-inoculated samples having a high acid consumption rate (Figure 5-3), which may have been due to lack of acidophilic microbial populations which facilitate the rate of Fe^{2+} oxidation. All inoculated samples had a similar profile for acid consumption, except for the flasks inoculated with 10^{10} cells/mL, for which lower acid consumption was observed. The lower acid consumption might be due to the presence of a significant concentration of iron and sulphur oxidising micro-organisms which enhanced the onset of ARD generation. The consumption of acid followed the order of different inoculum sizes used, with the highest inoculum having a lower acid consumption, and the lower inoculum size tests having acid consumption higher than the other inoculum sizes. The differences between other inoculated flasks and those containing 10^{10} were consistent with what was observed for leachate pH changes.

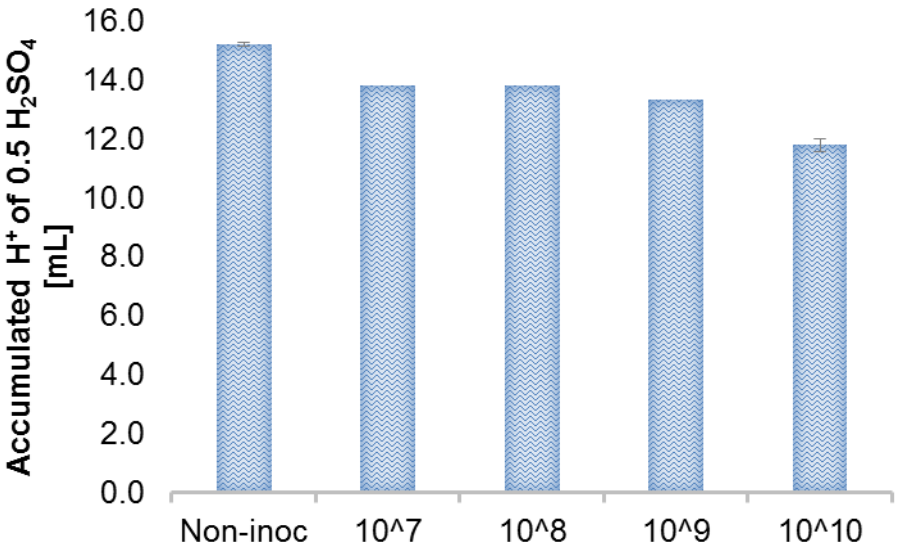

Figure 5-3: Cumulative addition of 0.5M H_2SO_4 for the control of flask pH to pH 2.0 for experimental flasks inoculated with different initial cell concentrations. Error bars represent the standard deviation of the mean (n=3).

The increase in solution pH as a result of readily soluble minerals with buffering ability for the first 3 to 5 days Figure 5-4) was mirrored by the decline in redox potential from 425 mV to 300 mV (Figure 5-4). The rate of increase of the redox potential was similar for all inoculated flasks except for flasks containing a 10^{10} cell inoculum which increased only after day 14, while others increased gradually from 300 mV to 700 mV over a 30 day period. The redox potential of the non-inoculated flasks also increased from day 20, albeit more gradually, reaching 600 mV on day 30 and 700 mV on day 70, with stabilisation being observed thereafter. These redox potential levels in the non-inoculated controls suggested the presence and activity of inherent Fe-oxidising micro-organisms in the samples used (without sterilisation) within the non-inoculated flasks.

In the pH-controlled Biokinetic tests, the ANC of the mineral was counter-balanced by the addition of a standardized acid such that microbial community accelerated the rate of ARD generation over a shortened time; whereas, in the non-controlled pH Biokinetic tests, inoculum concentration was greatly affected by the significant quantity of ANC, resulting in a significant increase of leachate pH. The rate of increase in the redox potential of the experimental flasks in relation to the initial inoculum concentration influenced redox potential development, with higher microbial concentration tests reaching a redox potential of 700 mV sooner than those flasks with a lower inoculum concentrations. A 10-day lag period was observed for the non-inoculated flasks before the redox potential increased to 700 mV by day 15. Thereafter, the redox potential remained above 700 mV for all test flasks for the

remainder of the experiment, indicating that the oxidative environment in the Biokinetic flasks was due to the presence of elevated ferric iron concentrations.

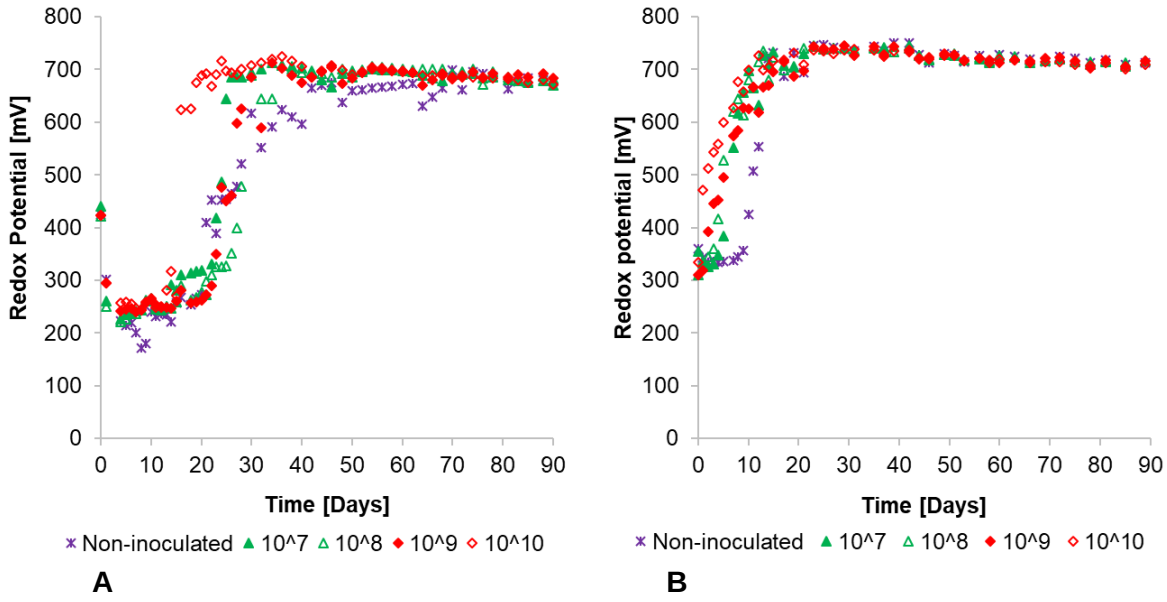

Figure 5-4: Redox potential of non-controlled pH (A) and controlled pH (B) for sample 1

The rate of change in ferrous concentrations and the total iron concentration quantified provided an insight into whether the activity of different inoculum cell concentrations in inoculated and non-inoculated shake flasks could influence such concentrations. Generally, the comparison of the ferrous iron and total iron concentrations confirmed the time period at which significant activity of the Fe-oxidising micro-organisms occurred Figure 5-5. In all flasks, an increase in ferrous iron concentration was observed over the first 10 days, suggesting leaching of sulphide-bearing minerals, such as pyrite observed in the mineralogical assessment. In all inoculated flasks except those inoculated with 10^{10} cells, the Fe^{2+} concentration continued to increase, albeit at a slower rate, to more than 500 mg/L Fe^{2+} before the onset of ferrous iron oxidation resulted in its depletion. In the flasks inoculated with 10^{10} cells, the ferrous iron concentration plateaued at a lower concentration 350 mg/L, presumably due to iron cycling and perhaps absorption by the high cell concentration, prior to an observable decrease from day 13, and depletion by day 16. The rapid increase in the redox potential for the flasks inoculated with 10^{10} cells accelerated the rapid decrease in the ferrous iron concentration under these conditions. For the other flasks, the rate of increase in ferrous iron concentration up to day 20, and the subsequent decrease in ferrous iron concentration thereafter, were similar to those observed for a higher inoculum concentration. The increase in ferrous iron concentration was delayed in the non-inoculated flasks, increasing to 240 mg/L on day 15, i.e. approximately half the value of that attained in the

inoculated flasks, due to iron cycling prior to natural proliferation of resident microbial species in the unsterilized ores used. The decrease of Fe^{2+} was evident from day 25, with depletion being observed by day 30, and with ferrous iron accumulated in the system hypothesised to arise from the further dissolution of Fe-bearing minerals in the leachate.

The ferrous oxidation rates of inoculated shake flasks occurred in the order of the initial inoculum concentrations, with the highest inoculum concentration facilitating ferrous oxidation rates within the 24 hours, and with others having a longer lag phase for ferrous oxidation rates. These results corresponded with a rapid increase in total iron concentration for tests having a higher oxidisation rates, with ferrous iron concentration reaching a high ferric iron concentration of ~850 mg/L on day 9. This was most probably due to mineral oxidation and drastic decline of ferrous iron suggesting microbial action (Figure 5-5 (A) and (B)), a phenomenon which occurred at later stage for non-inoculated tests. Furthermore, after 11 days of experimentation, ferrous concentration depleted for both set of tests. This suggested that the metabolic mechanisms of both iron and sulphur oxidising micro-organisms was high, with iron oxidisers embedded in the waste rock facilitating ferrous oxidation within the tests.

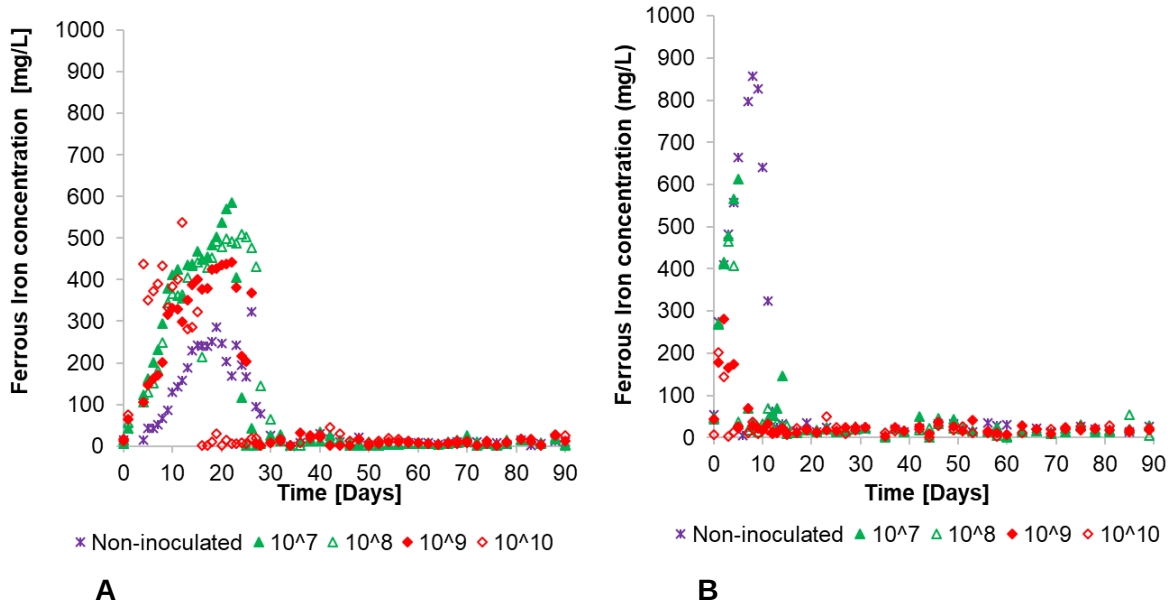

Figure 5-5: Ferrous iron concentration generated in Biokinetic test for sample 1 under non-controlled pH (A) and controlled pH (B)

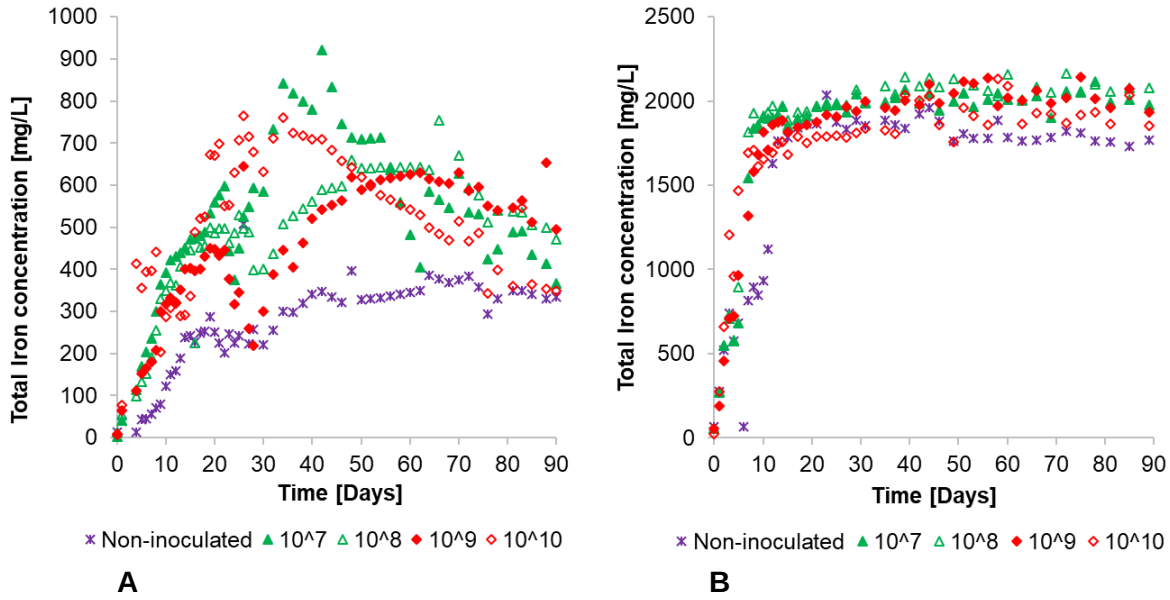

Figure 5-6: Total iron concentration of the Biokinetic test for sample 1 at non-controlled pH (A) and controlled pH (B)

Figure 5-7). These low sulphate concentrations observed at the beginning of the experiments coincided with a high pH, revealing a lack of accumulated sulphide minerals from waste rock samples. Sulphate concentrations increased gradually until day 40, revealing dissolution of acid generating minerals such as pyrite, as this correlated with a reduction in pH. This was followed by a decline, suggesting the ensuing precipitation of the sulphates. Furthermore, a constant concentration level of the sulphates was observed from day 50 to day 70, followed by a subsequent decline thereafter for samples inoculated with 10^7 to 10^{10} cells. By the end of the experiments, similar sulphate concentrations were observed within the Biokinetic test flasks, irrespective of the initial inoculum concentration. This suggested a depletion of available sulphurous species in the waste rock used, due to micro-organisms or oxidation facilitating species in solution, including a consequential precipitation indicated by a yellow bow within the test solutions. This might have coated the mineral and inhibited further oxidation of the remaining sulphides in the waste.

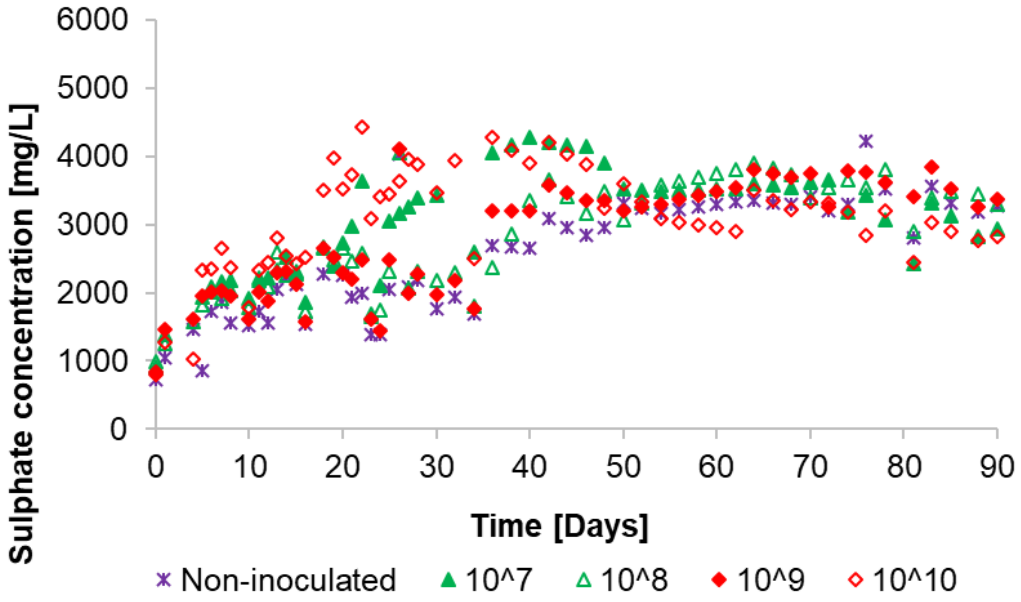

Figure 5-7: Sulphate profile for non-controlled pH on sample 1

The qRT-PCR used in this study to analyse the composition of the inoculum and microbial composition over time, i.e. at mid-leach, day 45, and at the end of the experiment, demonstrated species variations, and thus changes in the microbial composition, as shown in Figure 5-8. Genomic DNA (gDNA) extraction was taken from the inoculum and samples at mid-leach (day 45), and the end of the experiment (day 90) for the pH controlled Biokinetic tests. The DNA was extracted using a procedure described in section 3.4. As shown in Figure 5-8, the inoculum used in this study was dominated by *L. ferriphilum* and *A. caldus,* and insignificant amounts of archaea species. The inoculum also contained a significant concentration of unknown bacteria that could have consisted of sulphur oxidising bacteria such as *Salfobacillus acidophilus* and other iron oxidisers. The non-inoculated samples were composed of a nearly equal proportion of *L. ferriphilum*, *A. caldus*, unknown bacteria and minute quantities of unknown archaea. Additionally, equal distributions of *L. ferriphilum* and *A. caldus* present in small quantities were observed in 10^8 and 10^9 at mid-leach (day 45), together with a dominance of archaea species, *A. thermoplasma,* a minute quantity of *A. cupricumulans*, and unknown bacteria. The inoculum was dominated by a known quantity of bacterial species, whereas the leach solutions showed a significant increase in archaea species. This could be due to the insufficient substrate, or build-up of by-products in the tests. Tests comprising 10^{10} cells indicated better performance in solution chemistry due to their proportion in *A. caldus*. It was noteworthy that microbial composition was differentiated under different test conditions; in the non-controlled pH Biokinetic test, *A. caldus* and *L.*

ferriphilum decreased due to unfavourable pH conditions. Additionally, the speciation of the microbial community over a prolonged test might have been distorted due to insufficient substrates, which could have entrenched certain challenges.

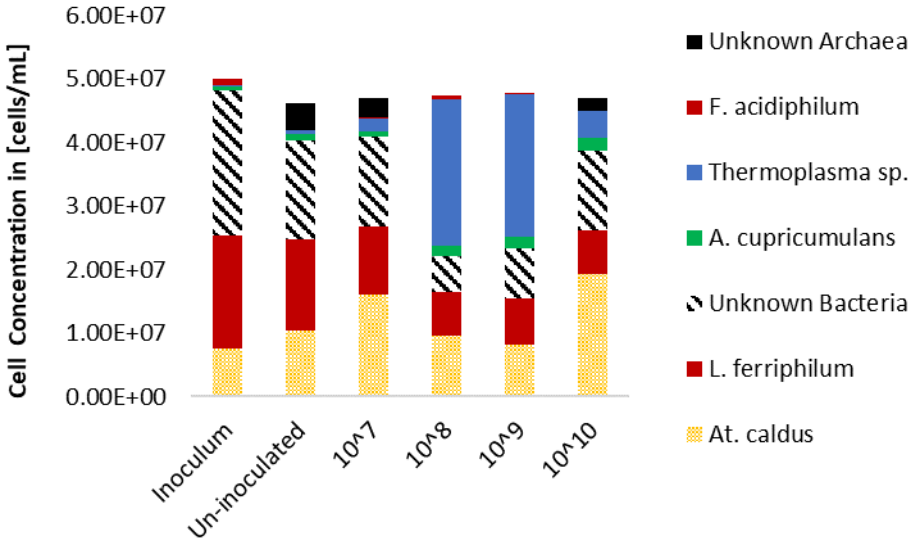

Figure 5-8: The microbial speciation determined at the mid-leach (day 45) of the pH controlled Biokinetic tests in terms of cell concentration (y-axis) as a function of initial cell concentrations

The microbial phase was further studied at the end of the test stage of 90 days, i.e. the cessation of the experimental tests. At this point, the microbial biomass was collected and DNA extracted for qPCR analysis as prescribed by Turpikina et al., (2013). The microbial copy numbers, presented in Figure 5-9 as a function of the test conditions, were evaluated. In the data, “other bacteria” represented a differentiation between the copy numbers determined using a UniBact primer and *Ferriphilum* and *A. caldus* primers, whereas other archaea represented by the difference between the copy numbers determined using the UniArch and *A. cupricumulans* primers. This data demonstrated the low copy numbers (of the order of 10^6) relative to the inoculum concentrations used. Furthermore, the dominant microbial species in these Biokinetic tests varied substantially from those observed in the inoculum used.

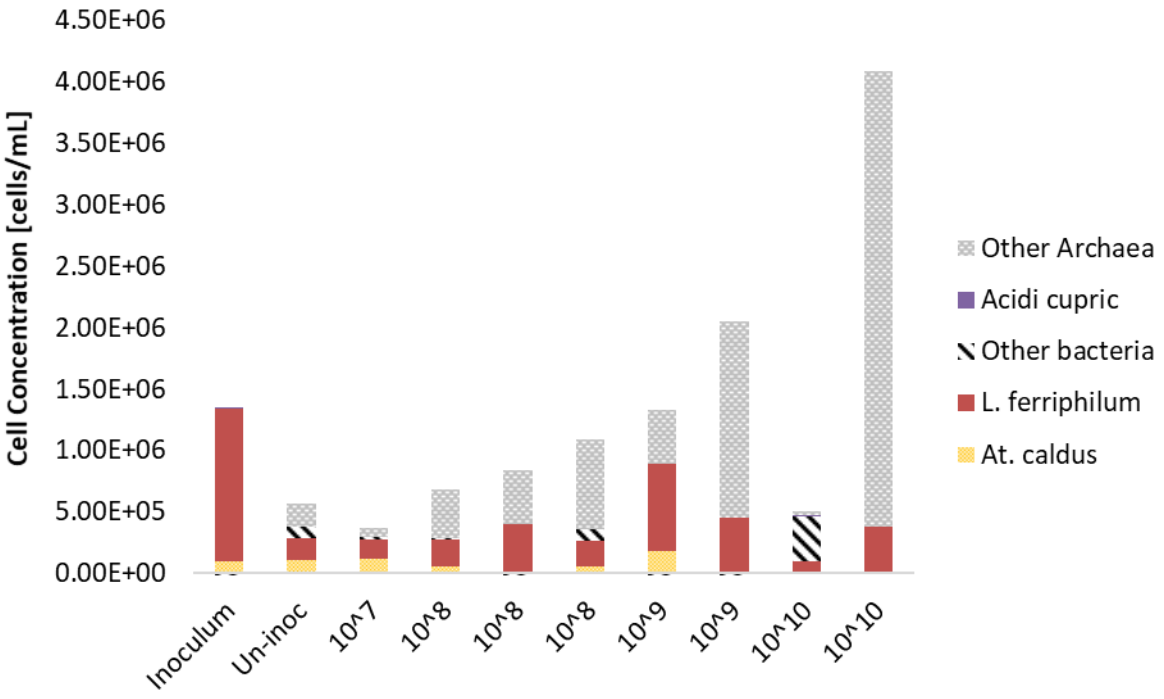

Figure 5-9: Microbial speciation determine on day 90 (end of experiment) in terms of copy numbers

Overall, the cell concentration in the planktonic state indicated a significant decline compared to the inoculum after 110 days of the tests. This could mean that as soon as the substrate (ferrous iron) was depleted, cell death occurred in the test systems. The composition of *A. thermoplasma* and *A. cupricumulans* was noted to increase slightly due to ideal pH conditions of 1.0-1.2, as shown in Figure 5-10, while the *A. caldus* and unknown bacteria decreased with *L. ferriphilum* not being detected. The presence of *A. caldus* throughout the experiment showed its important role as a sulphur-oxidising microbe during ARD generation, although lower cell concentrations were observed towards the end of the experiment. *A. cupricumulans* species were present throughout the experiment at lower concentration relative to other species, indicating that *cupricumulans* species could be one of the species serving as Fe and S-oxidising micro-organisms in the consortia, albeit in small numbers. This was probably due to the non-ideal pH conditions, as the species function optimally at pH 1.0 - 2.10. The *A. caldus* concentration depletion was considered a consequence of other Fe and S scavengers and the accumulation of inhibitory by-products within the tests, which might have led to non-detectable quantities of the species compared to those used in the inoculum. *A. thermoplasma* was not detected in the inoculum, although it was detected in the non-inoculated samples, suggesting a possibility of the species being

native to the waste ore. It is essential to note that as soon as the substrate became limited (Fe^{2+}), the inoculated microbial community disappeared, with microbial species endemic in the environment from which the ores were taken, especially archaea, becoming a dominant species.

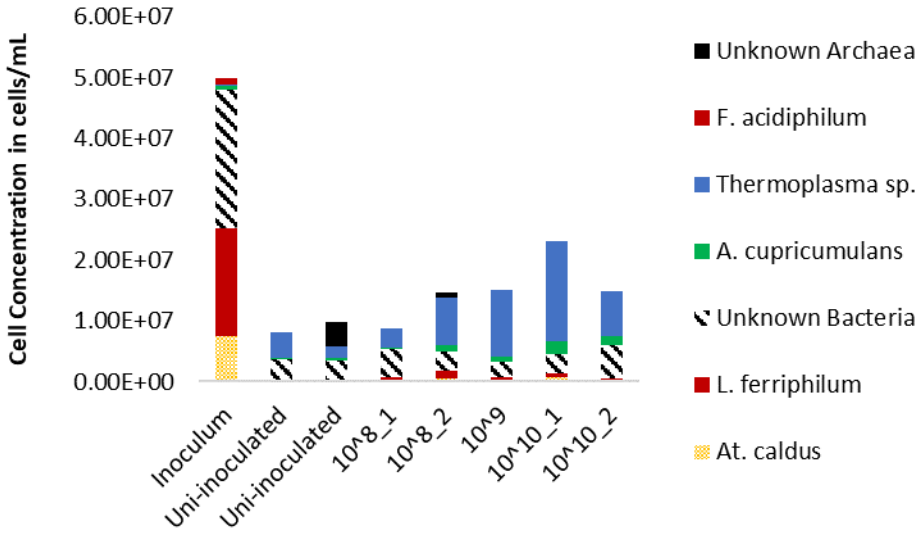

Figure 5-10: Microbial speciation determined at the end of experimental run of Biokinetic test in terms of cell concentration (y-axis) as a function of initial cell concentration

5.4 Effect of inoculum size on Biokinetic test profiles for copper-bearing waste rock under non-controlled pH conditions

Figure 5-11(A)), an initial increase in pH of the feed samples was noticed in all flasks, inoculated and non-inoculated, from day 1 to 14. The increase in pH is partly due to the easily leachable components in the waste with a neutralising ARD capacity. The non-inoculated samples increased to a pH of 2.60, while inoculated flasks pH increased up to 2.50. After 14 days, the pH decreased steadily, indicating a high dissolution of sulphide-containing minerals, including pyrite, observed in the bulk mineralogy of the waste. The pH decrease followed the same order of initial inoculum concentration size until day 20, with 10^{10} tests having the lowest pH. The pH remained stable between 1.8 and 2.10 from day 50 to 90, indicative of the dominance of acid generating minerals (sulphide-containing minerals) over those with an acid neutralising ability within the feed sample.

Figure 5-11(B)) increased following a similar trend, starting from the highest inoculum used (10^{10}) in tests. The redox potential for all different inoculum sizes and non-inoculated tests had an initial ~390 mV redox potential and remained unchanged for 4 days, with the exception of 10^{10} test experiments, which had no observable lag phase attributed to a high initial cell concentration. Thereafter, an exponential increase ensued for tests in which 10^{8}, 10^{9}, and 10^{7} inoculum sizes were used on day 5. However, the non-inoculated tests remained in lag phase until days 11 with the redox potential reaching 650 mV on day 12. This indicated that microbial activity of the indigenous community associated with waste as cross-contamination was minimised during the preparation of tests and during sampling. At the end of the exponential microbial growth phase, further increases in redox potential to 685 mV was observed, which remained stationary thereafter, with minimal changes. This corresponded with a gradual decrease in pH between 2.10 and 2.00 for non-inoculated and inoculated flasks respectively.

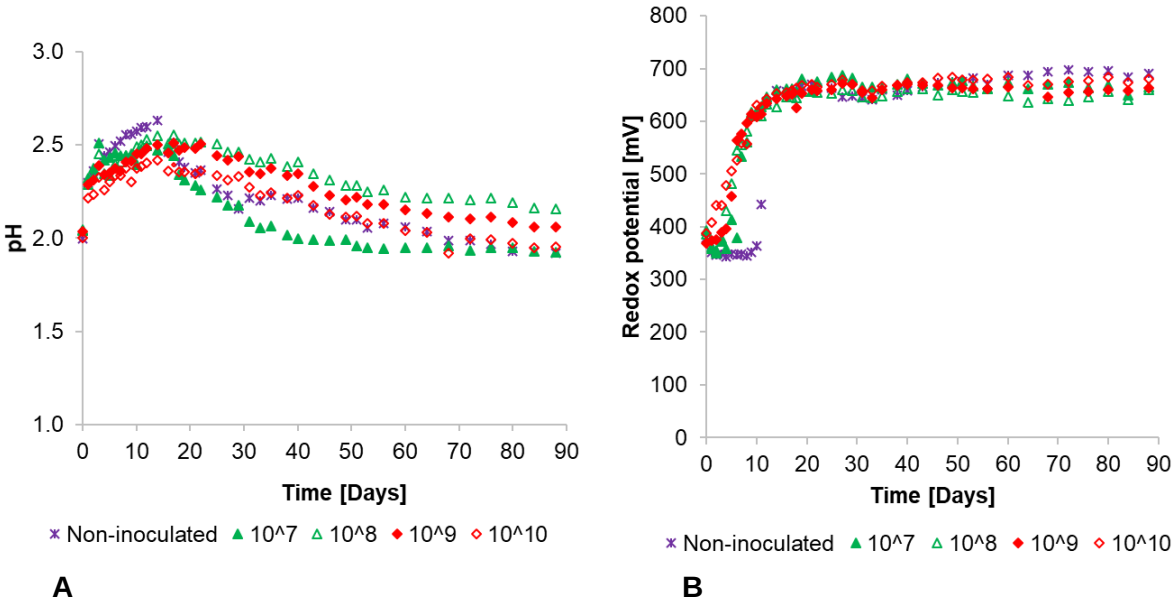

Figure 5-11: pH and Redox potential profiles under non-controlled pH for sample 2

The quantity of ferrous iron provides information on the leached Fe-bearing minerals including pyrite (Figure 5-12). Like waste from gold mining waste samples, the concentration of ferrous iron increased to maximums of 40 and 100 mg/L for inoculated and non-inoculated samples respectively. Subsequent to decreases in ferrous iron below 20 mg/L, as observed after day 3 and 7 for inoculated and non-inoculated samples respectively, the low ferrous oxidation in the non-inoculated samples was attributed to an absence of inoculum; however, on day 7, ferrous concentration declined, coinciding with an increase in redox potential. This suggested natural microbial community prevalence in the waste samples since the waste

material was not sterilized. The decline in ferrous iron concentration also suggested oxidation due to Fe-oxidising microbial community.

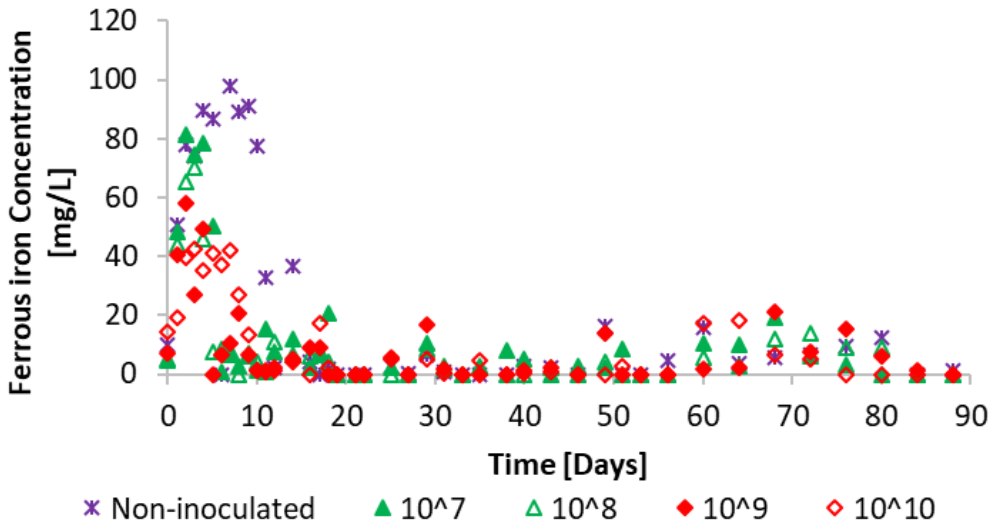

Figure 5-12: Ferrous iron profile for non-controlled pH on sample 2

5.5 Summary

The first sample used in the standard test had high ANC content which increased the pH above the pH optimum of the inoculum used in the study. Due to the significant quantities of the ANC, the inoculum had a minimal impact under non-controlled pH conditions. Additionally, when the pH was suppressed through the addition of dilute sulphuric acid, the effectiveness of the inoculum was noticed. Further research was conducted under similar conditions, using waste with a low ANC for the standardisation of the test. The differences noticed between sample one and two under non-controlled pH conditions was governed by the difference in mineralogical characteristics of waste rocks used. This was controlled by weathering of acid-consuming minerals, which ultimately increased the pH to cecum-neutral for sample 1, resulting in precipitation of ferric ion at pH above 3.5.

The results from sample 1 under non-controlled pH conditions were indicative of significant dissolution of minerals with neutralising potential, which was observed to cause a negative effect on the microbial community used as an inoculum as a result of the high pH. The dissolution of acid generating minerals was indicated by a reduction in the pH to acidic conditions. The pH below 2.5 favoured the microbial community of iron and sulphur oxidisers to regenerate lixiviate (ferric iron), which accelerated the rate of ARD generation. The results under pH controlled tests showed ideal conditions and the effect of the microbial consortium

used. Microbial speciation data presented supported the finding that the native microbial community associated with waste rock became dominant towards the end of the experiments.

The initial increase of feed samples in pH was noticed in all test flasks between days 1 to 14. The increase in pH was partly attributed to the easily leachable components of the waste, which had a neutralising ability as a result of its high magnetite content. The pH of non-inoculated samples increased to 2.60, while the pH of the inoculated flasks increased to 2.50. After 14 days the pH decreased steadily, indicating dissolution of sulphide-containing minerals, including pyrite, observed in the bulk mineralogy of the waste material used. The pH in tests remained stable between 1.8 and 2.10 from day 50 to 90, which indicated that the leaching of acid generating (sulphide containing) minerals proceeded more rapidly than the acid neutralising minerals within the feed samples.

The redox potential of inoculated and non-inoculated sample increased following a similar trend, starting from the highest inoculum to the lowest. The redox potential for all inoculum sizes and non-inoculated sample started at an average of ~390 mV, with increases being observed even for non-inoculated cultures; this was indicative of microbial activity in the indigenous community which became dominant towards the end of the tests, which must be researched further.

CHAPTER 6

RESULTS AND DISCUSSION: SEMI-CONTINUOUS BIOKINETICS TESTS

6 RESULTS AND DISCUSSION: SEMI-CONTINUOUS IN COMPARISON TO BATCH BIOKINETIC TESTS

6.1 Introduction

The UCT Batch Biokinetic test is a characterisation protocol used to gauge relative rates of acid neutralisation and acid generation in the presence of Fe and S-oxidising micro-organisms over 90 days. Under non-controlled pH Batch Biokinetic tests, minerals composed of high ANC content were observed to cause a negative effect on the inoculum, which led to a delay in acidification. To address the challenges associated with high ANC, which increases the pH beyond the pH optimum of the inoculum, pH-controlled and Semi-continuous/draw and fill Biokinetic tests effective for ARD prediction must be investigated. The Batch Biokinetic test provides relative kinetic data on neutralisation, and acidification potential also gives an insight into the potential onset of ARD generation. However, rapid initial neutralisation may mask potential for future acidification. The pH controlled Biokinetic test provides information on the neutralisation potential (but not kinetics), while also providing data on the microbial-assisted acid generation. In addition, in Batch pH controlled Biokinetic tests, neutralising components maybe affected by the effectiveness of the inoculum used. However, the severity of the decrease in solution pH in the pH-controlled experiment, did not allow for a reliable indication on the extent of pH increase under ARD generating conditions. This is where a Semi-continuous Biokinetic test would be beneficial, as the continuous removal of 10% of the leachate-containing dissolved components of ANC will limit inhibitory by-products seen in Batch tests. Further, the introduction of fresh media that aid the proliferation of micro-organisms used in the initiation of the tests will facilitate accurate prediction of the rate of ARD generation. This allows removal of neutralising capacity liberated prior to acid generation; therefore, a clear detection of acid neutralising and acid generating regions can be observed in the Semi-continuous Biokinetic test.

6.2 Aims and objectives

The objective of this chapter was to explore the use of a Semi-continuous Biokinetic to test ARD potential of the gold-bearing and copper-bearing waste rocks used in this study. This was achieved by:

- Determining the kinetics at which acid consuming and acid generating reactions occur, and their impact on the microbial activity when a Semi-continuous Biokinetic test is used;

- Assessing the microbial speciation that was performed over progressively elongated leaching periods using qPCR;
- Describing the kinetic results of acid neutralising and acid generating reactions for gold-bearing and copper-bearing waste rock samples.

6.3 Semi-continuous and Batch Biokinetic Test results for gold-bearing waste rock

The overall potential for acidity generation was tracked through measurement of solution pH. Measurements were recorded prior to removal of 10 % (v/v) solution and after addition of the ABS solution, with presentation of these results in Figure 6-1.The initial increase in pH observed for both Semi-continuous and Batch Biokinetic tests, was due to reaction of the acid neutralising minerals such as calcite. The pH in the Semi-continuous test increased to approximately pH 5.80 within the initial twenty-four hours for both inoculated and non-inoculated tests. This is similar to the pH levels attained within the inoculated and non-inoculated in the batch Biokinetic tests after three days. The decrease in solution pH with time, as observed from the profile for Semi-continuous test, was due to the addition of acidified ABS solution at pH 2.0, and the generation of acidity following sulfide` mineral oxidation. A gradual decrease in the pH for the Batch tests was observed to a plateau region of approximately pH 4.0 till day 30 suggesting dominance of the acid generating reaction. A pH of approximately 2.0 was attained after 20 and 35 days respectively for both tests.

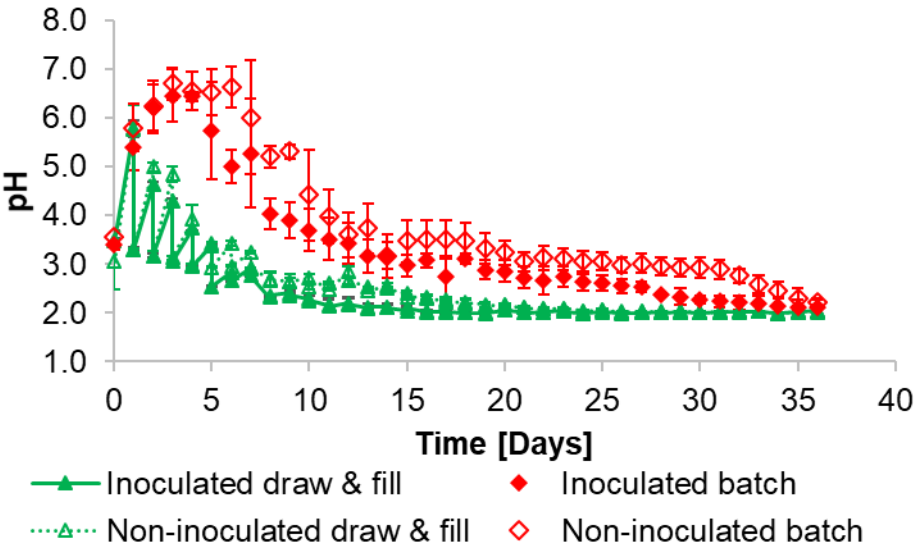

Figure 6-1: Variations in pH over time for Semi-continuous and Batch Biokinetic tests. Bottom data points shows pH after removing 10% of the supernatant and replacing it with an equal volume of ABS solution at pH 2. Dotted lines indicate pH before removing supernatant and replacing it with ABS media.

Figure 6-2 shows the accumulation of hydrogen ion concentration for both inoculated and non-inoculated samples in the Semi-continuous and Batch Biokinetic tests over the experimental test runs. These results are related to the pH variation data presented in Figure 6-1, showing the instance at which acid-consuming minerals occur at a high rate compared to the acid generating waste rock constituents in the sample used in the tests. A lag period of 6 days due to significant concentration of hydroxides from acid-consuming minerals was observed in the Semi-continuous test, and this corresponded to high pH values as shown in Figure 6-1. Thereafter, the concentration of hydrogen ions increased gradually with significant differentiation between inoculated and non-inoculated prior stabilizing 0.010 mole/L after twenty-five days. This was directly related to the relative rate of acid consumption caused by the rate of dissolution for acid-consuming leached by-products of sample under test conditions. In the Batch test hydrogen ion concentrations declined on day 1 and remain constant until day 15 to 20, suggesting an accumulation of hydroxide ions during this period in which minimal pH decreases were observed. This was attributed to the dissolution of fast weathering minerals with acid consuming abilities. Thereafter, an exponential increase in the hydrogen ions was observed on both inoculated and non-inoculated flaks, indicating an accumulation of hydrogen ions reaching a similar concentration of H^+ observed in the Semi-continuous Biokinetic test.

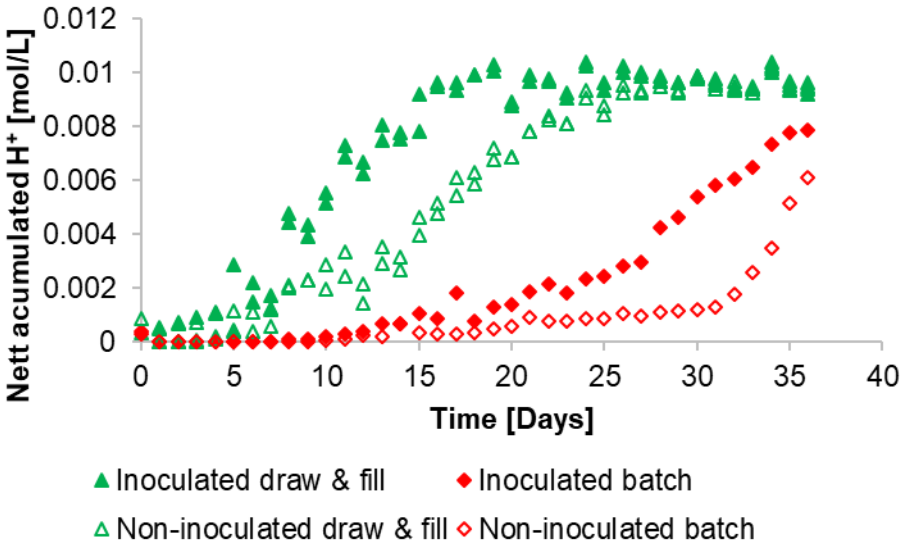

Figure 6-2: Net accumulation of H^+ as a function of time for inoculated and non-inoculated flasks under Semi-continuous and Batch Biokinetic tests conditions

For both set of tests in this waste sample, inoculation affected the extent of pH increase through the generation of acidity following iron precipitation and sulfide mineral oxidation.

This is particularly evident for the tests performed in this sample, where the acidity generated through microbial action reacts with the acid neutralising components, resulting in a lower solution pH value. The differences between inoculated and non-inoculated tests may be further observed in the redox potential data for both tests

Figure **6-3**, where the oxidation of soluble ferrous iron by the iron-oxidising micro-organisms within the inoculum results in a high solution potential to be reached over a shorter time period. Following an initial decrease in redox potential for all tests, a result of the increase in solution pH and the removal of soluble ferric iron by precipitation, the rates of increase differed between the inoculated and non-inoculated tests. Inoculated tests reached a potential of ~650 mV after approximately 8 days and 33 days for Semi-continuous and Batch test, as compared to the non-inoculated flasks which reached a similar value after approximately 13 days and 36 days for the same tests respectively. The lag phase period of 9 and 33 days for the non-inoculated in the Semi-continuous and Batch Biokinetic test indicated periodic requirements by which the native microbial community must adapt to the test conditions, further, the growth of cell numbers in the new environment might have been stunted, as it differed from the environment in which the samples were obtained. A maximum of approximately 700 mV was attained by all tests by day 36 of the experiments.

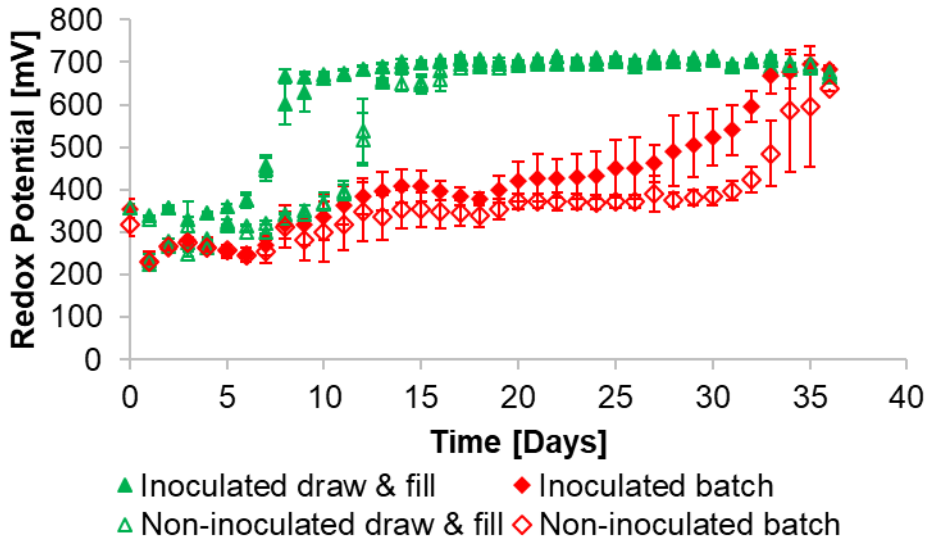

Figure 6-3: Redox potential profile under Semi-continuous and Batch Biokinetic test for gold-bearing sample. Error bars present standard deviation n=3 (where n represent number of flasks)

The increases in redox potential were mirrored by the changes in the ratio of ferrous iron to ferric iron with time across all test performed on both tests. The differing behaviour in soluble iron between the two tests was a result, primarily, of the increase in solution pH observed in the Semi-continuous and Batch Biokinetic tests. This increase resulted in a longer lag period prior to the dominance of the rate of microbial ferrous iron oxidation relative to the rate of chemical leaching of the Fe-bearing minerals in the Batch test. Substantial differences were also observed between the inoculated and non-inoculated tests performed on the Semi-continuous test. A greater concentration of ferrous iron attained within the inoculated flasks (~370 mg/L) relative to the non-inoculated tests (~200 mg/L) over the initial six days Figure 6-4, corresponding to redox potential values below 450 mV. The decline in ferrous iron concentration on day 5 in inoculated test samples was due to the activity of iron oxidising microbes as previously described, e.g. *L. ferriphilum.* This also corresponded to an increase in planktonic cell concentration in the solution drawn from the tests. A subsequent decline in ferrous iron concentration to below 10 mg/L was observed after 16 days for non-inoculated samples (see Figure 6-4).

The increase in total iron was dominated by ferric iron species up to a maximum value of approximately 480 mg/L by day 14. A plateau in the total iron concentration was observed for the non-inoculated tests over the same time, indicating the rate of removal of total iron was approximately that of the rate of deportment from the waste sample. The total iron concentration increased to a maximum concentration of approximately 350 mg/L by day 18. The decreases in the total iron concentration after day 20 for both inoculated and non-inoculated flasks in the Semi-continuous tests were a result of the removal of the soluble iron as part of the Semi-continuous method, and this may also suggest complete dissolution of iron bearing minerals within the mineral waste. A lag period of 5 days in the ferrous iron for Batch test was observed with the inoculated and non-inoculated flasks and this coincides with increase in the solution pH due to dissolution of acid neutralising minerals. Thereafter an exponential phase in the ferrous reaching similar concentrations below 250 mg/L suggested complete oxidation of iron species, prior subsequent decrease at day 28 and 30 for the inoculated and non-inoculated flask respectively. The gradual increase in the total iron for the inoculated and non-inoculated flasks indicated leaching of iron species within the mineral waste.

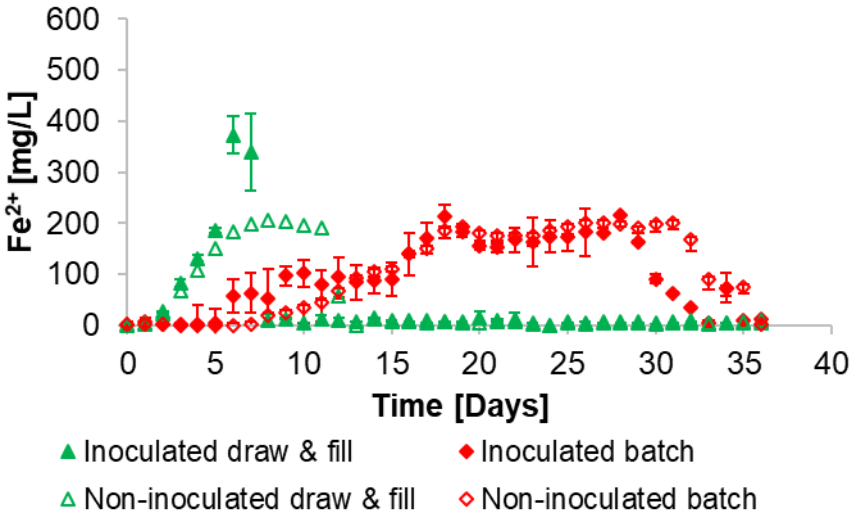

Figure 6-4: Ferrous iron concentration generated over time from the gold-bearing waste rock

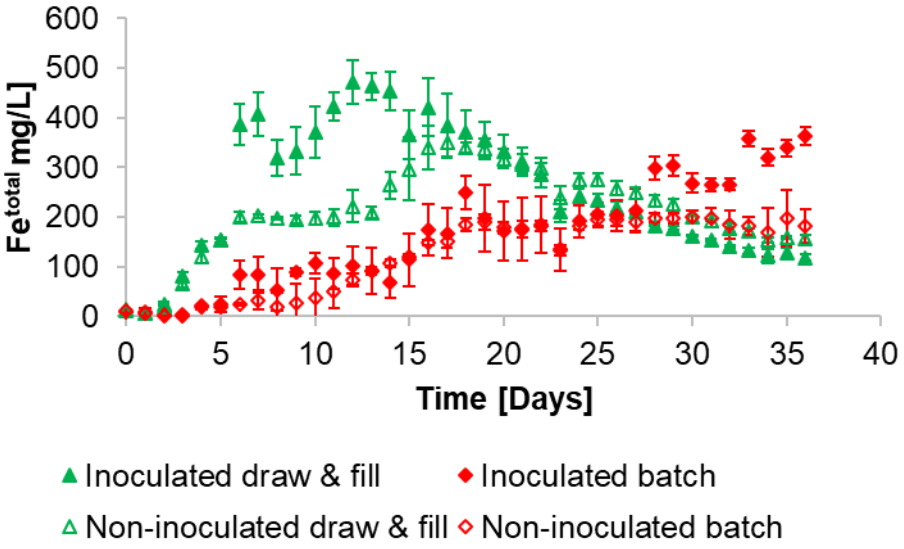

Figure 6-5: Total iron concentration profile as a function of time under Semi-continuous and Batch Biokinetic test for gold-bearing waste rock

A direct relationship between the initial sulphate concentrations and the solution pH's was observed, with greater sulphate concentrations observed for tests with lower pH values (inoculated flask). In the two sets of test, the rate of sulphide oxidation was affected directly by the concentration of ferric iron within the Biokinetic solutions. Over the initial six days, similar sulphate concentrations were observed for the inoculated and non-inoculated Semi-continuous test. An increase in the rate of change of the sulphate concentrations was observed at a time point corresponding to the increase in redox potential values for both inoculated and non-inoculated flaks on Semi-continuous and Batch Biokinetic tests. Under the elevated relative ferric iron concentrations, providing an increase in oxidant source, a similar rate of sulphate increase was perceived for both inoculated and non-inoculated flasks. Similar to the total iron concentrations, a decrease in sulphate concentrations was observed in the later stage of the tests in the Semi-continuous test, with the rate of removal of the sulphate within the flasks higher than the rate of supply from the oxidation of the sulphide minerals. This was also through for both inoculated and non-inoculated test in the Batch system ran for 90 days, presented in chapter 5, suggesting the removal of the oxidation by-products due to solution sampling. This suggests depletion of available sulphur or precipitation that was observed at the early stages of the test coated the mineral and inhibits oxidation of the remaining sulphide in the mineral. Fluctuation thereafter suggested dissolution of different forms of sulphur species within the mineral such pyrrhotite, as their dissolution rate, thus their availability in the leachates, would have been different. After day 30, sulphate concentration remained constant at ~2000 mg/L, suggesting the complete reaction of sulphide species with the waste rock used.

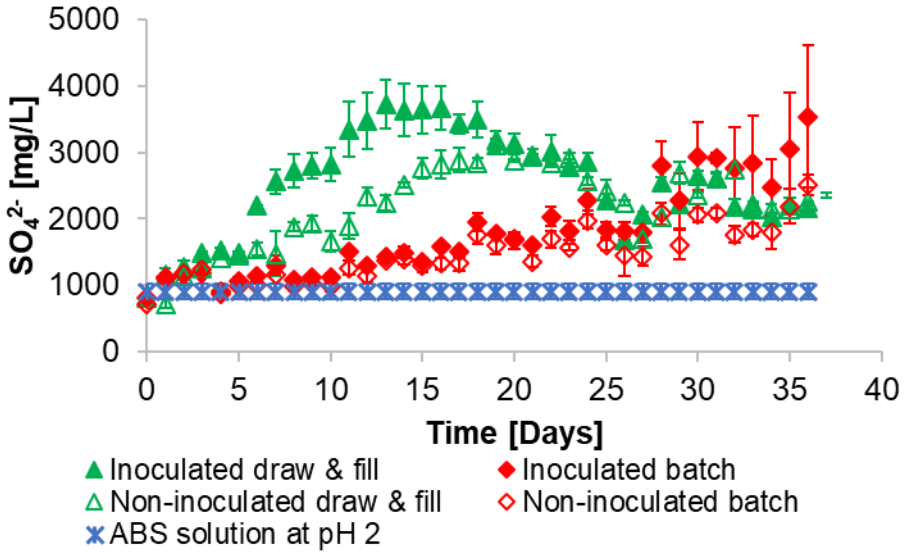

Figure 6-6: Sulphate profile for Semi-continuous and Batch Biokinetic test for gold-bearing sample. Dotted lines indicate ABS solution at pH 2.

6.4 Microbial speciation conducted at different stages of the experimental run for sample 1

The microbial speciation was conducted on the inoculum prior to commencement of the Semi-continuous Biokinetic test experiments, and during an operation in which sample collection occurred on days 5, 20, 25 and 30. The inoculum comprised an equal proportion of *A. caldus* and *L. ferriphilum* and a small portion of universal archaea. On day 5, only the *A. caldus* was predominant in the non-inoculated samples (see Figure 6-7(a)) and *L. ferriphilum* was absent, possibly due to unfavourable pH above 3.5 on day 5 (see Figure 6-7(b). Both *A. caldus* and *L. ferriphilum* species had an increased cell concentration on day 20. These observations corresponded with a decline in pH to a value close to 2, a point at which the rate of Fe^{2+} oxidation to Fe^{3+} was high, as indicated by an increase in the redox potential ~650 mV by day 20. This was followed by a gradual decrease in cell numbers of *A.caldus* on day 25 and day 30, correlating with a decrease in sulphate concentration, while the *L. ferriphilum* concentration remained unaltered due to ideal pH conditions and nutrient availability provided during replenishment of the removed supernatant.

The inoculated sample was mainly composed of *A. caldus* and a minute contributory portion of *L. ferriphilum* on day 5. The small concentration of *L. ferriphilum* corresponded with high pH (see Figure 6-7(b)). A significant increase in cell concentration for both *A. caldus* and *L. ferriphilum* was observed on day 10. These observations corresponded with similar increases in redox potential above 650 mV on day 10, suggesting a high rate of oxidation of Fe^{2+} to $Fe^{3+.}$ Furthermore, sulphate concentrations increased at this stage, suggesting dissolution of acid generating by-products facilitated by the accumulation of H^{+} iron (see Figure 6-7). Similar observations between inoculated and non-inoculated samples were with insignificant differences between the compositions of the cells inoculated in comparison with inherent micro-organisms from the mineral.

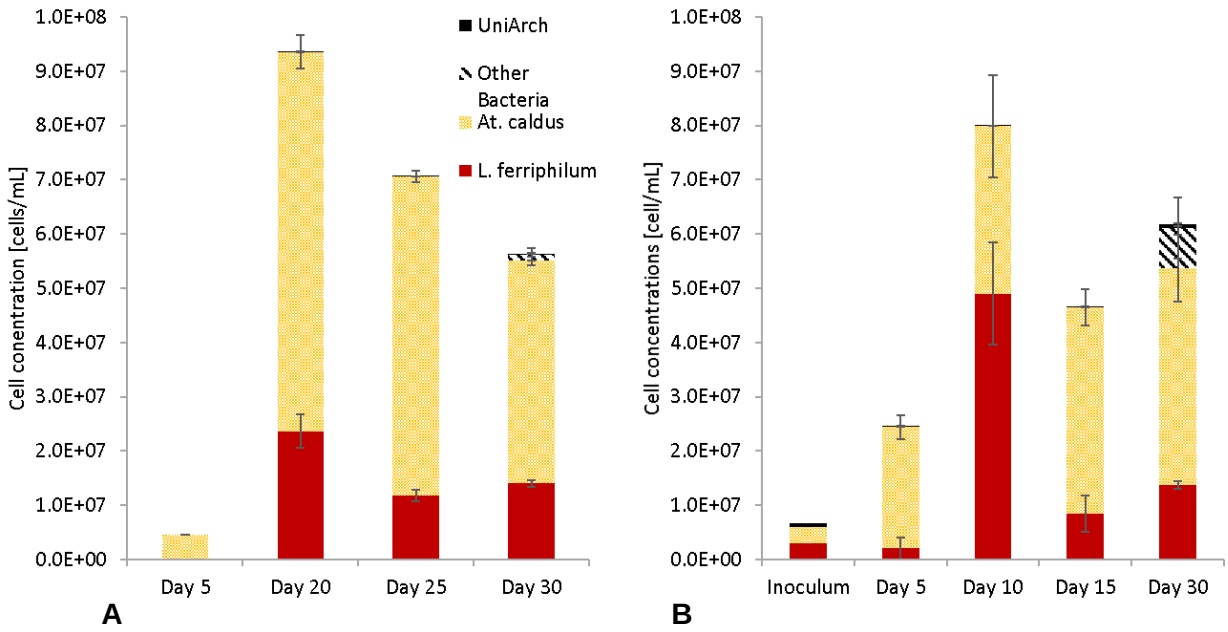

Figure 6-7: Microbial speciation determine in the non-inoculated (A) and inoculated (B) as a function of progressive leaching in terms of copy numbers with error bars showing standard deviation where n=3

6.4.1 Biokinetic test: comparing data provided by Semi-continuous and Batch tests for the gold-bearing sample

The Semi-continuous Biokinetic tests allowed for the removal of oxidation products with time, preventing the formation of a chemical equilibrium and allowing the oxidation reactions to occur to completion unlike in the Batch Biokinetic test where the oxidation products are retained in the solution. The daily replacement of 10% of the solution with fresh ABS solution at pH 2.0 within each flask allowed for downward control of the solution pH to levels more favourable for the acidophilic micro-organisms. The piece-wise control of solution pH resulted in a decrease in the lag period prior to oxidative conditions within the flask experiments, with approximately half the time required to attain 700 mV as compared to the Batch Biokinetic flask experiments in this sample. Furthermore, this decrease in lag time was comparable to that experienced within the pH-controlled experiments in chapter 5, where the daily control of the pH was performed through the drop-wise addition of H_2SO_4. The severity of the decrease in solution pH in the pH-controlled experiment, however, did not allow for a reliable indication on the extent of pH increase under ARD generating conditions, as is the case in the Semi-continuous Biokinetic tests.

Replacement of 10 % of the solution volume simulated a Semi-continuous, flow-through system to better represent a typical ARD generating environment within a waste deposit. The removal of test solution enabled the removal of oxidation products which may limit the chemical reactions, and provide a non-ideal environment for the micro-organisms within the tests, such as potentially toxic elements released from mineral dissolution and oxidation. For the tests performed on the gold-bearing sample, this was achieved through the lowering of the pH conditions within the Semi-continuous Biokinetic tests through the addition of ABS solution at pH 2.0, which negatively affected the inoculum within the Batch Biokinetic tests performed on the gold-bearing sample. Such removal, however, includes the removal of soluble reactant species used in oxidation reactions, and as nutrient sources by the iron and sulphur-oxidising micro-organisms, and may negatively affect the performance of the microbial populations within the Biokinetic tests when performed on other waste samples. In particular, negative consequences may occur under circumstances where the chemical leaching rate is slower than the rate of removal of the soluble species. This was observed after 15 and 20 days for the inoculated and non-inoculated tests, and suggests a shift in the primary source of the iron and sulphur elucidated from the waste sample from sulphide minerals to slow-dissolving iron-oxyhydroxides.

6.5 Semi-continuous and Batch Biokinetic test results for copper-bearing sample

A pH increase of approximately pH 2.4 and 2.70 in the inoculated test was observed in the initial four and thirteen days for the Semi-continuous and Batch tests performed on the copper-bearing sample Figure 6-8. This is attributed to the leaching of readily weathered minerals with significant neutralising potential. The steady decrease in solution pH with time, as observed from the profile for gold waste rock, was due to the addition of acidified ABS solution at pH 2.0, and the generation of acidity following sulphide mineral oxidation. For non-inoculated samples, such an increase was slightly above that observed for inoculated test experiments. A slight increase was observed in the copper-bearing sample due to low ANC content, unlike gold-bearing waste rock sample, which showed a high ANC. A pH of approximately pH 2.0 was attained after 20 days for all tests. A significant decline in the hydrogen ion concentration for the inoculated samples correlated with increase in pH in the two sets test. Thereafter, a gradual increase in the hydrogen ions from day 5 and 10 was observed in both tests suggesting accumulation of hydrogen iron due to dissolution of sulphide-containing minerals such pyrite, chalcopyrite and galena Figure 6-9.

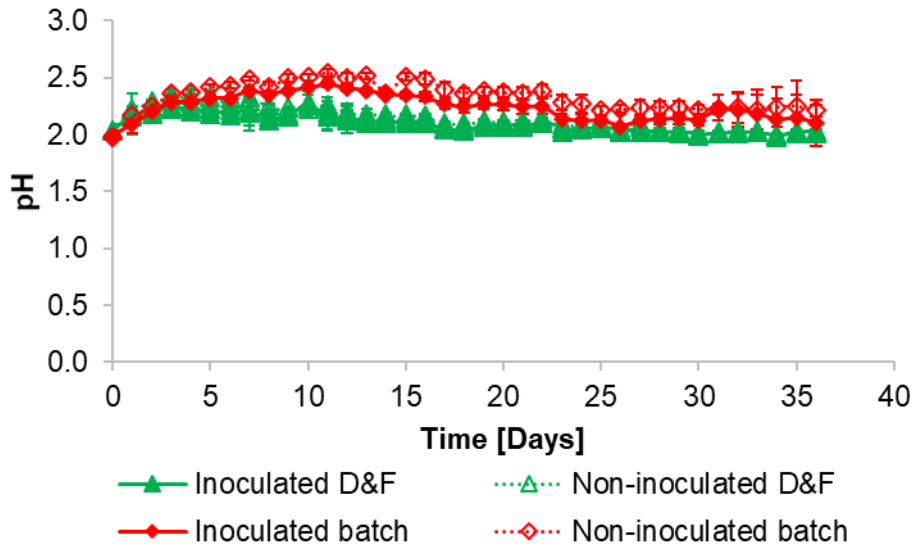

Figure 6-8: Solution pH of inoculated and non-inoculated flasks for Semi-continuous and Batch Biokinetic test for copper-bearing waste rock as a function of time. Note: D&F is abbreviation for draw and fill test

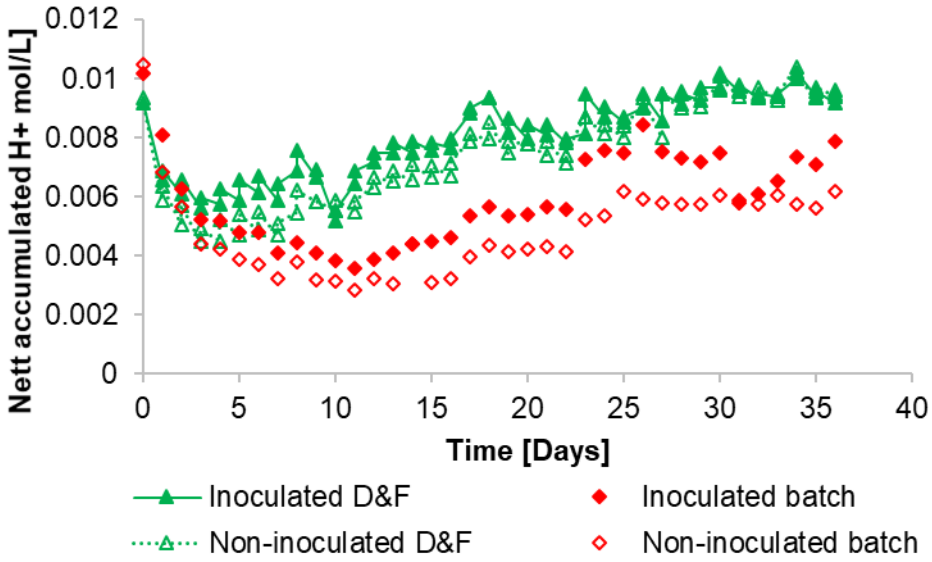

Figure 6-9: Net accumulation of H^+ as a function of time for inoculated and non-inoculated flasks under Semi-continuous and Batch Biokinetic tests conditions for copper-bearing waste rock

The redox potential of Semi-continuous and Batch tests for both inoculated and non-inoculated samples declined on the first day due to neutralisation of rapidly dissolved weathering minerals which consume acid Figure 6-10. The redox potential of the solution increased slowly from day 3 and 4 for inoculated flasks in the Semi-continuous and Batch Biokinetic tests respectively. A further rapid increase of redox potential from 410 mV was

observed on day 3 and 8 because of the growth of microbial community oxidising ferrous to ferric iron. These redox potential levels in the non-inoculated controls suggested the presence and activity of the indigenous microbial community of iron oxidising micro-organisms, but the absence of a ferrous iron scavenger such as *L. ferriphilum* until late in the test. Thereafter, the redox potential of inoculated and non-inoculated samples remained stable throughout the rest of experimental run, indicating the oxidative environment in the Biokinetic flasks due to the presence of elevated ferric iron concentrations.

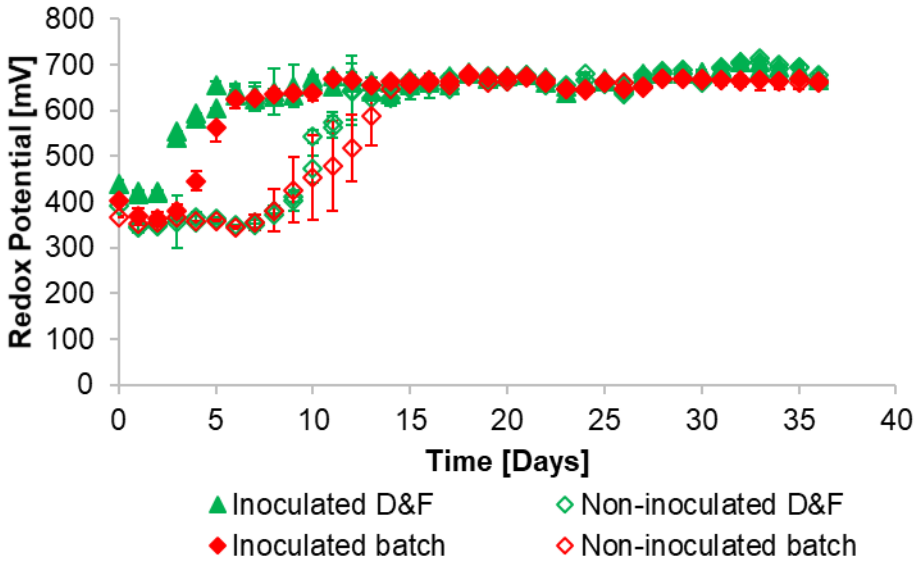

Figure 6-10: Redox potential of inoculated and non-inoculated Biokinetic samples over time for copper-bearing sample

The ferrous iron measured in the leachate is accumulated from the mineral as a result of Fe-bearing minerals such as pyrite, galena and chalcopyrite. A difference in the increase of ferrous concentration for both inoculated and non-inoculated samples was observed between the two tests. The subsequent decrease of ferrous iron was observed on day 2 and 4 for inoculated in the Semi-continuous and Batch Biokinetic tests respectively. The mineral oxidation was catalysed by the microbial community as this correlated with an increase in redox potential above 650 mV. A lag period of 5 days prior to the decrease, and a plateau below 10 mg/L in ferrous iron concentration for the non-inoculated samples, showed the required period of adaptation for the natural microbial community adaptation phase. This was followed by another 6 days of a steady decline and plateau under 20 mg/L on day 10 and 12 for non-inoculated Semi-continuous and Batch Biokinetic test respectively. The ferrous iron concentration in the Batch test was higher (100 mg/L) than the non-inoculated Semi-continuous test 60 mg/L due to the build-up of the accumulated iron products leached from the mineral. The total iron concentration was similar for both sets of tests for the first

days of the experiments. The total iron of inoculated increased progressively, reaching a maximum concentration of 153 and 120 mg/L in the Semi-continuous and Batch test respectively, while this was also similar for the non-inoculated tests until day 31. Thereafter a gradual decline showed that the oxidation by-products might have been removed or depleted in the non-inoculated tests.

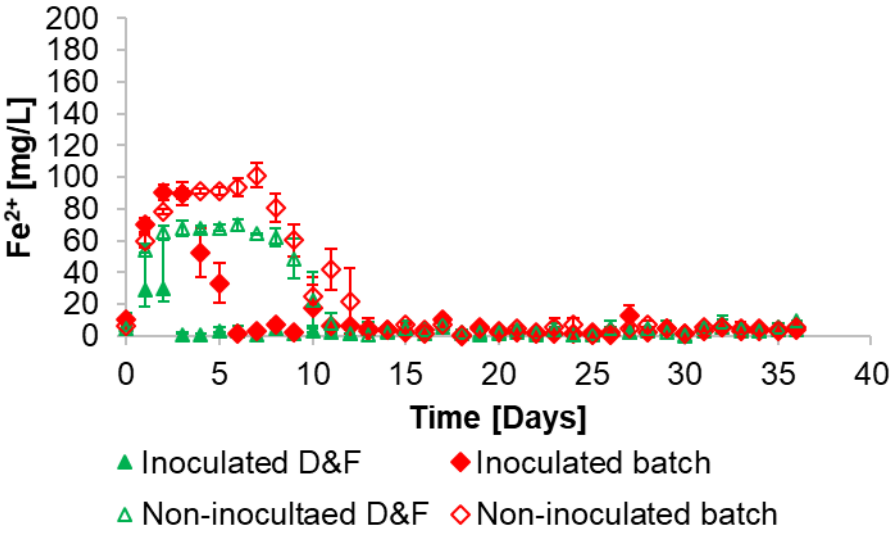

Figure 6-11: Ferrous iron concentration for copper-bearing sample

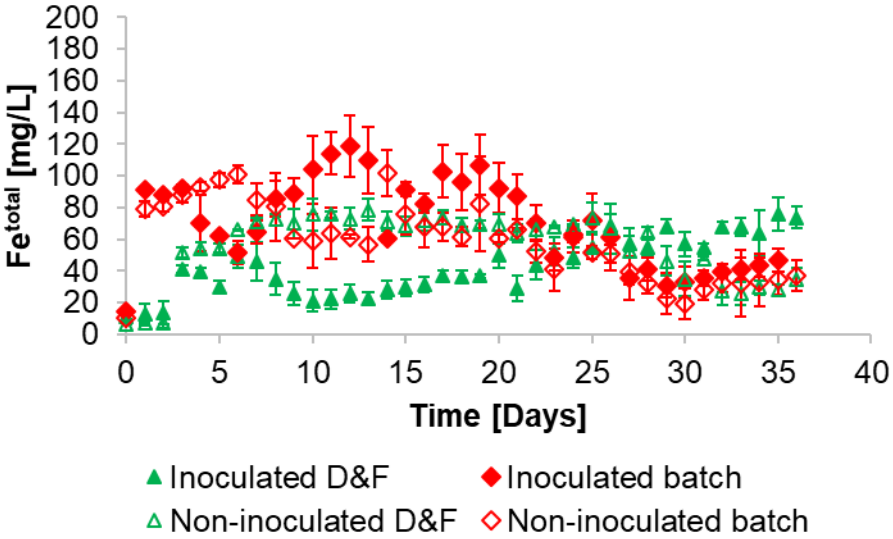

Figure 6-12: Total iron concentration for copper bearing sample

There was insignificant difference observed in the sulphate concentrations throughout the duration of the tests performed on the copper-bearing sample Figure 6-13. Here, the sulphate concentration oscillated around a mean of approximately 2000 mg/L. The deviations observed in the total iron profiles was absent for the sulphate concentrations due to the high concentrations in the acidic test environments, and the inherent accuracy of the turbidimetric sulphate measurements. The constant concentrations attained over the final five days of the experiment suggested a constant rate of sulphide oxidation, similar to that of the rate of removal of the oxidation products by solution sampling. Conversely, the sulphate concentration in the Batch for both inoculated and non-inoculated tests fluctuated around 2000 mg/L and 2500 mg/L for the first twenty-five days prior the gradual increase in the inoculated test above 3000 mg/L. The increase in sulphate concentration indicated oxidation of sulphide mineral such as pyrite and chalcopyrite.

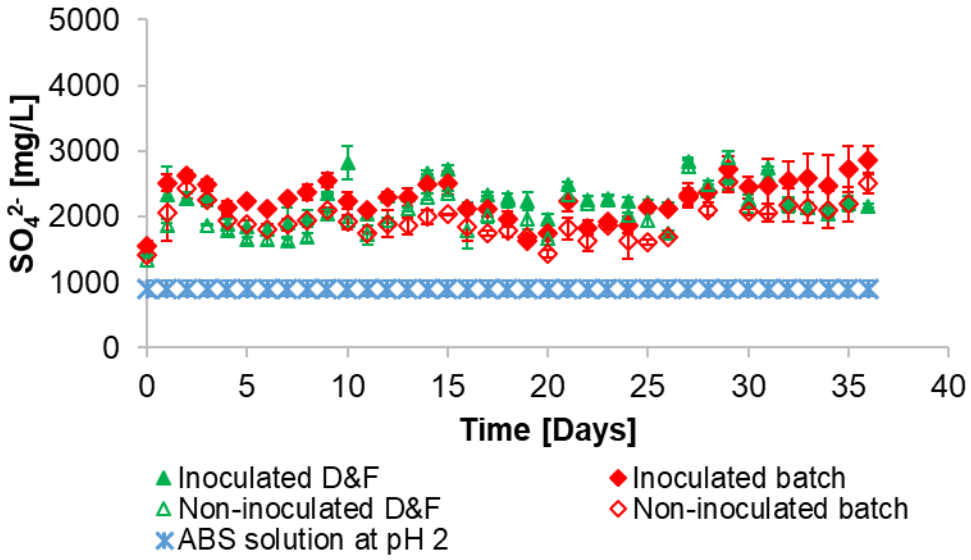

Figure 6-13: Sulphate concentration for copper-bearing sample

Since the inoculum was dominated by *L. ferriphilum* and a small quantity of *A. caldus,* the non-inoculated test samples obtained on day 5 were mostly composed of *A. caldus* and small portions of *L. ferriphilum*. A nearly equal distribution of *A. caldus* and *L. ferriphilum* was observed on day 5 and this corresponded with an increase in the redox potential above 650 mV, suggesting a high conversion rate of Fe^{2+} to Fe^{3+} governed by biological reactions of the micro-organisms embedded in the water rock used for the tests. This also correlated with a gradual decline of ferrous iron below 5 mg/L. The inoculated Semi-continuous Biokinetic tests indicated a nearly equal proportion of *A. caldus and L. Ferriphilum.* The ferrous iron concentration decreased during this period, suggesting high microbial activity. On day 15,

both species increased, suggesting sufficient substrate availability for microbial growth. However, on day 30, both species declined, although the *A. caldus* was still present in high cell concentrations compared to *L. ferriphilum* while archaea started appearing in the test solution. Some leached waste species were definitely in decline in residual rock in test flasks, culminating in a decrease in some microbial species. An alternative argument would thus suggest that an inhibition by-product with higher inhibition capabilities started to leach into the solution, limiting the growth of a vulnerable micro-organisms while promoting the proliferation of another.

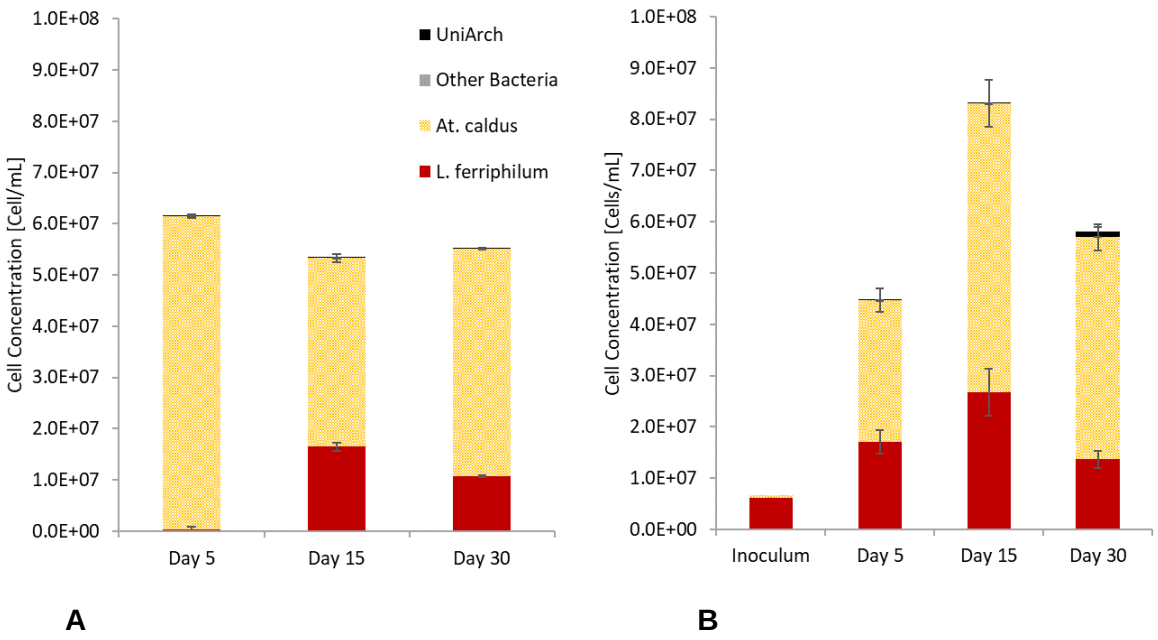

Figure 6-14: Microbial speciation determine of non-inoculated(A) and inoculated (B) samples as a function of progressive in terms of cell numbers

6.6 Comparison of speciation data on day 5 and 30 for sample 1 and sample 2

On day 5, the composition of *A. caldus* was significantly different, with a smaller portion in sample 1, and higher numbers in sample 2 in the non-inoculated samples. Both microbial species declined on day 30 for sample 1 while they increased in sample 2. This was associated with the different mineralogical characteristic observed in the solution chemistry of the Biokinetic tests. This suggested a negative impact of high ANC, which in turn may have affected the effectiveness of microbial species and delayed the rate of ARD generation. Under inoculated semi-continuous Biokinetic test conditions on day 5, *L. ferriphilum* was present in small amounts due to the high pH values close to 4 while *A. caldus* dominated as it has a wide optimum range of pH up to 4.5. Sample 1 and sample 2 showed an insignificant

shift in microbial species speciation. However, universal archaea and other bacteria started appearing as the test progressed beyond day 30.

6.7 Summary of the results for gold-bearing and copper-bearing samples under Semi-continuous and Batch Biokinetic test.

The composition of the waste samples used in the Biokinetic tests directly affected the results obtained. In particular, the acid neutralising capacity of the wastes affected the solution pH, with consequences for the rates of both chemical and biological ARD generation. The type of sulphide minerals within the wastes affected the nature of the test results as these constituent the sole supply of nutrients to the micro-organisms. The presence of easily soluble sulphides, which undergo dissolution under acidic conditions, results in the development of oxidative conditions earlier through the supply of nutrients to the microbial communities.

The similarities in community composition and dynamics between the inoculated and non-inoculated tests shows the growth of the indigenous micro-organisms under the favourable conditions. The elevated pH conditions with the tests performed on the gold bearing sample resulted in a lag in the increase in cell numbers. For the inoculated tests, however, the decrease in pH due to the daily replacement of ABS solution at pH 2.0, allowed for growth of the microbial populations over the initial 5 days of the experiment. This was in contrast to the Batch Biokinetic tests, where the prolonged elevated pH conditions had a detrimental effect on the inoculated micro-organisms. The initial dominance of *At. caldus* was observed in both inoculated and non-inoculated Biokinetic flasks, and was due to the readily available reduced sulphur species present initially due to the acid solubilisation of acid-soluble sulphide minerals. The presence of the reduced sulphur species, and their oxidation, may be inferred from the elevated sulphate concentrations for both sets of experiments above that of the ABS feed solution. The initial dominance of *At. caldus* over *L. ferriphilum* is in agreement with Hao et al. (2010), where dominance of an *At. caldus* and *Sulfobacillus thermotolerans* mixture was followed by a dominance of *L. ferriphilum* at a later stage of bio-oxidation of a gold-bearing sulphide ore. This progression was attributed to the initial availability of inorganic sulphur species, with the lower pH and high redox potential conditions observed in the latter stages more favourable for *L. ferriphilum*.

CHAPTER 7

CONCLUSIONS AND RECOMMENDATIONS

7 CONCLUDING REMARKS AND RECOMMENDATIONS

In this thesis, three different experimental approaches were used to characterise ARD potential of waste rocks, using standard ARD characterisation tests, biokinetic tests under pH controlled and non-controlled conditions, as well as a semi-continuous test. The primary findings of the study addressed the research questions listed in chapter 1 with recommendations for future research being presented in this chapter.

Accurate, informative and cost-effective ARD characterisation tools are necessary to develop mitigation measures for mining waste rock decomposed in the environment. Considering this, the overarching objective of this research was to use Biokinetic tests and ARD geochemical characterisation tests as a tool to aid the interpretation of the potential for ARD generation using two different waste rock samples of different neutralising capacity. The quantitative data obtained from the entire sets of tests were combined to contribute to the standardisation of Biokinetic test and to contribute to a greater understanding of the potential for ARD formation from these wastes. The potential for ARD generation from the gold-bearing and copper-bearing waste rocks was characterised using standard methods at the laboratory-scale, which involved static ARD characterisation tests; acid-base accounting (ABA); net acid generation (NAG); mineralogical assessment; and batch and semi-continuous Biokinetic tests.

7.1 Summary

7.1.1 Static test results for ARD characterisation of waste rock samples

The effect of acid consuming minerals (calcite, magnetite and other slow weathering minerals, including plagioclase-albite and acid generating minerals (pyrite, pyrrhotite and chalcopyrite) were identified from the waste rocks using mineralogical techniques. The minerals present in the waste rocks were leached under ARD characterisation tests. Static tests such as acid ABA and NAG tests were conducted to determine the behaviour of these samples under chemical conditions. The ABA tests indicated that Sample 1 with net acid producing a potential of 17.20 kg H_2SO_4/ton was classified as moderately acid-forming, while sample 2 was found to have a higher acid forming potential, namely an ABA value of 92.3 kg H_2SO_4/ton. However, these tests may overestimate the ARD potential due to the use of inorganic acids, with minimal information providing for the effect of microbial activity as well as relative rates of ARD generation in the environment.

7.1.2 Effect of inoculum size on Batch Biokinetic tests

The overall results of the Biokinetic test indicated that acid-consuming minerals, notably calcite, dissolved at a faster rate and increased the pH of the leachate beyond the optimum pH for Fe^{2+} and S-oxidising micro-organisms. This was observed by measuring redox potential to track the rate of ferrous oxidation to ferric iron. Under non-controlled pH, no effect of inoculum size on biokinetic tests for sample 1 was observed except for the higher inoculum size of 10^{10} used. This was due to the dissolution of minerals with a significant buffering capacity, which resulted in the precipitation of ferric iron at pH above 3.5. These caused long microbial lag phase periods and slowed the mineral leaching by the microbial community, while at 10^{10} inoculum cell concentration there was a short lag due to the high initial cell count. However, under controlled pH conditions, an increase of inoculum size on biokinetic tests accelerated the rate of acid generation.The neutralization potential provided by acid consuming minerals was suppressed, which created ideal environmental conditions for the microbial consortium to accelerate the rate of ferrous to ferric iron oxidation. The ferrous to ferric oxidation occurred sequentially, starting from the samples with highest inoculum cell concentration, which indicates the influence of inoculum size. It can therefore, be concluded that there was an effect of inoculum size on batch biokinetic tests when the mineral had a low content of ANC. The sample with high ANC increased the pH, ultimately creating an unfavourable environment for the microbial consortium used as inoculum. However, there is a need to understand the characteristics of the material being studied.

7.1.3 Microbial community used as inoculum on Batch Biokinetic test

The DNA extracted from the samples were isolated as described in chapter 3, and the qPCR was also conducted to speciate the microbial species present on day 45 and day 90 for the pH controlled tests, while it was only performed on day 90 for the non-controlled pH Batch Biokinetic test. The data of microbial speciation performed for sample 1 at the end of the experiment showed microbial community differentiation. This was mainly due to the high ANC content which increased the pH beyond the optimum pH for the inoculated consortium. However, there were species found which might have come from the waste samples themselves. The speciation data at mid-leach (day 45) indicated a representative of the microbial consortia dominated by *A. caldus* and *L. ferriphilum* for different inoculum sizes and for non-inoculated samples. This could have been due to the starvation of test consortia and dominant archaea species such as *A. cupricumulans*, which also oxidises iron. Based on the two different results obtained under pH controlled and non-controlled conditions at the

end of the experiment, a semi-continuous Biokinetic test was conducted to complement the data generated in Batch Biokinetic tests for better characterisation of ARD under microbial mediated conditions. One set was inoculated while the other was non-inoculated. The non-inoculated samples in both samples demonstrated delayed acidification due to the lack of inoculum. The instance at which redox potential increased correlated with the dominance of Fe and S-oxidising micro-organisms in the inoculum used. This data indicated that the removal of the supernatant containing dissolved ANC allowed the representative consortia to perform optimally such that the rate at which acid neutralisation and acid generating reactions occurring at a faster rate could be clearly observed from the test.

7.1.4 Semi-continuous Biokinetic test

The daily replacement of 10% of the solution with fresh ABS solution at pH 2.0 within each flask allowed for downward control of the solution pH to levels more favourable for the acidophilic micro-organisms to facilitate the rate of ARD generation in the ARD simulated system. The piece-wise control of solution pH resulted in a decrease in the lag period prior to oxidative conditions within the flask experiments, with approximately half the time required to attain 700 mV as compared to the Batch Biokinetic flask experiments performed on sample 1. Furthermore, this decrease in lag time was comparable to that experienced within the pH-controlled experiments presented in chapter 5, where the daily control of the pH was performed through the drop-wise addition of H_2SO_4. The severity of the decrease in solution pH in the pH-controlled experiment, however, did not allow for a reliable indication on the extent of pH increase under ARD generating conditions, as is the case in the Semi-continuous Biokinetic tests. The removal and replacement of 10% (v/v) with fresh ABS solution at pH 2.0 allowed for the control of the pH conditions, proving more favourable conditions for the mixed-microbial inoculum. In addition, the reduction in pH with time is less severe as compared to the addition of concentrated H_2SO_4, allowing for information to be gained on the extent of initial pH increase for the waste samples. Although the rate of removal of lixiviates and microbial nutrients did not negatively affect the Biokinetic tests performed in this study, the potential remains for negative consequences of solution removal in cases where the replenishment of lixiviates and nutrients is slower than the rate of their removal.

The relative composition of the microbial communities between the two waste samples remained unaffected by the difference in sample composition for the wastes used in this study. The microbial activity within the non-inoculated flasks was likely due to the daily sampling of the tests, and may not reliably reflect the composition of the indigenous micro-organisms within each waste sample. The use of a well-defined, mixed iron- and sulphur-

oxidising inoculum, however, provides a minimum time-frame for investigating microbial ARD generation. Tests conditions may not be suitable for pure abiotic Biokinetic tests, with the relevance of such conditions remaining questionable as compared to a waste deposit on site

7.2 Addressing the key questions

7.2.1 What are the effects of controlled pH and non-controlled pH on the Biokinetic test? Does this affect the quality of data or ease of interpretation?

Hypothesis I: An increase in the initial cell concentration of consortia in the Biokinetic test can enhance or accelerate the onset of the rate of acid generation in the test, until the established microbial community more rapidly regenerates the ferric iron and acid than it is consumed during mineral leaching. Above this concentration, no further impact of inoculum concentration can be observed.

The rate of ARD generation was expected to increase sequentially in the order related to inoculum size due to the concentration of the microbial community to initiate both pH-controlled and non-controlled Biokinetic tests. In the non-controlled pH Biokinetic tests, this was true for the 10^{10} inoculum test, and there was minimal difference associated with other inoculum sizes used. This was due to the high ANC content of the mineral which buffered the pH above optimum pH of Fe and S oxidising micro-organisms. At pH above 3.5, iron forms a precipitate which ultimately limits the regeneration of iron recycling, which in turn leaches the mineral. To address the challenge of a high ANC content in sample 1, pH controlled Biokinetic tests were conducted. In the experiment, dilute sulphuric acid was added in order to suppress the ANC influence. This was also to reduce the precipitation of ferric iron such that it remained in the solution to leach minerals in the waste rocks. The pH reduction also created ideal conditions for the inoculum to catalyse the ferrous oxidation to ferric iron. On completion of the exponential phase for redox potential increments, sufficient ferric iron was generated and there was an observable effect of different inoculum sizes. The results from sample 1 under pH controlled conditions and sample 2 for non-controlled pH indicated that the increase in inoculum size accelerated the rate of ARD generation.

7.2.2 Will there be any effect of inoculum size on biokinetic tests? If so, is the effect different under pH controlled or uncontrolled conditions?

Hypothesis II: By controlling the pH of the biokinetic test at pH 2 or below, ferric iron precipitation is minimised, favouring mineral leaching. Furthermore, a favourable

environment is maintained for the iron and sulphur oxidising micro-organisms such that the acid generating reactions can proceed in an accelerated manner, allowing for a representative but accelerated test.

The influence of inoculum size presented by 10^7, 10^8 10^9 and 10^{10} at 6 % w/v of 150 µm for the characterisation of waste rocks under Biokinetic tests conditions was investigated. This test was conducted to determine the standard initial cell concentrations which accelerate the rate of ARD generation in the Biokinetic tests. Under non-controlled pH Biokinetic tests, the pH increased to pH 5.5 due to the dissolution of the acid-consuming minerals. In the controlled pH Biokinetic test, the increase in pH was corrected to pH 2.0 through the addition of a standardised sulphuric acid solution. This limited the precipitation of ferric iron and created ideal conditions for different inoculum sizes to accelerate the rate of ARD generation. The ferric iron concentration was 2000 mg/L compared to 675 mg/L of that observed in the non-controlled pH biokinetic tests. This was supported by redox potential profiles which measured the ratio of ferrous oxidation to ferric iron, which in turn leached the mineral. This was illustrated by the high acid consumption rates which were found to be 15.18, 13.77, 13.80, 13.30 and 11.77 for non-inoculated reference tests respectively.

Hypothesis III: By using a semi-continuous operational strategy for the biokinetic test, acid neutralising capacity will be reduced, allowing regions of neutralisation and acid generation to be clearly observed, and thus allowing the flooding conditions to be more representative of field conditions.

The kinetics of acid generation and neutralisation reactions were investigated using the Semi-continuous Biokinetic test. The test was performed by conducting an experiment with one set inoculated with a mixed culture of Fe and S oxidising microorganisms and other being non-inoculated. The supernatant removed during sampling was used for microbial speciation. The data generated indicated a significant increase in pH due to the potential of acid neutralising capacity. The removal of the supernatant containing the dissolved component with neutralisation potential allowed the acid generating reaction to occur at a faster rate. The speciation data also showed that the microbial species were responsible for accelerating the rate of ARD generation.

7.3 Conclusions

7.3.1 Effects of inoculum size on biokinetic test for ARD generation potential

7.3.1.1 Non-controlled pH biokinetic test

Biokinetic tests were conducted under Batch and Semi-continuous/ draw and fill conditions. This was done to simulate long-term weathering of waste rocks in a disposal environment. Shake flasks simulating long-term weathering in a disposal environment were inoculated with various inoculum sizes of mixed cultures of iron and sulphur-oxidizing microorganisms. The Batch Biokinetic test was carried out under three different conditions: pH controlled non-inoculated, pH controlled inoculated, and pH non-controlled non-inoculated, tests. According to the results obtained from the batch Biokinetic test for sample 1 (with high ANC) under non-controlled pH conditions, there was minimal effect of inoculum size on Biokinetic tests except for the 10^{10} cell concentration tests. These results suggested ineffectiveness of the Fe and S-oxidising micro-orgasms used, as the inoculum pH was beyond the optimum range for these particular micro-organisms. The microbial speciation data also indicated a significant change in the microbial compositions dominated by archaea originating from the waste rock. Similar experiments were conducted using a different waste rock with a low ANC content. The results generated indicated an effect of the inoculum size on Biokinetic test profile. It was therefore concluded that there was an effect of inoculum size on Biokinetic tests when using low ANC content waste rock. However, there is a need to understand the mineral characteristics prior to conducting such a test.

For copper-bearing (sample 2) under non-controlled pH conditions, an effect of inoculum size was observed. Therefore, it can be concluded that there was an effect of inoculum size on Batch-based Biokinetic tests. However, there is a need to understand the characteristics of the material. For example, the gold-bearing waste rock had a high concentration of neutralising acid capacity which counteracted the increase in the pH, ultimately creating an unfavourable environment for microbial consortium used as inoculum. It was also noted that the microbial diversity used changes as leaching progresses due to depletion of the substrate, with the mineral itself being associated with containing both iron and sulphur oxidising organisms which accelerate the rate of ARD generation in the mine dumps.

7.3.1.2 Controlled pH

Under pH-controlled conditions, an effect of inoculum size was observed and the microbial speciation data at mid-leach indicated an equal distribution of iron and sulphur oxidising

organisms. However, the speciation data at the end of the experiment showed a significant shift in the microbial community as a result of substrate depletion and dominance of the native microbial community. This showed that the microbial community present in the test towards the end of the experiment does not necessarily indicate the micro-organisms that regenerated the reactant for leaching. This is because oxidation of ferrous iron to ferric iron mineral occurred in the early stages of the test, and the inoculum could have been starved as ferrous iron was depleted and native microbes become dominant in the system.

7.3.1.3 Semi-continuous Biokinetic tests

A Semi-continuous Biokinetic test was conducted by inoculating one set of experiments with an equal proportion of Fe and S oxidising micro-organisms, while the other set was not inoculated. During the test, 10% of the supernatant was removed and replaced with an equal volume of fresh ABS at pH 2. This study has demonstrated that the Semi-continuous Biokinetic test was a suitable method for removal of the easily soluble minerals with neutralising capacity, such that the acid generation reactions occurred at a faster rate. Furthermore, the addition of fresh media maintained ideal conditions for the micro-organisms to proliferate and accelerate the generation of reactants which leach the mineral. Therefore, the Semi-continuous Biokinetic test should be used to complement and confirm the Batch Biokinetic test to gain further insights into the relative rates of acid generation and acid neutralisation under microbial mediated conditions, in particular for a sample with high ANC content.

7.4 Recommendations

Based on the conclusions from this study the following recommendations are proposed:

7.4.1 The addition of a detailed mineralogical assessment of the metals dissociated under ANC, NAG, and Batch Biokinetic tests, including a draw and fill test, must be individually optimised to gain insight into the mineral mobility under different test conditions. Some of the minerals might be classified as non-acid forming and ignored, while they contain a high concentration of toxic metals above environmental standards and cause a detrimental effect on the ecosystem. Also, comparison of the results generated from the aforementioned tests with long-term kinetic tests, i.e. humidity cell and column leach, will provide a better prediction of ARD generation such that mitigation measures can be put in place. It will be of great importance to do analyse residues and do Fe and S balance to gain insight of how much each mineral leached under different test conditions for better characterisation of ARD potential.

7.4.2 As indicated in chapter 5, the importance of removing ANC in the system such that the rate of ARD can be accelerated in a reduced time-frame is paramount. Based on these observations, the data generated in the previous chapter, such as the redox plateau above 650 mV, indicated there was not much difference between inoculated and non-inoculated tests observed as a result of slow weathering waste rock. Therefore, reducing the duration of the Batch Biokinetic test from 90 days to 45 is advised. This will reduce the labour and many samples can be characterised to determine their relative rate of acid generation.

7.4.3 The removal and replacement of the supernatant for Semi-continuous/draw and fill Biokinetic tests may cause a decline in the microbial community under high ANC conditions because leachates have an influence on cell deactivation, which may cause ineffectiveness of the micro-organisms used. It is therefore recommended to re-inoculate the flasks when pH is close to 2 in the Semi-continuous test and Batch Biokinetic tests.

7.4.4 It has been observed that the waste rocks are composed of a diversity of microbial community which enhances the ARD generation in mine waste. Therefore, there is a necessity to perform speciation data in the early stages of the Batch and Semi-continuous Biokinetic test such that the micro-organisms associated with the waste rock which result in an increase in redox potential might better correlate the performance of the tests with changes in pH and microbial profile.

7.4.5 The use of Semi-continuous Biokinetic tests is, however, promising. In particular, refinement of the test method with respect to the volume removed and the frequency of removal may provide an easy option for waste samples with slower relative rates of mineral dissolution. A detailed knowledge of the sample mineralogy and chemistry, however, would be critical in the effective design of Semi-continuous Biokinetic tests for waste samples of interest, and in the fundamental understanding of microbial-mediated ARD generation obtained from the conducted test. Also varying the ratios of Fe and S-oxidisers within the inoculum for Biokinetic test is advised as they adapt and function at rate under different pH conditions to inform inoculation strategies within Biokinetic test**.**

REFERENCES

Adam, K., Kourtis, A., Gazea, B. and Kontopoulos, A. 1997. Evaluation of static tests used to predict the potential for acid drainage generation at sulphide mine sites. Transactions of the Institution of Mining and Metallurgy Section A-Mining Industry, 106: A1-A8.

Akcil, A. and Koldas, S. 2006. Acid Mine Drainage (AMD): causes, treatment and case studies. *Journal of Cleaner Production*, *14*(12-13): 1139-1145.

Baker, B.J. and Banfield, J.F. 2003. Microbial communities in acid mine drainage. *FEMS microbiology ecology*, *44*(2):139-152.

Becker, M., Dyantyi, N., Broadhurst, J.L., Harrison, S.T. and Franzidis, J.P. 2015. A mineralogical approach to evaluating laboratory scale acid rock drainage characterisation tests. *Minerals Engineering*, *80*:33-36.

Berry, R., Hunt, J., Parbhakar-Fox, A. and Lottermoser, B. 2015. Prediction of Acid Rock Drainage (ARD) from calculated mineralogy. In *10th International Conference on Acid Rock Drainage and IMWA Annual Conference*: 1-10.

Bhatti, T.M., Bigham, J.M., Carlson, L. and Tuovinen, O.H. 1993. Mineral products of pyrrhotite oxidation by Thiobacillus ferrooxidans. *Applied and environmental microbiology*, *59*(6):1984-1990.

Blowes, D.W., Ptacek, C.J., Jambor, J.L. and Weisener, C.G. 2005. The geochemistry of acid mine drainage. *Treatise on geochemistry. Environmental geochemistry*, *9*:149-204

Blowes, D.W., Ptacek, C.J., Jambor, J.L. and Weisener, C.G., 2003. The geochemistry of acid mine drainage. *Treatise on geochemistry*, *9*:612.

Bouzahzah, H., Benzaazoua, M., Bussiere, B. and Plante, B. 2013. Prediction of acid mine drainage: importance of the mineralogy knowledge and test protocols for static and kinetic tests. Mine water and the environment, 33(1):54-65.

Brantley, S.L. 2008. Kinetics of mineral dissolution. In Brantley, S.L., Kubicki, J.D. and White, A.F. (eds). *Kinetics of water-rock interaction*: 151-210. New York: Springer.

Bryan, C.G. 2006. *A study of the microbiological populations of mine wastes.* Doctoral dissertation, University of Wales, Bangor.

Bryan, C.G., Hallberg, K.B. and Johnson, D.B. 2006. Mobilisation of metals in mineral tailings at the abandoned São Domingos copper mine (Portugal) by indigenous acidophilic bacteria. *Hydrometallurgy*, *83*(1-4):184-194.

Broadhurst, J.L., Bryan, C.G., Becker, M., Franzidis, J. and Harrison, S.T.L. 2013. Characterising the acid generating potential of mine wastes by means of laboratory-scale static and biokinetic tests. *International Mine Water Association Colorado, USA*: 275-280.

Broadhurst, J.L. and Petrie, J.G. 2010. Ranking and scoring potential environmental risks from solid mineral wastes. *Minerals Engineering*, *23*(3):182-191.

Broadhurst, J.L. 2007. *Generalised strategy for predicting environmental characteristics of solid mineral wastes: a focus on copper.* Doctoral dissertation, University of Cape Town.

Caruccio, F.T., Hossner, L.R. and Geidel, G. 1988. Pyritic materials: acid drainage, soil acidity, and liming. *Reclamation of surface-mined lands*, 1:159-189.

Chotpantarat, S. 2011. A review of static tests and recent studies. *American Journal of Applied Sciences*, *8*(4):400.

Church, C.D., Wilkin, R.T., Alpers, C.N., Rye, R.O. and McCleskey, R.B. 2007. Microbial sulfate reduction and metal attenuation in pH 4 acid mine water. *Geochemical Transactions*, *8*(1):1-14.

Coastech Research. 1991. *Acid Rock Drainage Prediction Manual.* Energy Mines and Resources.

Colmer, A.R., Temple, K.L. and Hinkle, M.E. 1950. An iron-oxidizing bacterium from the acid drainage of some bituminous coal mines. *Journal of bacteriology*, *59*(3):317-328.

Dew, D.W., Rautenbach, G.F., van Hille, R.P., Davis-Belmar, C.S., Harvey, I.J. and Truelove, J.S. 2011. High temperature heap leaching of chalcopyrite: method of evaluation and process model validation. *Percolation leaching: the status globally and in southern Africa. The Southern African Institute of Mining and Metallurgy, Johannesburg*: 201-219.

Dyantyi, N. 2014. *Application of mineralogy in the interpretation of laboratory scale acid rock drainage (ARD) prediction tests: a gold case study.* Doctoral dissertation, University of Cape Town.

Erguler, Z.A. and Erguler, G.K., 2015. The effect of particle size on acid mine drainage generation: Kinetic column tests. *Minerals Engineering*, *76*, pp.154-167.

Evangelou, V.P. and Zhang, Y.L. 1995. A review: pyrite oxidation mechanisms and acid mine drainage prevention. *Critical Reviews in Environmental Science and Technology*, *25*(2):141-199.

Ferguson, K.D. and Erickson, P.M. 1988. Pre-mine prediction of acid mine drainage. In (eds) *Environmental Management of Solid Waste* (pp. 24-43). Berlin: Springer.

García, C., Ballester, A., González, F., Blázquez, M.L. and Acosta, M. 1996. Chemical and microbiological transformations in a pyritic tailing pond. *Minerals engineering*, *9*(11):1127-1142.

Gilcreas, F.W. 1966. Standard methods for the examination of water and waste water. *American Journal of Public Health and the Nation's Health*, *56*(3):387-388.

Goodall, W.R., 2008. Characterisation of mineralogy and gold deportment for complex tailings deposits using QEMSCAN®. *Minerals Engineering*, *21*(6):518-523.

Gunsinger, M.R., Ptacek, C.J., Blowes, D.W., Jambor, J.L. and Moncur, M.C. 2006. Mechanisms controlling acid neutralization and metal mobility within a Ni-rich tailings impoundment. *Applied Geochemistry*, *21*(8):1301-1321.

Hallberg, K.B. 2010. New perspectives in acid mine drainage microbiology. *Hydrometallurgy*, *104*(3-4):448-453.

Hammarstrom, J.M. and Smith, K.S. 2002. Geochemical and mineralogic characterization of solids and their effects on waters in metal-mining environments. In Seal, R.R. II and Foley, N.K., (eds.) *Progress on geoenvironmental models for selected mineral deposit types: US Geological Survey Open-File Report*:8-54.

Hao, C., Wang, L., Dong, H., Zhang, H., 2010. Succession of acidophilic bacterial community during bio-oxidation of refractory gold-containing sulphides. Geomicrobiology Journal 27, 683-691

Harrison, S., Broadhurst, J.L., van Hille, R., Oyekola, O., Bryan, C., Hesketh, A. and Opitz, A. 2010. A systematic approach to sulphidic waste rock and tailings management to minimise acid rock drainage formation. Insert journal name, issue (vol): page range.

Herrell, M.K., McRae, C., Salzssauler, K. and Waples, J.S. 2009. Practical application of accelerated methods of acid rock drainage and metal leaching prediction of mine materials 8th International Conference on Acid Rock Drainage. June 23-26 Sweden.

Hesketh, A.H., Broadhurst, J.L., Bryan, C.G., Van Hille, R.P. and Harrison, S.T.L. 2010. Biokinetic test for the characterisation of AMD generation potential of sulfide mineral wastes. *Hydrometallurgy*, *104*(3-4):459-464.

Hlongwane, P. 2015.The influence of solid loading and particle size on the characterisation of sulphide containing ores using the biokinetic test: copper tailing case study, MSc thesis. University of Cape Town.

Hornberger, R.J. and Brady, K.B.C. 1998. Kinetic (leaching) tests for the prediction of mine drainage quality. *Coal mine drainage prediction and pollution prevention in Pennsylvania:* Harrisburg, Pennsylvania Department of Environmental Protection:7-1.

Jambor, J.L., Nordstrom, D.K. and Alpers, C.N. 2000. Metal-sulfate salts from sulfide mineral oxidation. *Reviews in Mineralogy and Geochemistry*, *40*(1):303-350.

Jambor, J.L. 1994. Mineralogy of sulfide-rich tailings and their oxidation products. *The environmental geochemistry of sulfide mine-wastes*, *22*:59-102.

Johnson, D.B. 1998. Biodiversity and ecology of acidophilic microorganisms. *FEMS microbiology ecology*, *27*(4):307-317.

Kotelo, L.O. 2013. *Characterising the acid mine drainage potential of fine coal wastes.* Doctoral dissertation, University of Cape Town.

Komadel, P. and Stucki, J.W. 1988. Quantitative assay of minerals for Fe (super 2+) and Fe (super 3+) using 1, 10-phenanthroline; III, A rapid photochemical method. *Clays and Clay Minerals*, *36*(4):379-381.

Lapakko, K. 2002. Metal mine rock and waste characterization tools: an overview. *Mining, Minerals and Sustainable Development*, *67*:1-30.

Lapakko, K.A., Engstrom, J.N. and Antonson, D.A., 2006, March. Effects of particle size on drainage quality from three lithologies. In *Poster paper presented at the 7th International Conference on Acid Rock Drainage (ICARD)* (pp. 1026-1050).

Lawrence, R.W. and Wang, Y. 1997, May. Determination of neutralization potential in the prediction of acid rock drainage. In *Proceedings of the fourth international conference on acid rock drainage.* 1: 451-464).

Lawrence, R.W. and Wang, Y. 1996. *Determination of Neutralization Potential for Acid Rock Drainage Prediction: A Report of Laboratory Investigations Prepared for Environment Canada*. Insert page range if available.

Lawrance, R.W., Ritcey, G.M., Poling, G.W., (1989). Strategies for the prediction of acid mine drainage. 13th Annual British Columbia Mine Reclamation Symposium, Vernon, BC, June 7-9:1-50.

Liu, C.W., Lin, K.H. and Kuo, Y.M. 2003. Application of factor analysis in the assessment of groundwater quality in a blackfoot disease area in Taiwan. *Science of the Total Environment*, *313*(1-3):77-89.

Loos, M.A., Cleghorn, C. and Mödinger, H. 2000. Occurrence of bacteria causing acid mine drainage in the outer layers of coal waste dumps in relation to abiotic ecological determinants and soil covers used for dump rehabilitation. *WRC Report*, (454/1/00).

Lottermoser, B.G. 2010. Sulfidic mine wastes. In Insert editor surname, initial. (ed). *Mine Wastes.* Berlin: Springer: 43-117.

Lottermoser, B. 2003. Mine Water. In Insert editor surname, initial. (ed). *Mine wastes*. Berlin: Springer: 83-141.

Makgae, M. 2011. Key areas in waste management: A South African perspective. In Kumar, S. (ed). *Integrated Waste Management-Volume II*. InTech: 69-82.

Mbamba, C.K., Harrison, S.T.L., Franzidis, J.P. and Broadhurst, J.L. 2012. Mitigating acid rock drainage risks while recovering low-sulfur coal from ultrafine colliery wastes using froth flotation. *Minerals Engineering*, *29*:13-21.

Manders, P., Godfrey, L. and Hobb, P. 2009. Insert title. *CSIR.* Available at www.csir.co.za/nre/docs/BrifingNote2009 This link is not active.

Morin, K.A. and Hutt, N.M. 1998, December. Kinetic tests and risk assessment for ARD. In *Fifth Annual British Columbia Metal Leaching and ARD Workshop* (pp. 9-10).

Miller, S., Robertson, A. and Donahue, T. 1997. Advances in acid drainage prediction using the net acid generation (NAG) test. In *Proc. 4th international conference on acid rock drainage, Vancouver, BC* (pp. 0533-549).

Morin, K.A. and Hutt, N.M. 1997. *Environmental geochemistry of minesite drainage: practical and case studies:* Vancouver*:* Minesite Drainage Assessment Group (MDAG) Publishing.

Mphephu, N.F. 2002. Rehabilitation of Tailings Dams on the Central Rand; Johannesburg. *Center for Applied Mining and Exploration Geology, University of the Witwatersrand*. Available: http://citeseerx.ist.psu.edu/viewdoc/download?doi=10.1.1.529.6510&rep=rep1&type=pdf.

Nengovhela, A.C., Yibas, B. and Ogola, J.S. 2006. Characterisation of gold tailings dams of the Witwatersrand Basin with reference to their acid mine drainage potential, Johannesburg, South Africa. *Water SA*, *32*(4):499-506.

Nordstrom, D.K. and Southam, G. 1997. Geomicrobiology of sulfide mineral oxidation. *Reviews in mineralogy*, *35*:361-390.

Nordstorm, D.K. and Alpers, C.N. 1999. Geochemistry of acid mine waste. *Reviews in economic geology. The environmental geochemistry of ore deposits A*, *6*:133-160.

Norris, P.R., Davis-Belmar, C.S., Brown, C.F. and Calvo-Bado, L.A. 2011. Autotrophic, sulfur-oxidizing actinobacteria in acidic environments. *Extremophiles*, *15*(2):155-163.

Oelofse, S.H.H., Hobbs, P.J., Rascher, J. and Cobbing, J.E. 2007, December. The pollution and destruction threat of gold mining waste on the Witwatersrand: A West Rand case study. In *10th International Symposium on Environmental Issues and Waste management in Energy and Mineral Production (SWEMP, 2007), Bangkok:* 11-13.

Opitz, A., Broadhurst, J. and Harrison, S. 2015. Assessing environmental risks associated with ultrafine coal wastes using laboratory-scale tests. Available: https://open.uct.ac.za/bitstream/handle/11427/25141/Opitz_2015.pdf?sequence=1.

Opitz, A.K.B. 2013. *An investigation into accelerated leaching for the purpose of ARD mitigation.* Doctoral dissertation, University of Cape Town.

Paktunc, A.D. 1999. Mineralogical constraints on the determination of neutralization potential and prediction of acid mine drainage. *Environmental Geology*, *39*(2):103-112.

Parbhakar-Fox, A., Lottermoser, B. and Bradshaw, D. 2013. Evaluating waste rock mineralogy and microtexture during kinetic testing for improved acid rock drainage prediction. *Minerals Engineering*, *52*:111-124.

Parbhakar-Fox, A.K. 2012. *Establishing the value of an integrated geochemistry-mineralogy-texture approach for acid rock drainage prediction* (Doctoral dissertation, University of Tasmania).

Parbhakar-Fox, A.K., Edraki, M. Walters, S & Bradshaw, D. 2011. Development of a textual index for the prediction of acid rock drainage. Mineral Engineering, 24: 1277-1287.

Parker, G.K., and Robertson, A. 1999. Acid mine drainage. In AMEEF Occasional paper no 11. Melbourne: Australian Minerals and Energy Environment Foundation: 101-117

Plante, B., Bussière, B. and Benzaazoua, M. 2012. Static tests response on 5 Canadian hard rock mine tailings with low net acid-generating potentials. *Journal of Geochemical Exploration*, 114:57-69.

Plumlee, G.S. 1999. The environmental geology of mineral deposits. *The environmental geochemistry of mineral deposits. Society of Economic Geologists. Part A*:71-116.

Price, W.A. 2009. Prediction manual for drainage chemistry from sulphidic geologic materials. *MEND report*, *1*(1):579. Give the page range, not just the first page.

Price, W.A. and Kwong, Y.T.I. 1997, May. Guidelines for the prediction of add rock drainage and metal leaching for mines in British Columbia: Part III Waste Rock Weathering, Sampling and Analysis, Some Lessons from the Provincial Database. In *Proceedings of the Fourth International Conference on Acid Rock Drainage, Vancouver, BC Canada*:31-45).

Rawlings, D.E. 2005. Characteristics and adaptability of iron-and sulfur-oxidizing microorganisms used for the recovery of metals from minerals and their concentrates. *Microbial cell factories*, *4*(1):1-15.

Ritchie, A.I.M. 1994. Sulfide oxidation mechanisms: controls and rates of oxygen transport. *The Environmental Geochemistry of Sulfide Mine Wastes*:201-245.

Rohwerder, T. and Sand, W. 2007. Mechanisms and biochemical fundamentals of bacterial metal sulfide oxidation. In Donati, E.R. and Sands, W. (eds). *Microbial processing of metal sulfides*. Dordrecht: Springer:35-58.

Rosner, T. 2001. *A preliminary assessment of pollution contained in the unsaturated and saturated zone beneath reclaimed gold-mine residue deposits*. WRC. Incomplete citation. Insert journal/proceedings/source. page range, etc.

Rousseau, P.D. 2012. A critical review of static geochemical test methods applied to mining wastes, including their applicability to field conditions. In *International Mine Water Association Symposium, Bunbury Australia*:499-504.

Sapsford, D.J., Bowell, R.J., Dey, M. and Williams, K.P. 2009. Humidity cell tests for the prediction of acid rock drainage. *Minerals Engineering*, *22*(1):25-36.

Sand, W., Jozsa, P.G., Kovacs, Z.M., Săsăran, N. and Schippers, A. 2007. Long-term evaluation of acid rock drainage mitigation measures in large lysimeters. *Journal of Geochemical Exploration*, *92*(2-3):205-211.

Schippers, A. 2007. Microorganisms involved in bioleaching and nucleic acid-based molecular methods for their identification and quantification. In Donati, E.R. and Sands, W. (eds). *Microbial processing of metal sulfide*. Dordrecht: Springer *s*:3-33

Singer, P.C. and Stumm, W. 1970. Acidic mine drainage: the rate-determining step. *Science*, *167*(3921):1121-1123.

Skousen, J., Simmons, J., McDonald, L.M. and Ziemkiewicz, P. 2002. Acid–base accounting to predict post-mining drainage quality on surface mines. *Journal of Environmental Quality*, *31*(6):2034-2044.

Skousen, J., Renton, J., Brown, H., Evans, P., Leavitt, B., Brady, K., Cohen, L. and Ziemkiewicz, P. 1997. Neutralization potential of overburden samples containing siderite. *Journal of Environmental Quality*, *26*(3):673-681.

Smart, R., Skinner, W.M., Levay, G., Gerson, A.R., Thomas, J.E., Sobieraj, H., Schumann, R., Weisener, C.G., Weber, P.A., Miller, S.D. and Stewart, W.A. 2002. ARD test handbook: project P387A, prediction and kinetic control of acid mine drainage. *AMIRA, International Ltd, Ian Wark Research Institute, Melbourne, Australia*.

Sobek, A.A. 1978. *Field and laboratory methods applicable to overburdens and minesoils*. Industrial Environmental Research Laboratory, Office of Research and Development, US Environmental Protection Agency.

Stewart, W., Schumann, R.C., Miller, S. and Smart, R.S.C. 2009. Development of prediction methods for ARD assessment of coal process wastes. Securing the future and 8th ICARD Conference, June 22-26, Skelleftea, Sweden.

Stewart, W.A., Miller, S.D. and Smart, R. 2006. *Advances in acid rock drainage (ARD) characterisation of mine wastes*. 7th International Conference on Acid Rock Drainage (ICARD), March 26-30, 2006, St. Louis, Missouri.

Tupikina, O.V., Minnaar, S.V., Van Hille, R.P., Van Wyk, N., Rautenbach, G.F., Dew, D. and Harrison, S.T.L. 2013. Determining the effect of acid stress on the persistence and growth of

thermophilic microbial species after mesophilic colonisation of low grade ore in a heap leach environment. *Minerals Engineering*, *53*:152-159.

Tributsch, H. 2001. Direct versus indirect bioleaching. *Hydrometallurgy*, *59*(2-3):177-185.

Vassilev, S.V. and Vassileva, C.G. 1996. Occurrence, abundance and origin of minerals in coals and coal ashes. *Fuel processing technology*, *48*(2):85-106.

Yibas, B., Pulles, W., Lorentz, S. and Maiyana, B. 2011. Development of water balances for operational and post-closure situations for gold mine residue deposits to be used as input to pollution prediction studies for such facilities. *Water Research Commission (WRC). WRC Report*, (1460/1), p.11.

Weber, P.A., Thomas, J.E., Skinner, W.M. and Smart, R.S.C. 2005. A methodology to determine the acid-neutralization capacity of rock samples. *The Canadian Mineralogist*, *43*(4):1183-1192.

White III, W.W., Lapakko, K.A. and Cox, R.L. 1999. Static-test methods most commonly used to predict acid-mine drainage: practical guidelines for use and interpretation. *Reviews in economic geology*, *6*:325-338.

APPENDICES

List of Tables

Appendix A

Appendix F

Appendix G

Appendix H

List of Figures

APPENDIX A : ARD Characterisation tests

Acid neutralization capacity tests

Table A 1: Fizz Ratings" and associated acid quantities and concentrations to be used in the ANC determination

		HCl		
Reaction	*Fizz rating*	*Molarity (M)*	*Volume (ml)*	*NaOH molarity (M)*
No reaction	0	0.5	4	0.1
Slight reaction	1	0.5	8	0.1
Moderate reaction	2	0.5	20	0.5
Strong reaction	3	0.5	40	0.5
Very strong rxn	4	1	40	0.5
	5*	1	60	0.5

*5 is used for very high ANC material (> 400 kgH_2SO_4/t) e.g. limestone

The standard ANC test was modified from the methodology developed by Sobek *et. Al* (1978).

1. 2 gram of -75µm fraction dry sample was accurately weighed and transferred into clean 250ml dry Erlenmeyer flasks.
2. A certain amount of Hydrochloric acid was added into the sample based on fizz rating.
3. 20 ml of deionized water was also added constantly in each sample using measuring cylinder.
4. Flasks were weighed in an electronic balance and the mass was recorded. Four blank flasks containing deionized water and appropriate amount of HCl were prepared for each fizz rating.
5. The flasks were heated in a hot plate at 90°C for a maximum of two hours until reaction stops.
6. This was indicated by non-evolution of gas bubbles and particles settled evenly at the bottom of the flask.
7. During heating deionised water was added occasionally to avoid dryness of the sample.
8. Upon the completion of the reaction, flasks were cooled at room temperature and deionised water was added to make up to their original weighs before heating.

9. The pH of the ANC solution was measured to determine if sample was correctly fizz rated and this was confirmed by pH between 0.8 to 1.5.
10. Those samples that had pH above 1.5 were fizz rated low and were changed into the next higher fizz, and samples that had pH were 0.8 were repeated on lower fizz because too much acid was added.
11. Samples were filtered to avoid any oxidation that could result from pyrite on solid residue.
12. The clear liquid was then back titrated into two end points of pH 5 and 7 using 0.5 molar concentration of NaOH.
13. Two drops of 30% H_2O_2 were added at pH 5 to precipitate ferrous iron into ferric iron.
14. Samples were further titrated to pH 7 and the amount of NaOH used was recorded.
15. The amount of HCl consumed was converted into Kg H_2SO_4/t using formula below.

Calculation of ANC

$$ANC = \frac{[Volume_{HCl} * M_{acid} - Volume_{NaOH} * C] * 49}{W_{sample}}$$

$$C = \frac{Volume_{HCl\ in\ blank}}{Volume_{NaOH\ titrated\ in\ blank}}$$

Where:

Y = (Vol. of HCl added) - (Vol. of NaOH titrated x B)

B = (Vol. of HCl in blank) / (Vol. of NaOH titrated in blank)

MHCl = Molarity of HCls

wt = Sample weight in grams

C = Conversion factor

C = 49.0 (to calculate kg H_2SO_4/ton)

C = 5.0 (to calculate % $CaCO_3$ equivalent)

Net Acid Generation test

1. The net acid Generation (NAG) is a static test that was used to provides direct empirical estimate of the overall sample reactivity.

2. This method was also employed in this study to determine the semi-soluble acid minerals such as sulphate and other potential acid generating sulphur bearing minerals.
3. NAG testing was carried out in accordance with the method described in Sobek et al*.*, 1978).
4. 250 ml of 15% H_2O_2 was added into an Erlenmeyer flask containing 2.5g of pulverised sample less than -75 µm fraction.
5. The H_2O_2 was allowed to react with the sample overnight, and the following day the NAG solution was gently heated in a hot plate to 90°C for a maximum of 2 hours.
6. Deionised water was added continuously to avoid dryness of the flasks.
7. The heating was done to remove excess H_2O_2 and also to facilitate the release of inherent neutralizing capacity such as carbonate buffering.
8. The solution was then allowed to cool at room temperature for a maximum of two hours.
9. Evaporation was accounted by addition of deionised water to make up the flasks into their pre-weighed volumes and this was followed by measuring and recording the NAG pH. The test also reports the NAG value, measured in equivalent kilograms of sulphuric acid (H_2SO_4) per tonne.
10. The above method was adapted for the test samples in order to trfffack the pH change through the latter portion of the test

Table A. 1: Composition of autotrophic basal salt media

Chemical compound	Mass (g)
$(NH4)_2SO_4$	7.5
$Na_2SO_4.10H_2O$	7.5
KCl	2.5
$MgSO_4.7H_2O$	25
KH_2PO_4	2.5
$Ca(NO3)_2.4H_2O$	2.5

1. Add 80ml of deionised water and 1ml of trace elements top up the solution to 1 litre. Sterilize the solution in an autoclave.
2. Dilute the 50x stock solution to make 1x ABS solution.
3. Adjust the pH of ABS using concentrated H_2SO_4 to pH 2

APPENDIX B : Inoculum preparation

1. Co-culture equal volumes of mesophilic mixed culture dominated *by Leptospirilum ferriphilum* (iron oxidiser) with *Acidthiobacillus caldus* (sulphur oxidiser).
2. Grow the microbial consortium in 0 K media supplemented with 3% pyrite in a 1litre shake flasks.
3. Incubate the flask at 37ºC shaking platform at 140rpm.
4. Conduct cell count using counting chamber and a light microscope at 100X with use of oil immersion.
5. Scat cells after 7 days by removing 10% of supernatant and replacing it with equal volumes of 0 K media
6. At cell concentration of 10^8, remove an aliquot of 100 ml, filter it and wash with citrate buffer to remove any residual iron and protons prior inoculations.
7. Suspend cells in filter disc into 10ul of ABS (pH 2) repeat cell counts.
8. Measure initial redox potential and pH of the inoculum
9. Calculate the suitable volume from the inoculum prior inoculation.

APPENDIX C : Batch biokinetic tests

Procedure

1. Weigh mass of an empty flask in an electronic balance and zero the machine.
2. Add 7.5g of an ore sample 100% passed -150 microns.
3. Add 150ml of 1X ABS solution pH 2 into 250ml Erlenmeyer shake flasks.
4. Introduce calculated cell concentration into respective flasks.
5. Weigh and record the initial mass of each flask before placing in an orbital shaker.
6. Place the shake flask in an orbital shaker at 37 ºC agitating at 150rpm for minimum of 90 days.

Sampling

NB: This was done daily for the first two weeks and every second day thereafter

1. Weigh flasks and topped up with acidified water pH 2 for (pH controlled flasks using burette) and deionised water for uncontrolled pH) to their original initial weights to compensate for evaporation.
2. Allow the flasks to settle down and pipette 100ul and store in Eppendorf tubes for metal analysis.
3. Record redox potential, pH and perform iron assay using 1-10 phenanthroline method.
4. Analyse sulphates by turbidity test with use of barium chloride for pH uncontrolled sample (10^9 and control with uncontrolled pH).
5. On day 45 sacrifice one flask from each inoculum size and perfume microbial speciation and mineralogical assessment on the residue. Mineralogy will be done on the residue on completion of the experiment.
6. Measure the absorbance with Helios UV-Vis spectrophotometer at a wavelength of 510 nm and insert into standard calibration curve to determine the concentrations of ferrous and iron total. Determine the difference between the two calculate ferric iron.
7. Insert the measured absorbance in the sulphate standard equation to determine the concentration.
8. The values obtained under each condition will be averaged and the standard deviation will be calculated. The averaged values for all the measured parameters (pH, $Fe^{2+,}$ Fe total and redox potential) will be plotted on a set of axes.

Ferrous iron and total iron concentration

- 1000ppm of standard ferrous iron solution was used.
- 250g of ammonium acetate buffer was dissolved in 700ml of concentrated glacial acetic acid.
- 1-10 phenanthroline indicator was prepared by dissolving 2127,708 mg in 100ml of deionised water in a 1000ml volumetric flask and topped up with deionised water to make a 1-10 phenanthroline indicator**.**
- The standard curve of ferrous iron concentration was prepared by adding 2mL ammonium acetate, 2mL 1-10 phenanthroline indicator in 3.125, 6.26, 12.5, 25 and 50ppm of ferrous standard in test tubes. To this 2 scoops of hydroxylamine were added for total iron**.** Results generated are presented in below.

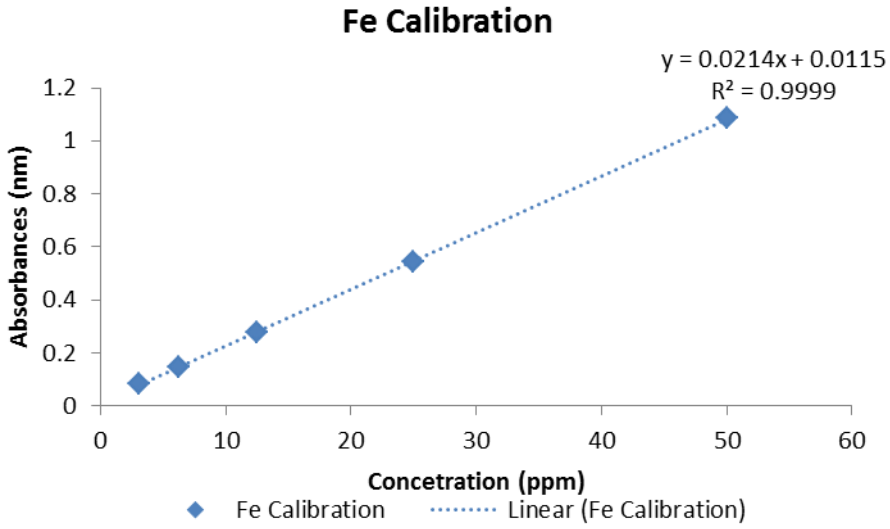

Figure C 1: Fe calibration curve

Prepare conditioning reagent as follows

- Dissolve 75 g NaCl in 30 of HCl (32%), 50 mL glycerol, and 100 mL of ethanol in 300mL of deionise water.
- Smash/grind barium chloride between 20 to 30 finer.

- Standard sulphate solution of 100mg/L is prepared by diluting 10.4 mL titrasol of 0.02 n H_2SO_4 in 100 mL of deionised water or dissolve 0.1479 g of Na_2SO_4 in 1 L deionised water.

Test procedure

- Add 5 mL of the diluted sample to a test tube.
- Add 0.25 mL of conditioning reagent and a scoop of finer barium chloride.
- Vortex for 1 minute.
- Read absorbance at 420 nm.
- The absorbance values were inserted into a sulphate standard curve to calculate the sulphate concentration.

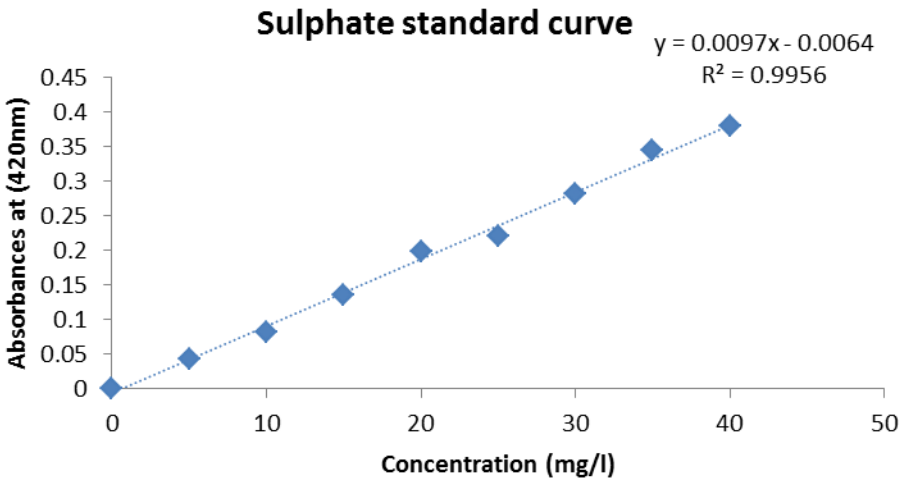

Figure C 2: Sulphate calibration curve

APPENDIX D : Draw and Fill Biokinetic test

Procedure

1. Add 7.5g of the ore sample to the flasks
2. Add 150 ml deionised water to a 250 ml Erlenmeyer flasks in the morning and incubate at 37 ^{O}C (150rpm).
3. Record the mass of each flask before placing in an orbital shaker.
4. In the afternoon remove flasks from the orbital shaker and allow the solids to settle down.
5. Withdraw 15ml of the supernatant and replace it with equal volume of deionised water
6. Prior to withdrawal of the supernatant, measure pH and redox potential and stored 2ml for metal analysis and store in Eppendorf tubes.
7. Sterilize the ABS solution in an autoclave.
8. Adjust the pH of ABS media using concentrated H_2SO_4 to pH 2.

Sampling

1. Sample every day, by removing 10% (15mL) of the supernatant using syringe and replace with equal volume of ABS at pH 2.
2. Pellet cells every fifth day for microbial speciation.
3. Replace flasks on shaking incubator.

APPENDIX E : Microbial Speciation

Washing of cells from biokinetic tests

1. Allow the flask to settle down for 2 hours.
2. Label 5x2ml Eppendorf tubes for each flask.
3. Pipette 2ml of the liquid from each flask into each tube.
4. Centrifuge at 13000rpm for 10 minutes.
5. Remove supernatant and add another 2ml of the liquid from the flask into the same tube.
6. Centrifuge at 13000rpm for 10 minutes.
7. Add 1ml of 10mMcitrate buffer to each tube and flick each tubes to wash cells.
8. Centrifuge at 13000rpm for 10 minutes.
9. Repeat steps 7 and 8.
10. Add 1ml TE buffer, flick gentle to wash the pellets.
11. Centrifuge at 13000rpm for 10 minutes, remove supernatant.
12. Repeat 10 and 11.
13. Add 200µl TE buffer to each tube, re-suspend gently and combine the 5 tubes from each flask into 1 tube.
14. Centrifuge at 13000rpm for 10 minutes.
15. Remove the supernatant and store the pellet at -20^{O}C.

APPENDIX F : Experimental results

ARD characterisation

Table F 1: Summery of ARD characterisation tests results obtained from ANC and NAG test

Waste Sample	Sulphur Grade [%]	MPA [kg H_2SO_4/ton]	ANC [kg H_2SO_4/ton]	NAPP [kg H_2SO_4/ton]	NAG pH	ARD Classification
Sample 1	2.3 ± 0.0	70.2 ± 0.7	53.2 ± 1.8	17.0 ± 1.9	2.5 ± 0.0	Potentially acid forming
Sample 2	3.15 ± 0.1	96.3 ± 1.7	3.39 ± 0.2	92.9 ± 1.7	2.63 ± 0.0	Potentially acid forming

Table F 2: Measured pH and standard deviation for non-controlled pH batch Biokinetic test sample 1

	Non-inoculated		10^7		10^8		10^9		10^10	
Day	pH	Stdev	pH	Stdev	pH	Stdev	pH	Stdev	Stdev	
0	2.45	0.22	2.51	0.17	2.55	0.15	2.52	0.08	pH	Stdev
1	3.94	0.09	4.83	0.77	4.74	0.47	4.09	0.56	2.58	0.02
4	4.91	0.14	4.70	0.03	4.78	0.09	4.43	0.36		0.13
5	5.45	0.21	4.39	0.26	4.74	0.11	4.42	0.42	4.01	0.21
6	5.21	0.11	4.22	0.16	4.51	0.15	4.25	0.29	3.98	0.48
7	5.11	0.04	3.90	0.44	4.26	0.21	4.16	0.20	3.82	0.03
8	5.14	0.14	3.81	0.01	3.93	0.02	3.96	0.04	3.75	0.02
9	5.06	0.10	3.69	0.13	3.73	0.05	3.77	0.12	3.69	0.22
10	4.36	0.52	3.66	0.11	3.68	0.03	3.67	0.12	3.67	0.23
11	4.31	0.48	3.71	0.13	3.70	0.03	3.78	0.16	3.63	0.24
12	4.32	0.40	3.67	0.11	3.68	0.03	3.79	0.15	3.64	0.13
13	4.05	0.66	3.70	0.09	3.67	0.05	3.75	0.15	3.61	0.13
14	3.96	0.65	3.70	0.10	3.66	0.02	3.66	0.10	3.63	0.14
15	3.99	0.37	3.25	0.10	3.72	0.01	3.72	0.10	3.47	0.04
16	3.93	0.37	3.43	0.10	3.82	0.02	3.81	0.11	3.11	0.04
17	3.96	0.35	3.48	0.10	3.83	0.05	3.85	0.11	2.41	0.05
18	3.87	0.23	3.39	0.10	3.78	0.05	3.77	0.07	2.28	0.04
19	4.03	0.54	3.49	0.49	3.77	0.04	3.78	0.08	2.19	0.05
20	3.76	0.63	3.55	0.47	3.80	0.06	3.83	0.06	2.17	0.06
21	3.05	0.13	3.83	0.49	3.68	0.13	3.79	0.06	2.15	0.05
22	2.89	0.21	3.52	0.43	3.58	0.15	3.77	0.06	2.12	0.06
23	3.09	0.07	2.85	0.37	3.43	0.13	3.34	0.44	2.12	0.05
24	2.81	0.32	2.51	0.43	3.41	0.10	3.08	0.79	2.07	0.07

25	2.81	0.26	2.30	0.40	3.37	0.09	3.08	0.78	2.07	0.08
26	2.76	0.28	2.20	0.38	3.21	0.08	2.88	0.56	2.08	0.08
27	2.64	0.23	2.19	0.39	2.98	0.02	2.57	0.16	2.08	0.07
28	2.63	0.23	2.20	0.41	2.72	0.12	2.52	0.20	2.11	0.07
30	2.32	0.09	2.09	0.43	2.31	0.11	2.29	0.17	2.14	0.07
32	2.27	0.10	2.06	0.35	2.27	0.19	2.26	0.17	2.05	0.08
34	2.20	0.13	2.07	0.28	2.21	0.15	2.22	0.15	2.07	0.12
36	2.19	0.08	2.06	0.27	2.13	0.08	2.13	0.08	2.07	0.17
38	2.20	0.09	2.08	0.30	2.14	0.08	2.15	0.08	2.07	0.77
40	2.20	0.10	2.09	0.37	2.16	0.07	2.18	0.08	2.09	0.03
42	2.22	0.09	2.13	0.44	2.18	0.07	2.19	0.05	2.11	0.26
44	2.19	0.08	2.13	0.46	2.16	0.06	2.16	0.04	2.16	0.16
46	2.16	0.07	2.12	0.46	2.13	0.05	2.14	0.04	2.16	0.44
48	2.08	0.06	2.05	0.08	2.06	0.04	2.07	0.03	2.15	0.01
50	2.14	0.06	2.14	0.12	2.12	0.04	2.14	0.02	2.08	0.13
52	2.06	0.07	2.10	0.17	2.07	0.04	2.10	0.02	2.18	0.11
54	1.99	0.07	2.06	0.77	2.02	0.03	2.06	0.02	2.14	0.13
56	2.01	0.07	2.07	0.03	2.04	0.02	2.07	0.02	2.10	0.11
58	2.03	0.07	2.08	0.26	2.06	0.02	2.09	0.02	2.11	0.09
60	2.05	0.07	2.09	0.16	2.07	0.01	2.10	0.02	2.12	0.10
62	2.07	0.07	2.10	0.44	2.09	0.01	2.12	0.01	2.12	0.10
64	2.08	0.06	2.12	0.01	2.11	0.01	2.15	0.06	2.13	0.10
66	2.07	0.06	2.11	0.13	2.10	0.01	2.12	0.03	2.16	0.10
68	2.05	0.06	2.10	0.11	2.09	0.01	2.09	0.00	2.16	0.10
70	2.05	0.03	2.11	0.13	2.07	0.02	2.07	0.00	2.15	0.49
72	2.05	0.03	2.13	0.08	2.09	0.02	2.09	0.01	2.16	0.47
74	2.07	0.03	2.17	0.12	2.10	0.03	2.12	0.01	2.16	0.49
76	2.05	0.03	2.14	0.17	2.08	0.04	2.08	0.00	2.19	0.43
78	2.05	0.03	2.14	0.77	2.07	0.03	2.09	0.01	2.15	0.37
81	2.05	0.02	2.15	0.03	2.09	0.02	2.10	0.01	2.16	0.43
83	2.07	0.02	2.15	0.26	2.10	0.03	2.10	0.00	2.16	0.40
85	2.09	0.02	2.19	0.16	2.13	0.03	2.12	0.00	2.18	0.38
88	2.07	0.02	2.18	0.44	2.11	0.04	2.12	0.01	2.20	0.23
90	2.06	0.02	2.21	0.01	2.13	0.04	2.13	0.02	2.19	0.35

Table F 3: Redox potential measured and standard deviation

	Non-inoculated		10^7		10^8		10^9		10^10	
Day	**Redox**	**Stdev**	**Redox**	**Stdev**	**Redox**	**Stdev**	**Redox**	**Stdev**	**Redox**	**Stdev**
0	424	6	440	13	422	6	424	7	424	1
1	302	5	260	82	250	33	294	36	295	89
4	223	19	226	10	220	8	241	23	258	58
5	214	12	234	15	227	11	244	23	258	36
6	219	11	241	12	238	14	247	23	255	54

7	200	7	242	16	237	15	241	18	247	47
8	171	31	244	18	243	9	243	6	246	12
9	180	65	260	19	263	2	258	7	257	16
10	239	30	265	8	265	2	266	5	264	17
11	231	36	244	10	250	4	254	3	249	0
12	236	26	244	7	243	7	248	6	251	1
13	235	45	250	6	249	5	249	7	281	1
14	222	70	291	14	246	3	247	6	317	1
15	257	39	281	13	259	6	260	4	271	1
16	267	53	310	10	289	17	282	5	624	3
17				12						3
18	254	52	313	11	262	4	257	10	625	3
19	266	57	317	10	267	8	258	4	675	6
20	272	65	320	10	277	7	262	5	688	5
21	410	53	272	10	297	10	273	1	692	2
22	452	89	331	5	309	16	290	3	668	5
23	389	22	418	4	326	18	349	72	690	5
24	452	110	487	6	325	11	477	245	716	7
25	454	97	645	14	327	11	451	204	697	6
26	464	94	686	15	352	13	461	136	694	1
27	478	72	686	7	400	18	598	104	691	4
28	521	89	685	9	478	52	625	76	700	4
30	617	59	689	10	695	10	686	2	707	1
32	552	68	700	8	645	77	589	69	712	3
34	590	23	713	9	645	58	712	11	720	10
36	623	44	707	6	708	14	702	13	725	11
38	610	48	705	7	701	9	688	3	716	2
40	597	53	703	6	694	4	675	19	706	2
42	664	27	694	6	697	6	686	15	686	2
44	670	12	681	5	691	25	697	10	695	2
46	675	28	667	7	685	44	708	6	704	11
48	637	48	693	8	700	2	673	50	699	29
50	659	10	698	8	686	28	683	3	690	22
52	662	25	700	38	696	15	694	3	695	26
54	665	44	701	42	705	2	705	4	700	35
56	667	34	700	40	704	1	702	2	699	1
58	669	25	699	38	702	1	700	1	697	1
60	671	18	697	32	701	2	697	1	696	2
62	673	18	696	33	700	3	695	2	694	3
64	630	42	689	48	700	3	671	40	688	3
66	647	34	684	49	700	3	681	24	688	3
68	664	31	679	31	700	5	692	8	688	5
70	699	3	691	26	692	14	686	7	682	14
72	661	44	690	15	695	8	685	10	689	8

74	695	4	692	23	700	4	696	1	685	4
76	691	11	683	26	671	26	685	6	684	26
78	688	6	686	29	695	5	693	0	684	5
81	663	50	681	50	686	5	685	5	682	5
83	677	13	678	54	680	8	690	1	680	8
85	683	8	675	54	677	10	685	1	675	10
88	681	3	679	57	687	5	693	4	681	5
90	676	5	670	52	682	5	684	5	672	5

Table F 4: Ferrous iron measured and standard deviation

	Non-inoculated		10^7		10^8		10^9		10^10	
Day	**[Fe^{2+}]**	**Stdev**	**[Fe^{2+}]**	**Stdev**	**[Fe^{2+}]**	**Stdev**	**[Fe^{2+}]**	**Stdev**	**[Fe^{2+}]**	**Stdev**
0	14.399	0.138	6.603	1.225	13.763	0.994	15.513	0.861	13.286	0.276
1	40.016	2.714	41.687	34.331	56.563	2.894	64.757	7.830	75.815	37.205
4	14.161	24.527	123.389	14.851	105.489	2.578	105.012	12.345	437.947	0.138
5	42.243	7.267	162.768	20.902	130.231	0.066	145.823	27.198	351.631	2.714
6	43.198	6.089	200.318	43.889	150.438	20.051	162.609	33.253	373.588	24.527
7	51.392	6.068	231.504	57.146	182.021	30.318	171.440	38.294	389.419	7.267
8	66.985	43.914	294.352	65.542	249.403	44.201	200.636	59.868	432.617	6.089
9	86.794	50.341	378.361	44.153	344.789	30.383	316.229	19.636	334.368	6.068
10	129.117	30.023	412.251	60.007	365.951	34.694	331.424	26.615	383.453	43.914
11	142.482	27.934	424.264	82.065	362.132	67.677	328.958	27.571	401.114	50.341
12	157.677	21.618	354.654	63.413	363.246	59.450	298.329	39.280	538.186	30.023
13	188.703	20.902	435.959	24.302	405.489	40.511	350.756	34.157	280.907	27.934
14	228.958	43.889	438.663	19.914	433.890	33.857	388.425	25.145	285.919	21.618
15	242.641	57.146	468.894	35.943	442.562	38.867	401.074	32.233	322.673	176.483
16	240.732	65.542	449.006	37.128	213.206	18.239	377.088	41.853	1.193	181.633
17	239.936	44.153	456.165	20.210	429.594	30.590	378.520	29.702	1.193	194.583
18	250.915	60.007	483.930	50.589	453.620	41.077	425.776	21.601	10.740	191.291
19	286.794	82.065	503.182	48.888	492.045	39.692	426.014	10.126	28.640	195.246
20	246.937	63.413	538.186	35.554	478.918	40.990	435.800	8.776	0.477	198.381
21	202.705	133.986	570.883	62.008	497.693	43.498	436.754	11.476	14.797	185.743
22	169.610	142.936	586.158	53.959	492.761	50.642	441.050	24.302	5.728	208.121
23	243.119	80.029	404.296	27.583	487.033	49.084	382.339	47.253	6.683	211.410
24	193.954	160.489	115.990	66.815	508.831	70.722	216.229	276.092	8.115	188.059
25	165.314	145.338	0.477	60.859	502.466	86.245	204.296	288.243	5.251	215.412
26	323.628	281.469	42.959	16.817	476.929	80.186	367.303	512.020	17.661	263.781
27	94.670	161.906	1.193	53.583	431.185	101.973	5.967	1.688	17.900	254.374
28	78.361	133.659	4.773	50.657	144.391	152.936	1.193	0.000	1.193	187.065
30	24.662	26.852	26.253	35.640	65.235	59.908	7.757	2.531	8.353	160.897
32	11.456	3.789	26.730	59.139	11.774	6.006	12.649	9.113	16.706	157.773
34	0.252	6.890	0.706	56.296	0.426	0.000	0.374	0.844	0.637	154.197
36	8.353	12.401	10.740	52.664	1.193	0.000	31.026	0.016	8.353	172.095

38	19.491	5.213	11.933	59.752	17.900	6.229	26.253	5.063	17.900	169.361
40	30.628	14.237	13.126	172.286	34.606	12.459	21.480	28.689	27.446	156.922
42	16.706	17.659	25.060	176.261	15.115	13.727	2.387	24.567	45.346	183.014
44	10.143	10.888	13.723	178.744	11.734	12.577	1.790	0.844	29.236	157.280
46	3.580	4.134	2.387	53.558	8.353	12.401	1.193	0.000	13.126	207.152
48	21.480	16.054	1.193	58.834	8.751	6.785	15.513	5.063	15.513	201.796
50	1.193	0.000	1.193	67.214	9.944	7.579	1.193	0.000	7.160	27.378
52	3.978	4.823	2.387	66.454	6.961	1.378	5.967	6.750	13.126	25.895
54	6.762	9.645	3.580	66.534	3.978	4.823	10.740	13.501	19.093	18.395
56	6.862	7.757	4.475	69.551	4.574	3.534	9.696	10.337	15.513	4.823
58	6.961	5.886	5.370	63.877	5.171	2.259	8.652	7.172	11.933	9.645
60	7.060	4.061	6.265	49.031	5.768	1.048	7.607	4.008	8.353	7.757
62	7.160	7.160	7.160	60.270	6.364	1.048	6.563	3.519	4.773	5.886
64	3.182	3.182	3.580	67.598	5.569	0.689	2.983	0.844	3.580	4.061
66	6.364	6.364	5.967	69.390	10.342	3.646	4.773	3.375	7.757	7.160
68	9.547	9.547	8.353	53.568	15.115	3.646	6.563	7.594	11.933	3.182
70	7.955	7.955	25.060	52.237	10.740	7.672	8.950	0.844	11.933	6.364
72	10.342	19.093	10.740	51.845	1.591	7.672	2.387	1.688	1.193	9.547
74	2.784	2.784	4.773	60.934	7.160	3.157	12.530	2.531	4.773	7.955
76	8.751	8.751	1.193	53.848	1.193	0.689	1.193	0.000	1.193	19.093
78	3.580	14.320	4.773	43.841	15.115	10.762	10.143	2.531	7.160	2.784
81	14.320	14.320	14.320	57.753	16.706	8.605	16.110	9.282	16.706	8.751
83	2.387	5.967	14.320	50.517	15.115	9.719	17.303	17.720	10.740	14.320
85	5.967	5.967	5.967	35.525	7.160	0.006	3.580	0.000	1.193	14.320
88	12.331	12.331	20.286	22.840	16.309	6.890	24.463	9.282	27.446	5.967

Table F 5: Total iron measured and standard deviation for sample

	Non-inoculated		**10^7**		**10^8**		**10^9**		**10^10**	
Day	**[Fe^{Tot}]**	**Stdev**	**[Fe^{Tot}]**	**Stdev**	**[Fe^{Tot}]**	**Stdev**	**[Fe^{Tot}]**	**Stdev**	**[Fe^{Tot}]**	**Stdev**
0	13.604	6.024	2.864	1.654	13.206	4.568	9.467	2.139	7.080	2.552
1	39.459	3.478	40.095	34.340	54.654	2.711	63.564	6.188	77.247	42.033
4	12.888	22.322	114.797	0.138	98.568	3.423	112.411	2.128	414.558	17.551
5	44.232	5.370	168.496	2.714	133.811	16.449	151.790	26.427	356.722	0.138
6	46.142	6.156	202.784	24.527	153.302	19.583	164.916	33.140	394.590	2.714
7	56.563	6.068	236.356	7.267	191.249	34.030	180.111	39.863	397.454	24.527
8	70.167	44.273	301.114	6.089	254.336	42.763	207.001	58.151	441.766	7.267
9	80.589	44.217	363.723	6.068	329.435	31.169	300.477	17.746	204.057	6.089
10	122.912	28.785	392.363	43.914	349.642	35.105	317.741	25.211	286.814	6.068
11	149.324	28.370	422.514	50.341	367.940	74.456	331.185	26.595	307.876	43.914
12	159.348	21.533	431.583	30.023	361.177	63.052	319.173	49.682	321.599	50.341
13	189.737	20.407	439.857	27.934	406.444	41.073	351.472	34.523	289.976	30.023
14	237.550	40.580	449.722	21.618	450.915	25.732	400.000	38.140	291.647	27.934
15	242.482	54.936	470.883	37.717	444.630	39.295	403.938	32.908	336.993	21.618
16	227.526	61.288	472.872	38.533	224.901	39.295	397.136	41.178	489.260	186.875

17	248.210	52.072	479.236	21.729	452.029	36.921	401.671	35.440	521.480	209.249
18	251.949	60.349	489.021	49.712	456.484	43.621	429.952	23.458	523.866	204.334
19	287.987	81.008	533.811	47.735	500.000	32.484	450.477	4.219	671.838	207.141
20	251.074	66.982	559.905	34.104	486.714	35.574	448.449	4.219	671.122	199.127
21	225.776	114.380	575.656	63.178	496.420	44.668	433.652	17.889	697.375	187.153
22	201.114	125.784	597.136	55.004	496.738	52.439	445.823	10.463	550.835	211.101
23	245.823	63.175	443.914	25.563	462.053	46.651	377.566	23.626	553.699	215.088
24	225.139	107.171	374.224	62.311	485.760	67.116	317.422	166.060	629.117	192.877
25	241.687	75.370	449.642	54.781	529.992	90.808	344.630	123.533	706.444	216.002
26	508.035	139.291	525.060	23.931	496.897	82.748	644.391	174.836	763.723	72.736
27	223.150	102.347	547.733	50.877	488.067	107.060	258.353	54.847	714.797	122.520
28	256.563	46.047	594.272	48.336	398.170	60.805	219.570	27.002	678.998	6.497
30	221.559	68.190	584.726	36.356	400.159	95.423	300.716	96.194	631.265	6.497
32	256.165	36.805	732.220	58.032	436.277	134.898	387.112	128.933	712.172	7.510
34	300.318	28.473	842.482	52.489	508.751	167.670	445.704	145.978	760.143	10.126
36	297.136	47.553	818.616	40.232	526.253	197.713	405.728	28.689	724.344	10.126
38	318.616	31.278	799.523	55.455	544.153	196.362	463.604	74.255	717.184	2.025
40	340.095	22.767	780.430	53.561	562.053	195.475	521.480	119.820	710.024	14.345
42	346.858	29.481	920.048	51.509	589.101	190.857	541.169	151.041	708.831	14.345
44	333.731	20.377	832.339	58.280	593.477	171.565	552.506	134.165	683.771	11.307
46	320.605	15.891	744.630	59.018	597.852	153.577	563.842	117.289	658.711	26.327
48	395.784	18.729	712.411	55.254	659.507	181.840	618.735	103.788	643.198	22.837
50	328.958	36.456	708.831	65.165	640.016	148.300	589.499	81.005	619.332	27.367
52	330.748	28.642	710.621	62.172	640.811	140.982	601.432	91.131	597.852	24.879
54	332.538	22.777	712.411	60.831	641.607	135.883	613.365	101.256	576.372	21.095
56	336.913	27.222	635.740	68.501	642.104	108.610	617.393	84.169	564.737	33.759
58	341.289	31.836	559.069	64.245	642.601	81.768	621.420	67.082	553.103	47.092
60	345.664	36.555	482.399	53.972	643.099	55.981	625.447	49.995	541.468	114.913
62	350.040	41.343	405.728	61.797	643.596	33.759	629.475	32.908	529.833	276.909
64	385.839	0.027	584.726	62.095	636.436	47.092	613.962	48.097	500.000	75.560
66	376.889	47.976	565.036	58.317	754.972	114.913	609.189	83.536	484.487	22.526
68	367.940	65.863	545.346	55.150	873.508	276.909	604.415	118.976	468.974	35.527
70	375.099	72.157	627.685	54.292	669.849	75.560	628.878	118.976	514.320	48.340
72	383.850	100.921	535.800	53.758	593.477	22.526	587.112	42.190	467.780	31.625
74	357.200	86.195	531.026	62.023	575.577	35.527	595.465	20.251	485.680	40.096
76	293.158	85.963	424.821	57.820	513.126	48.340	550.716	9.282	342.482	59.094
78	330.151	78.108	448.687	54.228	540.971	31.625	539.379	8.438	398.568	70.000
81	349.642	96.644	489.260	55.606	536.993	40.096	546.539	45.565	359.189	48.868
83	348.449	85.877	491.647	49.976	536.595	59.094	563.842	26.158	546.539	59.054
85	341.289	85.877	434.368	18.228	505.967	70.000	512.530	4.219	363.962	23.098
88	330.549	101.277	412.888	20.542	498.807	48.868	653.938	141.759	354.415	33.450
90	334.5267	84.459	366.3484	27.0017	471.3604	59.0541	494.0334	10.1256	348.4487	21.213

Table F 6: Sulphate measured and standard deviation

	Non-inoculated		10^7		10^8		10^9		10^10	
Day	**$[SO_4^{2-}]$**	**Stdev**	**$[SO_4^{2-}]$**	**Stdev**	**$[SO_4^{2-}]$**	**Stdev**	**$[SO_4^{2-}]$**	**Stdev**	**$[SO_4^{2-}]$**	**Stdev**
0	719.271	62.701	907.813	240.381	990.104	385.796	808.854	133.521	847.396	66.316
1	1056.250	41.340	1389.063	308.649	1257.292	209.260	1462.500	141.895	1275.521	285.335
4	1456.848	5.756	2965.625	164.623	1578.125	212.132	1609.375	135.564	1033.594	125.953
5	853.646	35.642	1939.583	0.138	1818.750	150.228	1950.000	99.363	2330.208	150.228
6	1734.375	32.626	2079.167	2.714	2018.750	66.144	2015.625	88.609	2357.292	66.144
7	1865.625	32.626	2160.417	24.527	1912.500	99.853	2035.417	130.516	2662.500	99.853
8	1565.625	263.076	2189.583	7.267	2029.167	242.391	1958.333	42.197	2378.125	242.391
9	1734.375	32.626	2079.167	2.714	2018.750	66.144	2015.625	88.609	2357.292	66.144
10	1513.542	153.804	1912.500	6.068	1784.375	105.002	1606.250	36.039	1778.125	105.002
11	1734.375	273.219	2172.917	43.914	2215.625	91.590	2010.417	70.318	2329.167	91.590
12	1550.000	194.956	2210.417	50.341	2083.333	87.964	1873.958	368.171	2454.167	87.964
13	2045.833	104.785	2341.667	30.023	2595.833	126.566	2290.625	275.692	2810.417	126.566
14	2244.792	223.221	2529.167	27.934	2265.625	136.609	2307.813	37.565	2540.625	136.609
15	2123.958	92.773	2313.542	21.618	2284.375	156.531	2125.000	88.388	2428.125	156.531
16	1541.667	219.114	1864.583	184.622	1736.458	96.892	1571.875	145.841	2515.625	96.892
17	1734.375	32.626	2079.167	2.714	2018.750	66.144	2015.625	88.609	2357.292	66.144
18	2266.667	232.730	2675.000	95.828	2655.208	107.089	2660.938	19.887	3503.125	316.942
19	2430.208	248.085	2382.292	145.952	2481.250	219.352	2523.438	130.373	3971.875	459.379
20	2253.125	90.409	2726.563	144.259	2652.083	163.886	2285.938	236.439	3521.875	515.107
21	1934.375	10.825	2968.750	145.651	2464.583	85.086	2201.563	121.534	3731.250	441.134
22	1986.458	337.621	3634.375	101.406	2570.833	61.264	2478.125	79.550	4428.125	383.909
23	1388.542	164.540	1643.750	72.439	1687.500	186.115	1607.813	90.598	3093.750	237.972
24	1387.500	94.580	2109.375	82.107	1738.542	109.702	1448.438	6.629	3409.375	306.521
25	2041.667	187.717	3059.375	99.437	2319.792	318.341	2485.938	298.311	3443.750	324.827
26	4028.125	209.072	3171.875	0.090	4050.000	430.786	4109.375	154.680	3631.250	321.463
27	2084.375	103.125	3250.000	86.532	2067.708	494.188	1996.875	4.419	3962.500	305.132
28	2189.583	203.253	3400.000	23.123	2317.708	189.812	2275.000	464.039	3878.125	265.098
30	1770.833	240.530	3431.250	2.210	2181.250	384.654	1979.688	497.184	3471.875	192.245
32	1933.333	393.952	3478.045	138.032	2303.125	424.966	2190.625	605.460	3937.500	319.897
34	1692.708	171.579	2593.750	189.992	1809.896	314.479	1773.438	563.476	2507.813	485.536
36	2687.500	497.091	4062.500	68.916	2361.458	355.005	3206.250	813.173	4284.375	576.190
38	2673.958	560.309	4175.000	30.352	2860.417	453.917	3200.000	815.383	4089.063	194.964
40	2660.417	718.861	4287.500	92.492	3359.375	553.954	3193.750	817.592	3893.750	276.599
42	3081.250	221.479	4203.125	153.391	3659.375	681.959	3581.250	234.229	4203.125	385.711
44	2960.938	250.366	4175.000	174.170	3411.979	375.392	3464.063	282.843	4040.625	527.980
46	2840.625	294.281	4146.875	149.424	3164.583	302.856	3346.875	95.017	3878.125	645.184
48	2965.625	184.136	3900.000	90.697	3482.292	469.763	3354.688	643.025	3234.375	761.866
50	3325.000	112.283	3525.000	273.546	3061.458	173.721	3195.313	254.116	3603.125	620.895

52	3247.917	87.519	3506.250	231.847	3322.917	287.017	3250.000	134.792	3343.750	587.145
54	3170.833	67.194	3487.500	147.052	3584.375	400.329	3304.688	134.792	3084.375	112.283
56	3212.240	59.878	3497.656	127.488	3642.188	344.272	3364.453	255.774	3039.844	87.519
58	3253.646	65.780	3507.813	247.586	3700.000	288.314	3424.219	376.755	2995.313	67.194
60	3295.052	82.096	3517.969	283.331	3757.813	177.080	3483.984	497.737	2950.781	59.878
62	3336.458	104.036	3528.125	248.478	3815.625	232.529	3543.750	618.718	2906.250	65.780
64	3353.125	30.136	3603.125	360.749	3905.208	117.524	3817.188	19.887	3496.875	82.096
66	3322.396	82.032	3575.000	287.200	3821.354	129.615	3753.906	54.138	3354.688	104.036
68	3291.667	136.299	3546.875	76.056	3737.500	142.213	3690.625	128.163	3212.500	30.136
70	3405.208	195.315	3609.375	106.066	3386.458	718.018	3745.313	50.823	3331.250	82.032
72	3201.042	89.286	3656.250	98.980	3537.500	533.534	3257.813	541.379	3318.750	136.299
74	3295.833	194.287	3175.000	86.342	3662.500	81.908	3793.750	57.452	3175.000	195.315
76	4229.167	82.765	3421.875	76.549	3538.542	462.736	3770.313	209.922	2834.375	89.286
78	3528.125	100.146	3075.000	209.922	3815.625	126.823	3620.313	218.761	3200.000	194.287
81	2803.125	81.250	2431.250	157.091	2909.375	145.338	3409.375	366.812	2450.000	89.012
83	3554.167	206.872	3321.875	154.753	3385.417	620.652	3840.625	366.812	3028.125	100.146
85	3314.583	152.753	3125.000	36.039	3487.500	18.750	3531.250	26.517	2909.375	81.250
88	3180.208	319.077	2815.625	373.255	3453.125	139.614	3253.125	22.097	2771.875	206.872
90	3279.167	122.727	2943.750	479.507	3295.833	98.094	3368.750	287.262	2825.000	152.753

Table F 7: Avarage16sRNA copy number for non-controlled pH Biokinetic test per 10ng of DNA for sample 1 end of experiment (day 90)

samples	UniBact	*Acidithiobacillus caldus*	*Leptospirillum ferriphilum*	UniArch	*Acidiplasma cupricumulans*
Inoculum	6.12E+05	9.96E+04	1.25E+06	3.10E+03	6.32E+03
B1	2.88E+05	5.39E+04	2.25E+05	4.00E+05	5.92E+02
B2	3.00E+05	1.16E+05	1.60E+05	7.11E+04	7.35E+02
B3	6.57E+05	1.70E+05	4.33E+05	9.64E+04	1.15E+03
B4	4.05E+05	3.27E+03	4.54E+05	1.60E+06	6.70E+02
B5	1.99E+05	4.45E+03	3.96E+05	4.41E+05	7.19E+02
B6	3.56E+05	5.76E+04	2.10E+05	7.37E+05	1.21E+03
B7	6.85E+05	1.78E+05	7.11E+05	4.41E+05	1.14E+03
B9	3.67E+05	1.15E+04	3.64E+05	3.71E+06	1.16E+03
B10	4.69E+05	3.70E+03	9.85E+04	3.89E+04	1.64E+03
B18	4.40E+04	6.18E+02	1.62E+04	2.71E+04	8.88E+02

Table F 8: pH measured and standard deviation for sample 1

	Non-inoculated		10^7		10^8		10^9		10^10	
Day	pH	Stdev	pH	Stdev	pH	Stdev	pH	Stdev	pH Std	
0	2.00		2.00		2.00		2.00		2.00	
1	3.18	0.19	2.85	0.02	3.07	0.06	3.18	0.12	3.25	0.05
2	2.44	0.10	2.44	0.02	2.40	0.03	2.98	1.10	2.43	0.08
3	2.36	0.21	2.32	0.03	2.22	0.06	2.29	0.07	2.40	0.24
4	2.17	0.04	2.16	0.04	2.14	0.04	2.20	0.04	2.29	0.12
5	2.13	0.03	2.08	0.03	2.06	0.02	2.26	0.10	2.25	0.18
6	2.12	0.03	2.23	0.23	2.44	0.03	2.19	0.06	1.70	0.75
7	2.07	0.02	6.00	2.44	6.00	2.41	2.16	2.16	1.86	1.99
8	2.02	0.02	2.41	0.03	2.12	0.03	2.09	0.11	1.86	0.13
9	1.79	0.03	2.05	0.36	1.73	0.03	1.95	0.33	1.63	0.08
10	2.07	0.01	1.93	0.19	1.86	0.09	1.95	0.01	1.81	0.10
11	2.20	0.17	1.90	0.17	1.84	0.09	1.98	0.08	1.80	0.10
12	2.25	0.03	1.81	0.09	1.80	0.09	1.95	0.10	1.78	0.10
13	2.33	0.26	1.78	0.07	1.75	0.07	1.89	0.05	1.77	0.08
14	2.09	0.08	1.80	0.06	1.76	0.06	1.89	0.04	1.79	0.08
15	1.95	0.03	1.79	0.06	1.75	0.06	1.87	0.04	1.79	0.09
16	1.83	0.05	1.72	0.07	1.69	0.07	1.82	0.02	1.74	0.08
18	1.78	0.05	1.71	0.08	1.69	0.08	1.82	0.02	1.75	0.06
20	1.82	0.06	1.74	0.04	1.72	0.04	1.79	0.01	1.75	0.06
22	1.75	0.05	1.72	0.06	1.71	0.06	1.80	0.02	1.77	0.05
24	1.72	0.06	1.70	0.06	1.69	0.06	1.79	0.03	1.78	0.06
26	1.66	0.04	1.65	0.07	1.64	0.06	1.74	0.02	1.70	0.06
28	1.66	0.05	1.65	0.06	1.65	0.06	1.73	0.04	1.72	0.06
30	1.68	0.05	1.68	0.07	1.68	0.05	1.78	0.03	1.74	0.04
32	1.68	0.05	1.64	0.01	1.66	0.06	1.76	0.02	1.74	0.06
36	1.68	0.06	1.66	0.05	1.64	0.05	1.75	0.04	1.74	0.06
38	1.67	0.03	1.67	0.06	1.65	0.06	1.76	0.04	1.74	0.04
40	1.66	0.04	1.67	0.05	1.65	0.05	1.74	0.03	1.73	0.06
43	1.66	0.06	1.66	0.04	1.63	0.04	1.72	0.03	1.70	0.04
45	1.65	0.06	1.67	0.05	1.66	0.05	1.75	0.02	1.73	0.04
47	1.64	0.04	1.66	0.05	1.65	0.05	1.75	0.02	1.72	0.04
50	1.67	0.04	1.66	0.03	1.68	0.04	1.74	0.02	1.71	0.03
52	1.65	0.04	1.64	0.03	1.67	0.04	1.71	0.02	1.69	0.01
54	1.69	0.04	1.69	0.04	1.72	0.05	1.77	0.02	1.76	0.02
57	1.67	0.04	1.66	0.04	1.67	0.03	1.72	0.01	1.70	0.01
59	1.70	0.04	1.69	0.04	1.72	0.03	1.75	0.01	1.75	0.01
61	1.63	0.04	1.63	0.04	1.66	0.02	1.69	0.02	1.70	0.02
64	1.70	0.06	1.67	0.04	1.70	0.02	1.72	0.02	1.73	0.01
67	1.71	0.05	1.73	0.06	1.73	0.01	1.73	0.04	1.77	0.02
70	1.66	0.04	1.69	0.00	1.72	0.01	1.69	0.02	1.72	0.00

73	1.68	0.04	1.69	0.06	1.72	0.01	1.71	0.02	1.75	0.00
76	1.68	0.04	1.68	0.06	1.70	0.01	1.69	0.02	1.74	0.01
79	1.70	0.04	1.71	0.06	1.73	0.00	1.71	0.01	1.77	0.01
82	1.72	0.04	1.73	0.05	1.73	0.00	1.72	0.02	1.77	0.02
86	1.69	0.04	1.71	0.06	1.73	0.01	1.71	0.03	1.78	0.02

Table F 9: Redox potential measured and standard deviation for sample 1

	Non-inoculated		**10^7**		**10^8**		**10^9**		**10^10**	
Day	Redox	Stdev	Redox	Stdev	Redox	Stdev	Redox	Stdev	Redox	stdev
0										
1	359	5	355	4	310	56	310	45	334	58
2	342	20	335	2	332	14	319	86	471	49
3	334	7	326	6	344	4	392	46	512	45
4	336	8	331	3	361	4	445	92	544	20
5	335	8	347	1	416	17	452	113	558	13
6	336	6	383	3	527	19	496	120	600	67
7		343	0	489	0	549	0	500		620
8	337	8	552	13	620	53	574	80	627	12
9	344	12	617	47	644	43	585	5	676	43
10	356	26	655	31	614	66	628	48	658	54
11	424	98	697	18	680	56	626	78	699	29
12	507	68	666	52	665	14	666	45	666	45
13	554	72	632	69	715	3	619	44	726	4
14	725	4	726	13	735	2	666	89	698	36
15	722	8	710	22	681	76	670	98	703	50
16	731	4	734	4	722	23	696	62	716	22
18	687	34	707	1	700	27	715	3	718	3
20	732	6	704	32	706	59	687	54	732	5
22	693	4	729	18	740	3	698	58	710	35
24	746	3	744	3	745	3	743	3	736	4
26	747	5	739	2	739	3	740	1	735	3
28	741	8	739	6	740	4	738	6	731	6
30	738	15	740	6	742	3	745	4	736	3
32	735	7	736	5	734	2	726	29	739	4
36	744	4	742	7	739	4	744	5	737	3
38	734	5	741	7	742	3	728	18	724	8
40	751	3	744	7	734	15	744	6	736	7
43	751	4	745	9	740	3	734	10	737	5
45	728	6	727	6	727	4	720	9	721	3
47	712	11	717	5	720	3	720	3	723	2
50	729	13	728	3	729	2	729	4	726	6
52	727	18	731	6	727	1	727	1	728	5

54	715	7	717	3	718	1	719	2	716	4
57	727	1	719	1	723	1	722	4	722	2
59	713	6	713	4	716	1	718	3	714	1
61	728	1	722	2	726	3	713	13	720	0
64	725	3	723	2	725	1	717	18	718	1
67	719	3	717	1	713	6	716	3	713	1
70	715	4	716	6	718	1	722	6	715	2
73	725	0	722	3	720	1	723	2	715	2
76	721	3	715	5	716	5	717	5	709	5
79	713	6	715	5	710	1	702	7	707	6
82	717	4	717	2	715	2	718	0	713	1
86	710	3	714	2	707	2	706	1	702	1
90	713	9	716	4	716	1	716	1	710	2

Table F 10: Ferrous iron measured and standard deviation for sample

	Non-inoculated		**10^7**		**10^8**		**10^9**		**10^10**	
Day	Fe^{2+}	Stdev	Fe^{2+}	Stdev	Fe^{2+}	Stdev	Fe^{2+}	Stdev	Fe^{2+}	stdev
0	273.628	12.969	43.898	0.511	48.075	1.580	43.161	1.397	6.470	0.751
1	409.255	38.639	267.322	2.736	269.943	2.650	177.232	121.751	201.966	115.543
2	481.736	50.009	410.483	3.336	416.052	19.937	281.491	31.582	143.571	242.289
3	556.511	65.399	478.624	5.200	464.373	39.523	164.783	0.198	1.802	3.121
4	665.029	70.839	565.930	26.272	407.043	56.462	174.038	240.411	13.104	0.709
5	4.372	97.798	613.432	43.648	37.265	26.243	26.003	24.984	21.294	3.546
6	796.069	743.653	19.641	189.599	8.888	56.921	60.100	48.321	29.946	30.303
7	857.903	124.782	69.206	80.618	17.199	12.826	68.387	113.171	11.876	3.949
8	827.191	130.397	34.398	22.351	25.389	8.362	27.437	3.753	36.036	32.834
9	639.640	155.323	23.342	16.252	12.285	2.457	21.294	26.272	8.190	2.837
10	322.686	524.789	22.113	1.229	32.760	60.033	18.428	1.229	17.609	3.546
11	61.835	277.903	42.998	24.662	70.025	52.164	33.579	11.415	17.609	11.415
12	23.751	60.613	55.692	41.919	50.778	48.215	13.923	3.753	8.190	3.092
13	32.351	18.886	70.025	87.275	34.398	38.790	11.876	0.709	12.285	5.355
14	15.971	0.262	145.373	109.690	28.256	16.065	22.523	6.766	20.885	3.250
15		10.496	9.828	1.229	28.665	30.524	11.466	0.110	6.143	3.686
17	16.380	16.380	10.647	3.753	11.876	6.183	10.238	3.949	20.885	19.190
19	35.627	24.199	18.837	3.753	18.428	3.250	17.609	9.302	18.837	5.674
21	13.104	1.419	17.609	3.092	14.333	1.419	14.333	4.314	10.647	1.877
23	24.161	15.360	18.837	3.949	23.342	6.143	16.790	2.557	49.550	48.682
25	15.971	7.473	14.742	2.128	13.104	2.557	14.742	2.457	23.751	15.604
27	13.923	11.415	14.742	4.429	20.066	13.476	22.932	18.482	8.190	1.419
29	17.199	3.686	25.389	6.766	19.656	0.000	23.342	5.630	16.790	5.540
31	18.837	4.651	22.932	8.887	21.294	1.877	23.342	5.355	23.751	2.557
35	2.867	1.877	1.229	1.229	4.505	3.949	2.048	0.709	11.466	3.092
37	20.475	6.766	21.294	5.540	22.005	5.329	23.342	3.250	14.742	2.128

39	12.695	1.877	14.333	3.546	15.892	4.890	15.152	1.877	15.971	3.250
42	22.523	3.753	50.369	48.955	17.522	3.735	25.799	3.250	18.837	4.314
44	4.095	7.093	0.410	0.709	22.005	7.436	9.828	10.496	0.819	1.419
46	32.351	16.589	33.170	10.919	44.825	11.025	37.674	11.932	27.846	3.753
49	32.510	20.043	42.998	27.798	22.005	5.187	25.184	6.081	17.199	5.212
51	19.656	13.899	19.656	1.737	18.949	2.593	15.971	1.737	26.413	19.980
53	12.899	11.293	14.742	0.000	15.892	5.187	41.155	40.828	10.442	7.818
56	34.398	29.535	12.899	2.606	15.892	13.831	15.971	1.737	11.057	3.475
58	28.870	40.828	23.955	25.194	4.279	0.864	10.442	11.293	2.455	3.472
60	31.327	16.505	3.070	4.342	0.000	0.000	7.371	6.949	6.755	0.870
63	17.813	9.555	12.900	4.342	17.726	6.051	27.641	0.869	10.445	0.870
66	22.113	15.636	15.971	12.162	15.281	4.322	19.042	2.606	19.656	10.424
69	14.128	0.869	9.214	0.869	12.225	0.000	7.985	2.606	19.656	3.475
72	14.128	0.869	12.899	0.869	22.616	7.780	24.570	0.000	20.270	2.606
75	25.184	0.869	30.713	17.374	28.729	0.864	18.428	5.212	25.799	1.737
78	20.270	6.081	12.285	158.100	19.560	3.458	20.270	0.869	20.885	0.000
81	15.356	9.555	13.514	1.737	18.337	3.458	17.199	13.899	27.641	21.717
85	14.128	2.606	20.270	11.293	53.178	63.104	14.128	7.818	17.813	2.606
89	26.413	2.606	28.256	1.737	4.890	1.729	17.199	5.212	22.113	6.949

Table F 11: Total iron measured and standard deviation for sample 1

	Non-inoculated		**10^7**		**10^8**		**10^9**		**10^10**	
Day	Fe^{Tot}	Stdev	Fe^{Tot}	Stdev	Fe^{Tot}	Stdev	Fe^{Tot}	Stdev	Fe^{Tot}	stdev
0.00	64.62	13.21	53.07	1.23	56.35	2.63	52.01	5.04	23.18	3.86
1.00	276.33	37.67	270.52	3.07	273.22	2.14	186.08	126.54	271.58	58.02
2.00	520.88	257.80	544.80	231.67	549.30	220.27	455.77	250.61	661.26	252.72
3.00	741.44	450.86	730.96	431.95	709.17	371.00	707.04	488.18	1205.41	490.01
4.00	571.25	71.73	581.49	61.53	572.89	93.61	724.41	222.66	958.64	685.88
5.00	681.41	96.83	680.59	37.28	895.99	19.05	967.24	366.46	1467.65	170.71
6.00	66.57	748.98	144.32	904.18	12.21	1452.50	12.39	1193.69	6.74	1597.46
7.00	814.50	115.63	1542.59	187.02	1814.50	70.13	1320.23	507.56	1694.51	34.75
8.00	893.53	115.85	1838.25	70.08	1926.70	33.20	1580.67	507.56	1708.03	144.44
9.00	847.26	123.04	1858.31	88.33	1852.58	8.06	1681.41	326.27	1610.97	91.48
10.00	934.48	116.12	1902.54	76.88	1911.55	60.03	1817.77	191.03	1656.02	108.38
11.00	1120.39	42.40	1896.81	85.01	1935.71	13.81	1710.07	120.77	1710.07	120.77
12.00	1628.58	98.28	1901.31	115.68	1969.29	28.57	1860.77	100.41	1692.47	110.92
13.00	1762.90	296.10	1904.18	69.61	1914.82	4.65	1873.46	72.86	1746.93	104.85
14.00	1873.87	321.73	1966.83	85.01	1971.74	29.36	1887.80	123.90	1757.17	143.62
15.00	1781.74	319.51	1855.45	74.05	1885.75	34.20	1815.32	135.08	1683.05	122.87
17.00	1841.93	316.01	1895.99	95.45	1931.20	31.94	1841.11	42.92	1788.29	124.05
19.00	1863.23	301.98	1914.41	113.30	1938.17	61.11	1859.54	39.74	1748.98	129.09
21.00	1866.50	330.20	1965.19	55.95	1970.11	79.86	1873.05	25.57	1791.15	119.34
23.00	2032.76	530.13	1971.33	73.61	1985.67	68.36	1918.92	62.85	1791.56	126.97

25.00	1872.24	365.79	1975.02	64.15	1988.94	45.29	1907.04	26.95	1794.02	112.42
27.00	1833.74	393.43	1936.12	75.69	1975.43	68.10	1964.37	92.68	1785.83	96.11
29.00	1884.93	389.76	2043.00	152.31	2065.93	36.70	1941.44	20.72	1810.81	103.61
31.00	1855.04	430.67	1991.81	60.19	1987.31	76.92	1998.77	48.40	1836.61	76.20
35.00	1884.93	455.24	1994.68	58.84	2088.04	29.70	1959.87	15.84	1825.14	11.01
37.00	1858.31	412.83	2021.29	133.32	2040.13	58.54	1944.72	73.78	1803.85	78.44
39.00	1836.61	380.34	2067.98	74.57	2140.46	88.37	2001.64	85.35	2035.63	87.79
42.00	1924.65	449.71	1987.71	115.42	2087.63	101.37	1975.02	27.26	2001.64	124.91
44.00	1961.10	488.99	2047.50	76.53	2135.95	55.90	2098.28	152.91	2031.53	160.67
46.00	1879.20	422.42	1946.36	101.23	2081.49	22.83	1988.12	78.03	1858.72	60.83
49.00	1761.06	515.13	1997.54	57.33	2133.29	185.03	2044.23	173.74	1759.21	1.74
51.00	1807.13	529.90	2046.68	36.48	2046.68	36.48	2113.02	187.64	1960.07	212.83
53.00	1779.48	492.54	1967.44	46.04	2094.59	93.82	2105.04	2.61	1914.00	45.17
56.00	1778.26	365.71	2006.14	29.54	2062.04	52.99	2138.21	152.02	1856.88	73.84
58.00	1886.36	695.81	2047.91	3.48	2030.12	26.93	1971.74	34.75	2129.61	37.36
60.00	1781.33	510.78	2006.14	69.49	2156.64	212.83	2016.58	47.78	2089.07	178.08
63.00	1760.44	496.89	2003.08	33.88	2008.08	42.53	2005.53	7.82	1861.80	80.79
66.00	1769.04	489.94	2027.64	125.96	2083.54	26.06	2059.58	125.96	1929.98	86.87
69.00	1781.94	469.96	1903.56	2.61	2051.60	13.90	1989.56	58.20	1925.06	15.64
72.00	1820.64	399.59	2058.97	130.30	2163.39	81.66	2017.81	25.19	1867.32	59.07
75.00	1808.35	550.74	2056.51	138.99	2050.98	11.29	2141.28	180.69	1915.23	85.13
78.00	1764.13	481.25	2116.71	158.10	2101.35	18.24	2013.51	8.69	1933.66	5.21
81.00	1754.30	528.16	1992.01	49.51	2054.67	18.24	1961.92	90.34	1862.41	17.37
85.00	1730.96	545.53	2011.06	46.91	2080.47	132.91	2072.48	135.51	2035.63	175.47
89.00	1765.97	551.61	1975.43	85.13	2080.47	132.91	1936.12	13.90	1851.97	25.19

Table F 12: Avarage16sRNA copy number for non-controlled pH biokinetic test per 10ng of DNA for sampl 1 end of experiment (day 45)

	UniBact	**Atc**	**LH**	**Atf**	**Att**	**LT**	**UniArch**	**JTC3**	**JTC1/2**
I0	1.37E+07	2.14E+06	5.08E+06	0.00E+00	4.67E+02	1.47E+03	3.25E+05	1.82E+05	5.67E+04
A1	2.44E+06	3.05E+04	1.65E+05	0.00E+00	0.00E+00	0.00E+00	1.31E+06	1.71E+05	2.81E+06
A2	1.90E+06	7.17E+03	2.14E+05	0.00E+00	0.00E+00	0.00E+00	3.58E+06	3.36E+05	1.00E+06
A3	1.39E+07	3.61E+06	4.92E+06	0.00E+00	1.28E+03	1.93E+03	2.00E+06	3.56E+05	2.03E+05
B3	1.34E+07	5.25E+06	3.53E+06	0.00E+00	2.44E+03	1.49E+03	1.99E+06	2.56E+05	6.58E+05
C1	3.29E+06	1.59E+04	3.70E+05	0.00E+00	0.00E+00	0.00E+00	1.06E+06	1.14E+05	1.90E+06
C2	1.86E+06	2.22E+05	4.40E+05	0.00E+00	0.00E+00	0.00E+00	3.62E+06	4.28E+05	2.88E+06
C3	3.87E+06	1.67E+06	1.20E+06	0.00E+00	6.16E+02	0.00E+00	3.67E+06	2.95E+05	4.01E+06
D1	1.95E+06	2.27E+04	3.75E+05	0.00E+00	0.00E+00	0.00E+00	3.83E+06	4.29E+05	6.49E+06
D3	5.86E+06	2.07E+06	1.84E+06	0.00E+00	7.27E+02	0.00E+00	3.72E+06	4.65E+05	5.68E+06
E1	1.89E+06	3.24E+05	2.28E+05	0.00E+00	0.00E+00	0.00E+00	4.24E+06	8.67E+05	6.84E+06
E2	1.98E+06	7.14E+03	1.71E+05	0.00E+00	0.00E+00	0.00E+00	2.10E+06	4.69E+05	2.36E+06
E3	8.98E+06	4.49E+06	1.61E+06	0.00E+00	1.75E+03	0.00E+00	1.94E+06	5.02E+05	9.60E+05
F3	1.59E+07	8.74E+06	2.87E+06	0.00E+00	2.45E+03	0.00E+00	3.56E+05	1.52E+02	2.83E+06
G3	3.81E+06	8.18E+05	6.50E+05	0.00E+00	3.22E+02	9.74E+02	3.45E+06	8.56E+04	8.76E+06

Table F 13: pH measured and standard deviation for sample 2

	Non-inoculated		10^7		10^8		10^9		10^10	
Day	pH	Stdev	pH	Stdev	pH	Stdev	pH	Stdev	pH	Stdev
0	2.00	0.01	2.04	0.01	2.04	0.00	2.04	0.01	2.00	0.03
1	2.30		2.32		2.29		2.29		2.21	
2	2.36	0.02	2.37	0.05	2.33	0.02	2.31	0.02	2.23	0.02
3	2.50		2.51		2.45		2.39		2.33	
4	2.44	0.02	2.42	0.03	2.35	0.03	2.34	0.04	2.26	0.04
5	2.46		2.43		2.34		2.35		2.30	
6	2.50	0.01	2.46	0.07	2.40	0.00	2.37	0.01	2.34	0.05
7	2.52		2.44		2.41		2.36		2.33	
8	2.55	0.01	2.44	0.01	2.44	0.03	2.41	0.01	2.38	0.06
9	2.56		2.44		2.45		2.41		2.30	
10	2.57	0.04	2.39	0.08	2.49	0.03	2.45	0.01	2.37	0.05
11	2.59		2.48		2.50		2.45		2.38	
12	2.60	0.02	2.49	0.06	2.53	0.04	2.48	0.01	2.40	0.06
14	2.63	0.01	2.47	0.09	2.55	0.05	2.50	0.05	2.42	0.06
16	2.46		2.48		2.51		2.46		2.36	
17	2.52		2.44		2.55		2.51		2.39	
18	2.41		2.34		2.51		2.47		2.35	
19	2.38		2.31		2.51		2.48		2.36	
21	2.35	0.06	2.28	0.22	2.51	0.01	2.48	0.04	2.34	0.04
22	2.36	0.07	2.26	0.22	2.52	0.01	2.51	0.05	2.36	0.05
25	2.26	0.08	2.22	0.22	2.51	0.03	2.44	0.08	2.33	0.08
29	2.16	0.13	2.17	0.27	2.46	0.02	2.44	0.08	2.33	0.14
33	2.20	0.11	2.06	0.31	2.41	0.03	2.35	0.07	2.23	0.11
38	2.21	0.12	2.02	0.31	2.38	0.02	2.34	0.07	2.21	0.10
40	2.22	0.13	2.00	0.21	2.41	0.03	2.35	0.07	2.23	0.10
46	2.14	0.13	1.99	0.28	2.31	0.03	2.23	0.11	2.13	0.10
49	2.10	0.13	1.99	0.23	2.28	0.04	2.20	0.13	2.11	0.11
51	2.10	0.13	1.96	0.24	2.28	0.04	2.22	0.12	2.12	0.12
53	2.05	0.11	1.95	0.25	2.25	0.04	2.18	0.10	2.08	0.11
56	2.08	0.13	1.94	0.25	2.26	0.05	2.18	0.10	2.08	0.11
60	2.06	0.12	1.95	0.23	2.22	0.05	2.15	0.07	2.04	0.10
64	2.03	0.11	1.95	0.23	2.22	0.04	2.13	0.06	2.03	0.10
68	1.99	0.11	1.96	0.22	2.21	0.03	2.11	0.08	1.92	0.06
72	1.99	0.09	1.93	0.23	2.21	0.04	2.10	0.08	2.00	0.11
76	1.97	0.09	1.95	0.22	2.22	0.05	2.11	0.09	1.99	0.10
80	1.93	0.08	1.95	0.21	2.19	0.05	2.08	0.10	1.97	0.09
84	1.93	0.07	1.93	0.21	2.16	0.06	2.06	0.10	1.95	0.10
88	1.92	0.08	1.92	0.00	2.16	0.03	2.06	0.11	1.95	0.09

Table F 14: Redox potential measured and standard deviation for sample 2

	Non-inoculated		10^7		10^8		10^9		10^10	
Day	Redox	Stdev	Redox	Stdev	Redox	Stdev	Redox	Stdev	Redox	Stdev
0	379	9	393	19	386	3	369	10	387	27
1	352		358		362		373		408	
2	347	3	350	3	355	3	375	25	441	2
3	347		372		378		388		441	
4	343	3	359	12	431	6	397	41	479	24
5	347		412		481		458		507	
6	347	2	379	23	544	13	564	5	526	15
7	347		533		555		575		559	
8	345	1	560	30	581	9	597	12	557	27
9	352		610		617		614		606	
10	364	28	617	4	618	15	608	12	630	14
11	442		628		609		614		627	
12	637	15	646	6	632	9	635	4	643	18
14	658	3	659	9	627	13	643	4	653	15
16	657		661		645		647		655	
17	653		661		646		651		658	
18	659		656		644		626		664	
19	667		681		656		654		668	
21	669	3	657	5	657	5	659	1	669	7
22	663	5	675	20	655	3	658	4	666	9
25	663	4	683	7	653	4	659	1	670	2
29	648	18	683	21	659	5	670	5	670	12
33	640	22	666	22	644	9	645	18	658	14
38	649	18	669	13	656	11	668	2	668	9
40	658	13	681	2	662	8	669	6	673	1
46	674	16	668	16	650	4	668	8	682	7
49	675	15	673	11	661	14	664	8	684	8
51	675	14	677	20	656	21	663	12	679	5
53	682	14	666	23	655	23	662	9	679	3
56	670	32	662	28	662	28	662	9	680	3
60	688	13	674	26	649	16	666	7	684	13
64	688	11	662	21	635	2			669	13
68	693	10	669	22	642	8	645	24	670	27
72	698	4	674	21	640	13	654	18	676	19
76	694	5	663	14	646	9	657	16	677	17
80	695	8	668	13	656	4	660	17	683	14
84	683	8	650	13	641	6	657	15	673	16
88	691	5	664	6	659	3	663	10	681	15

Table F 15: Ferrous iron measured and standard deviation

	Non-inoculated		**10^7**		**10^8**		**10^9**		**10^10**	
Day	$[Fe^{2+}]$	Stdev	$[Fe^{2+}]$	Stdev	$[Fe^{2+}]$	Stdev	$[Fe^{2+}]$	Stdev	$[Fe^{2+}]$	Stdev
0	9.86	8.12	4.53	0.48	5.01	0.72	6.92	1.45	14.24	1.10
1	50.91		48.13		43.75		40.57		19.09	
2	77.96	3.84	81.54	15.34	65.23	3.00	58.07	18.54	39.78	42.30
3	73.99		74.38		70.01		27.05		42.56	
4	89.50	15.51	78.36	11.09	46.14	30.76	49.32	2.76	35.00	60.63
5	86.71		50.12		7.56		0.00		40.97	
6	0.00	0.00	0.80	0.69	8.75	7.95	6.76	6.79	37.39	62.71
7	97.85		6.76		7.96		10.50		42.16	
8	89.10	1.82	2.78	3.84	0.00	0.00	20.68	35.83	27.05	36.08
9	91.09		5.97		7.16		6.76		13.52	
10	77.57	27.96	1.19	2.07	3.98	6.89	1.19	1.19	1.19	1.19
11	33.02		15.51		0.80		1.19		0.80	
12	2.39	3.16	7.56	9.04	11.14	17.22	1.19	0.00	1.99	1.38
14	36.60	46.91	11.93	4.13	6.36	1.82	4.38	2.48	5.17	4.82
16	4.38		1.99		5.97		9.15		0.00	
17	0.00		7.56		6.36		9.15		17.10	
18	1.63		20.68		3.98		0.00		1.99	
19	0.00		0.00		0.00		0.00		0.00	
21	0.00	0.00	0.00	0.00	0.00	0.00	0.00	0.00	0.00	0.00
22	0.00	0.00	0.00	0.00	0.00	0.00	0.00	0.00	0.00	0.00
25	2.78	4.82	1.99	3.44	0.00	0.00	5.17	8.96	5.57	9.65
29	6.76	11.71	10.34	2.48	8.35	7.45	16.71	7.95	5.17	5.38
33	0.00	0.00	0.00	0.00	0.00	0.00	0.00	0.00	0.00	0.00
38	0.00	0.00	7.96	1.82	0.00	0.00	0.00	0.00	0.00	0.00
40	2.78	4.82	5.17	6.99	0.00	0.00	0.40	0.69	1.19	2.07
46	0.00	0.00	2.78	4.82	0.00	0.00	0.00	0.00	0.00	0.00
49	16.31	5.38	1.99	2.48	3.98	0.69	13.92	1.82	0.00	0.00
51	0.00	0.00	8.75	6.89	0.00	0.00	0.00	0.00	2.78	2.48
53	0.00	0.00	0.00	0.00	0.00	0.00	0.00	0.00	0.00	0.00
56	4.77	8.27	0.00	0.00	0.00	0.00	0.00	0.00	0.00	0.00
60	15.91	11.28	10.34	4.82	5.57	1.82	1.59	2.76	17.10	1.38
64	3.58	3.16	9.94	3.84	2.78	0.69	1.99	3.44	18.30	3.65
68	5.57	1.38	19.09	2.39	11.93	1.19	21.08	16.29	6.36	2.48
72	6.48	4.63	5.97	2.07	13.92	0.69	7.56	4.52	5.17	1.82
76	9.55	1.19	3.18	5.51	9.15	0.69	15.53	0.00	0.00	0.00
80	12.33	2.76	0.00	0.00	9.15	0.69	5.97	1.19	0.00	0.00
84	0.00	0.00	0.00	0.00	0.00	0.00	1.19	2.07	0.00	0.00
88	1.19	1.19	0.00	0.00	0.00	0.00	0.00	0.00	0.00	0.00

APPENDIX G : Draw and fill biokinetic test results for sample 1

Table G 1: pH measured and standard deviation

	Non-inoculated			Inoculated		
Day	**pH**	**Stdev**	**$[H^+]$**	**pH**	**Stdev**	**$[H^+]$**
0	3.05	0.58	0.001	3.47	0.06	0.000
1	5.80	0.47	0.000	5.77	0.18	0.000
1	3.28	0.04	0.001	3.31	0.05	0.000
2	5.00	0.09	0.000	4.63	0.07	0.000
2	3.15	0.12	0.001	3.17	0.04	0.001
3	4.84	0.16	0.000	4.29	0.06	0.000
3	3.13	0.04	0.001	3.05	0.01	0.001
4	3.91	0.30	0.000	3.74	0.06	0.000
4	2.97	0.04	0.001	2.95	0.01	0.001
5	3.42	0.04	0.000	3.38	0.02	0.000
5	2.93	0.01	0.001	2.54	0.01	0.003
6	3.42	0.05	0.000	2.83	0.01	0.001
6	2.96	0.01	0.001	2.65	0.02	0.002
7	3.24	0.03	0.001	2.92	0.19	0.001
7	2.90	0.02	0.001	2.76	0.12	0.002
8	2.69	0.14	0.002	2.32	0.01	0.005
8	2.67	0.14	0.002	2.35	0.01	0.004
9	2.64	0.15	0.002	2.41	0.05	0.004
9	2.64	0.08	0.002	2.36	0.04	0.004
10	2.71	0.08	0.002	2.29	0.10	0.005
10	2.54	0.05	0.003	2.26	0.09	0.006
11	2.61	0.03	0.002	2.16	0.14	0.007
11	2.47	0.03	0.003	2.14	0.13	0.007
12	2.85	0.09	0.001	2.20	0.13	0.006
12	2.67	0.07	0.002	2.18	0.12	0.007
13	2.53	0.01	0.003	2.09	0.10	0.008
13	2.45	0.01	0.004	2.13	0.07	0.007
14	2.57	0.04	0.003	2.12	0.07	0.008
14	2.50	0.03	0.003	2.11	0.06	0.008
15	2.40	0.07	0.004	2.04	0.05	0.009
15	2.33	0.05	0.005	2.11	0.05	0.008
16	2.32	0.06	0.005	2.02	0.03	0.009
16	2.29	0.05	0.005	2.02	0.03	0.010
17	2.26	0.06	0.005	2.03	0.03	0.009
17	2.21	0.05	0.006	2.02	0.02	0.010
18	2.23	0.07	0.006	2.00	0.02	0.010
18	2.20	0.07	0.006	2.00	0.02	0.010
19	2.17	0.05	0.007	2.00	0.03	0.010

19	2.14	0.05	0.007	1.99	0.03	0.010
20	2.16	0.04	0.007	2.06	0.03	0.009
20	2.16	0.03	0.007	2.05	0.03	0.009
21	2.11	0.02	0.008	2.01	0.03	0.010
21	2.11	0.03	0.008	2.00	0.02	0.010
22	2.08	0.02	0.008	2.01	0.03	0.010
22	2.08	0.02	0.008	2.01	0.02	0.010
23	2.09	0.01	0.008	2.04	0.05	0.009
23	2.09	0.01	0.008	2.03	0.03	0.009
24	2.04	0.01	0.009	1.99	0.02	0.010
24	2.03	0.01	0.009	1.98	0.02	0.010
25	2.07	0.01	0.008	2.03	0.02	0.009
25	2.06	0.01	0.009	2.02	0.02	0.010
26	2.03	0.01	0.009	1.99	0.02	0.010
26	2.02	0.01	0.010	2.00	0.02	0.010
27	2.03	0.01	0.009	2.01	0.03	0.010
27	2.03	0.01	0.009	2.00	0.02	0.010
28	2.02	0.01	0.009	2.01	0.01	0.010
28	2.01	0.01	0.010	2.01	0.01	0.010
29	2.03	0.01	0.009	2.02	0.02	0.010
29	2.03	0.01	0.009	2.02	0.02	0.010
30	2.01	0.03	0.010	2.01	0.02	0.010
30	2.01	0.01	0.010	2.01	0.02	0.010
31	2.03	0.01	0.009	2.02	0.02	0.010
31	2.02	0.01	0.010	2.01	0.02	0.010
32	2.03	0.02	0.009	2.03	0.01	0.009
32	2.01	0.01	0.010	2.02	0.02	0.009
33	2.03	0.01	0.009	2.03	0.01	0.009
33	2.03	0.01	0.009	2.02	0.02	0.009
34	1.98	0.01	0.010	2.00	0.01	0.010
34	1.99	0.01	0.010	1.99	0.01	0.010
35	2.03	0.02	0.009	2.03	0.02	0.009
35	2.01	0.01	0.010	2.02	0.01	0.010
36	2.03	0.02	0.009	2.04	0.02	0.009
36	2.02	0.01	0.010	2.02	0.02	0.009

Table G 2: Redox potential measured and standard deviation

	Non-inoculated		Inoculated	
Day	**Eh**	**Stdev**	**Eh**	**Stdev**
0	358	10	356	10
1	234	13	224	2
1	329	6	338	1
2	266	5	280	4
2	357	8	357	1
3	249	6	275	1
3	315	57	329	7
4	263	13	285	1
4	345	3	346	3
5	314	1	318	1
5	323	6	360	7
6	301	2	375	19
6	316	1	374	14
7	301	4	449	27
7	322	4	455	24
8	343	2	667	17
8	333	12	602	49
9	342	21	665	5
9	350	12	630	46
10	365	28	663	7
10	369	14	671	7
11	395	25	670	9
11	391	22	675	9
12	518	62	683	9
12	537	75	682	8
13	660	3	690	8
13	654	4	690	7
14	651	19	689	4
14	655	10	701	5
15	647	23	699	4
15	654	12	699	3
16	658	27	704	3
16	679	9	700	3
17	694	7	711	4
17	685	4	707	4
18	690	1	707	2
18	694	4	704	5
19	694	1	705	4
19	687	2	695	1
20	692	2	704	1
20	700	6	704	2

21	704	2	707	3
21	695	1	700	1
22	712	2	712	1
22	694	2	698	1
23	704	7	701	4
23	697	1	696	2
24	710	1	707	4
24	695	2	695	2
25	711	1	710	1
25	703	1	703	1
26	706	2	702	5
26	697	1	688	5
27	713	1	709	1
27	699	3	701	1
28	714	1	711	1
28	701	2	702	2
29	709	1	707	1
29	696	2	695	1
30	714	1	706	3
30	711	1	706	2
31	696	2	695	1
31	691	2	691	2
32	702	2	705	1
32	706	0	705	1
33	713	1	690	26
33	705	1	705	1
34	699	1	693	1
34	693	1	683	4
35	695	7	685	2
35	695	2	690	1
36	665	1	666	2
36	677	2	676	2

Table G 3: Ferrous iron measured and standard deviation

	Non-inoculated		Inoculated	
Day	**$[Fe^{2+}]$**	**Stdev**	**$[Fe^{2+}]$**	**Stdev**
0	0.246	0.246	1.310	0.618
1	3.522	2.461	2.785	2.001
2	21.704	9.055	25.799	2.099
3	67.158	5.888	82.310	6.383
4	106.306	6.413	131.204	7.138
5	149.222	1.580	184.439	4.922
6	183.620	8.740	372.973	35.764
7	199.345	5.043	339.722	75.123
8	205.569	4.404	10.156	12.911
9	203.440	10.811	12.285	1.772
10	196.560	16.112	3.276	0.751
11	190.827	22.098	11.957	8.373
12	57.166	56.867	8.354	5.538
13	0.000	0.000	5.897	0.000
14	11.138	2.473	13.595	0.751
15	9.992	3.345	7.371	1.772
16	8.845	5.315	6.061	1.580
17	8.354	2.736	4.259	1.023
18	7.207	0.751	6.880	0.491
19	5.242	0.567	6.552	1.023
20	5.242	1.023	14.414	11.391
21	6.716	0.284	9.500	1.580
22	5.733	0.567	12.776	12.344
23	1.147	1.023	3.931	0.983
24	0.000	0.000	0.000	0.000
25	5.569	0.284	4.586	0.284
26	1.802	0.284	2.948	3.838
27	5.569	0.751	4.914	0.000
28	5.897	0.491	4.259	0.567
29	6.880	0.491	4.750	0.284
30	5.242	2.322	1.802	1.023
31	5.733	1.023	3.440	0.851
32	8.681	4.002	5.242	1.860
33	4.750	0.284	2.785	0.284
34	2.948	1.772	3.112	0.751
35	5.569	0.284	3.931	0.491
36	9.337	0.491	3.604	1.419
37				

Table G 4: Total measured and standard deviation

	Non-inoculated		Inoculated	
Day	**[Fe^{Tot}]**	**Stdev**	**[Fe^{Tot}]**	**Stdev**
0	11.057	0.246	12.367	0.751
1	5.405	1.300	6.061	1.212
2	19.656	8.145	24.488	2.581
3	64.619	7.383	80.016	8.061
4	118.919	12.077	143.325	7.294
5	152.007	4.947	152.498	5.674
6	198.853	10.428	386.077	41.969
7	201.638	4.179	406.388	43.269
8	198.034	2.142	319.247	35.321
9	194.595	8.859	332.351	47.811
10	197.052	12.077	371.335	52.260
11	198.690	16.374	422.768	28.987
12	221.458	31.787	470.925	43.528
13	208.845	10.977	463.063	27.046
14	263.391	27.505	454.382	38.654
15	296.478	63.191	365.766	49.273
16	340.213	44.407	421.130	59.259
17	348.731	28.016	383.456	64.623
18	339.885	9.758	371.499	43.419
19	338.084	19.278	354.791	37.566
20	317.117	19.860	332.678	32.477
21	306.634	20.015	311.712	28.714
22	298.608	20.167	285.012	24.614
23	238.493	23.450	211.138	22.755
24	274.038	14.049	242.097	15.956
25	275.348	12.570	233.579	13.745
26	257.166	14.447	217.363	14.117
27	247.830	11.807	209.009	7.294
28	232.760	11.838	182.473	0.751
29	224.734	10.781	177.396	3.069
30	200.983	10.665	161.671	1.772
31	192.629	1.300	153.972	2.879
32	177.559	9.405	140.704	3.272
33	170.516	7.239	131.859	5.821
34	153.645	4.432	121.048	14.329
35	158.395	3.451	128.092	10.428
36	155.774	7.272	118.264	7.127
37				

Table G 5: Sulphate measured and standard deviation

	Non-inoculated		Inoculated	
Day	**SO_4^{2+}**	**Stdev**	**SO_4^{2+}**	**Stdev**
0				
1	1133.333	31.920	1160.417	102.714
2	1247.917	84.568	1273.958	90.373
3	1414.583	18.311	1483.333	26.578
4	1131.250	29.811	1205.208	38.570
5	1542.708	88.902	1477.083	28.868
6	1472.917	340.185	2206.250	3.125
7	1878.125	61.476	2563.542	185.045
8	1934.375	118.132	2721.875	256.479
9	1654.167	155.194	2794.792	196.188
10	1887.500	192.917	2811.458	253.536
11	2333.333	131.114	3345.833	412.752
12	2236.458	117.607	3476.042	423.600
13	2510.417	44.451	3728.125	368.432
14	2759.375	149.511	3636.458	397.678
15	2811.458	215.655	3638.542	351.008
16	2880.208	179.744	3592.708	233.359
17	2830.208	78.146	3428.125	140.729
18	3109.375	95.043	3490.625	265.827
19	2873.958	14.091	3181.250	144.867
20	2951.042	98.442	3132.292	156.417
21	2519.792	20.807	2834.375	180.278
22	2913.542	77.455	3018.750	239.037
23	2566.667	49.047	2773.958	115.512
24	2418.750	162.380	2858.333	125.481
25	2239.583	31.612	2280.208	102.333
26	1705.208	53.247	1671.875	132.693
27	2033.333	3.608	2071.875	36.039
28	2689.583	159.232	2554.167	78.208
29	2351.042	43.787	2220.833	53.247
30	2611.458	91.126	2638.542	90.265
31	2740.625	29.811	2606.250	80.344
32	2219.792	40.785	2183.333	117.607
33	2145.833	63.763	2138.542	73.243
34	2141.667	17.770	2034.375	12.500
35	2251.042	11.831	2198.958	113.938
36	2357.292	34.422	2164.583	31.458
37				

APPENDIX H : Draw and fill Biokinetic test results for sample 2

Table H 1: pH measured and standard deviation

		Non-inoculated			Inoculated	
Day	**pH**	**Stdev**	**$[H^+]$**	**pH**	**Stdev**	**$[H^+]$**
0	2.03	0.01	0.01	2.04	0.01	0.01
1	2.23	0.02	0.01	2.18	0.01	0.01
1	2.20	0.01	0.01	2.16	0.01	0.01
2	2.30	0.01	0.01	2.22	0.01	0.01
2	2.24	0.01	0.01	2.18	0.01	0.01
3	2.35	0.01	0.00	2.25	0.00	0.01
3	2.31	0.01	0.00	2.22	0.01	0.01
4	2.35	0.01	0.00	2.24	0.02	0.01
4	2.28	0.01	0.01	2.20	0.01	0.01
5	2.33	0.01	0.00	2.23	0.01	0.01
5	2.27	0.01	0.01	2.18	0.02	0.01
6	2.31	0.01	0.00	2.21	0.02	0.01
6	2.26	0.00	0.01	2.17	0.02	0.01
7	2.33	0.01	0.00	2.23	0.01	0.01
7	2.29	0.01	0.01	2.19	0.01	0.01
8	2.26	0.01	0.01	2.16	0.02	0.01
8	2.21	0.01	0.01	2.12	0.01	0.01
9	2.23	0.01	0.01	2.18	0.02	0.01
9	2.23	0.01	0.01	2.16	0.02	0.01
10	2.26	0.01	0.01	2.29	0.10	0.01
10	2.23	0.01	0.01	2.26	0.09	0.01
11	2.26	0.00	0.01	2.19	0.02	0.01
11	2.23	0.01	0.01	2.16	0.02	0.01
12	2.20	0.01	0.01	2.14	0.01	0.01
12	2.18	0.01	0.01	2.13	0.02	0.01
13	2.19	0.01	0.01	2.13	0.02	0.01
13	2.16	0.01	0.01	2.11	0.02	0.01
14	2.18	0.01	0.01	2.13	0.02	0.01
14	2.15	0.00	0.01	2.10	0.02	0.01
15	2.18	0.01	0.01	2.12	0.01	0.01
15	2.15	0.01	0.01	2.11	0.02	0.01
16	2.17	0.01	0.01	2.12	0.02	0.01
16	2.15	0.01	0.01	2.10	0.01	0.01
17	2.10	0.01	0.01	2.05	0.01	0.01
17	2.09	0.00	0.01	2.05	0.02	0.01
18	2.10	0.00	0.01	2.03	0.01	0.01
18	2.07	0.00	0.01	2.03	0.01	0.01
19	2.13	0.01	0.01	2.09	0.02	0.01

19	2.10	0.01	0.01	2.06	0.01	0.01
20	2.11	0.00	0.01	2.10	0.01	0.01
20	2.11	0.00	0.01	2.07	0.01	0.01
21	2.13	0.00	0.01	2.09	0.01	0.01
21	2.10	0.00	0.01	2.07	0.01	0.01
22	2.15	0.01	0.01	2.11	0.01	0.01
22	2.13	0.00	0.01	2.10	0.01	0.01
23	2.06	0.02	0.01	2.09	0.03	0.01
23	2.06	0.01	0.01	2.02	0.01	0.01
24	2.09	0.02	0.01	2.06	0.02	0.01
24	2.07	0.02	0.01	2.04	0.02	0.01
25	2.10	0.01	0.01	2.07	0.03	0.01
25	2.08	0.01	0.01	2.06	0.03	0.01
26	2.04	0.02	0.01	2.05	0.02	0.01
26	2.03	0.01	0.01	2.02	0.02	0.01
27	2.10	0.05	0.01	2.07	0.03	0.01
27	2.02	0.01	0.01	2.02	0.01	0.01
28	2.05	0.01	0.01	2.04	0.02	0.01
28	2.02	0.00	0.01	2.02	0.01	0.01
29	2.04	0.01	0.01	2.03	0.01	0.01
29	2.02	0.01	0.01	2.01	0.01	0.01
30	2.02	0.01	0.01	2.01	0.01	0.01
30	2.00	0.01	0.01	1.99	0.01	0.01
31	2.03	0.01	0.01	2.02	0.02	0.01
31	2.02	0.01	0.01	2.01	0.02	0.01
32	2.03	0.02	0.01	2.03	0.01	0.01
32	2.01	0.01	0.01	2.02	0.02	0.01
33	2.03	0.01	0.01	2.03	0.01	0.01
33	2.03	0.01	0.01	2.02	0.02	0.01
34	1.98	0.01	0.01	2.00	0.01	0.01
34	1.99	0.01	0.01	1.99	0.01	0.01
35	2.03	0.02	0.01	2.03	0.02	0.01
35	2.01	0.01	0.01	2.02	0.01	0.01
36	2.03	0.02	0.01	2.04	0.02	0.01
36	2.02	0.01	0.01	2.02	0.02	0.01
37			1.00			1.00

Table H 2: Redox potential measured and standard deviation

	Non-inoculated		Inoculated	
Day	**Eh**	**Stdev**	**Eh**	**Stdev**
0		4	439	5
1	347	1	422	18
1	343	1	417	16
2	350	1	423	13
2	346	1	421	13
3	364	1	555	7
3	356	1	541	14
4	365	1	593	26
4	355	0	583	14
5	363	1	604	20
5	360	2	655	1
6	346	1	634	6
6	349	1	644	5
7	349	1	625	3
7	356	3	636	5
8	373	18	630	7
8	380	23	641	16
9	402	20	631	5
9	412	19	2553	3300
10	472	67	663	7
10	543	85	671	7
11	564	76	653	3
11	574	81	673	2
12	640	9	660	3
12	644	19	674	2
13	628	2	640	2
13	655	3	664	3
14	628	7	635	6
14	654	2	661	2
15	647	4	654	1
15	666	1	668	4
16	655	1	659	2
16	661	1	665	3
17	646	1	655	4
17	671	2	675	1
18	678	6	683	2
18	677	1	680	1
19	662	3	670	2
19	674	2	669	4
20	663	1	675	1
20	673	1	675	2

21	678	1	678	1
21	675	1	678	2
22	656	2	661	1
22	668	1	671	2
23	645	4	638	27
23	655	6	652	4
24	667	6	662	6
24	680	7	662	4
25	658	3	663	2
25	664	5	668	2
26	634	5	657	2
26	642	3	661	3
27	673	3	672	3
27	678	1	679	2
28	686	1	686	1
28	680	2	682	1
29	690	1	690	1
29	680	7	681	1
30	663	31	684	2
30	660	31	682	2
31	696	2	695	1
31	691	2	691	2
32	702	2	705	1
32	706	0	705	1
33	713	1	690	26
33	705	1	705	1
34	699	1	693	1
34	693	1	683	4
35	695	7	685	2
35	695	2	690	1
36	665	1	666	2
36	677	2	676	2

Table H 3: Ferrous iron measured and standard deviation

	Non-inoculated		Inoculated	
Day	**$[Fe^{2+}]$**	**Stdev**	**$[Fe^{2+}]$**	**Stdev**
0	4.341	0.375	7.043	0.567
1	54.300	1.950	28.911	10.823
2	65.029	3.972	30.139	8.740
3	67.486	4.773	0.983	0.491
4	67.649	2.046	0.655	0.284
5	68.141	2.046	2.948	0.491
6	69.943	3.622	3.112	0.284
7	64.537	0.284	0.819	0.751
8	61.916	5.538	4.750	0.284
9	48.485	12.570	1.638	0.751
10	22.441	17.727	3.276	0.751
11	8.190	6.105	2.457	0.851
12	1.310	0.284	1.802	0.284
13	0.983	0.491	4.423	0.491
14	2.457	0.851	2.785	0.751
15	4.423	0.491	4.750	1.237
16	3.604	0.751	1.474	0.851
17	7.862	1.300	5.242	0.284
18	2.129	1.580	1.638	0.284
19	2.293	0.751	0.983	0.491
20	2.129	1.237	1.638	0.751
21	3.604	1.023	2.621	0.284
22	2.129	0.751	0.819	0.284
23	3.767	1.419	4.095	1.023
24	0.819	0.567	0.819	0.284
25	1.802	0.284	0.655	0.284
26	4.750	0.751	4.914	0.491
27	1.966	0.983	2.621	0.284
28	4.750	1.023	2.785	0.284
29	2.293	1.135	4.750	0.751
30	0.983	0.491	0.033	0.057
31	5.733	1.023	3.440	0.851
32	8.681	4.002	5.242	1.860
33	4.750	0.284	2.785	0.284
34	2.948	1.772	3.112	0.751
35	5.569	0.284	3.931	0.491
36	9.337	0.491	3.604	1.419

Table H 4: Total iron measured and standard deviation

	Non-inoculated		Inoculated	
Day	**[Fe^{Tot}]**	**Stdev**	**[Fe^{Tot}]**	**Stdev**
0	6.962	0.511	12.531	1.300
1	53.399	1.560	36.691	5.899
2	69.615	3.345	43.243	7.436
3	73.710	3.405	22.932	2.322
4	74.201	3.900	25.389	2.706
5	71.253	2.736	32.596	3.817
6	69.124	0.284	40.950	7.522
7	65.684	2.216	41.769	11.916
8	69.943	3.486	57.166	10.241
9	54.382	9.224	59.787	7.059
10	36.691	10.194	59.787	7.059
11	27.682	1.986	69.124	6.005
12	40.459	6.885	74.038	5.413
13	40.131	6.599	74.529	3.753
14	53.071	6.274	78.624	5.958
15	59.623	5.863	76.986	5.115
16	66.830	6.138	77.969	4.670
17	75.348	4.645	84.848	3.721
18	73.055	4.237	84.521	3.838
19	84.848	2.522	98.116	1.237
20	83.374	6.413	90.090	7.634
21	85.012	5.667	88.616	7.898
22	85.504	6.611	88.943	9.180
23	67.158	0.751	76.167	8.886
24	62.735	0.284	70.106	6.690
25	71.744	9.414	79.443	7.554
26	89.435	15.702	84.193	7.898
27	99.263	14.469	107.125	4.688
28	85.995	3.222	87.469	4.840
29	85.012	9.008	84.521	4.504
30	83.538	10.642	85.504	7.723
31	192.629	1.300	153.972	2.879
32	177.559	9.405	140.704	3.272
33	170.516	7.239	131.859	5.821
34	153.645	4.432	121.048	14.329
35	158.395	3.451	128.092	10.428
36	155.774	7.272	118.264	7.127

Table H 5: Sulphate measured and standard deviation

	Non-inoculated		Inoculated	
Day	**SO_4^{2+}**	**Stdev**	**SO_4^{2+}**	**Stdev**
0				
1	1570.833	91.447	2331.250	425.241
2	2276.042	69.900	1273.958	90.373
3	1869.792	10.045	2311.458	158.802
4	1377.083	545.089	1875.000	81.729
5	1639.583	57.820	1851.042	82.817
6	1655.208	83.639	1809.375	60.354
7	1635.417	60.944	1905.208	239.105
8	1678.125	76.355	1976.042	129.389
9	2038.542	64.069	2348.958	18.311
10	1937.500	36.039	2811.458	253.536
11	1721.875	145.640	2047.917	78.458
12	1935.417	38.822	2308.333	66.316
13	2108.333	25.259	2328.125	94.837
14	2294.792	49.047	2672.917	32.526
15	2347.917	34.564	2729.167	57.820
16	1782.292	268.502	2152.083	55.581
17	2011.458	105.389	2339.583	25.452
18	2244.792	104.036	2289.583	71.421
19	1954.167	150.043	2243.750	132.288
20	1677.083	44.231	1957.292	91.073
21	2326.042	86.396	2487.500	38.017
22	2187.500	11.267	2257.292	64.221
23	2256.250	61.555	2267.708	58.072
24	2015.625	42.962	2239.583	55.581
25	1951.042	113.980	2208.333	41.615
26	1742.708	52.042	2179.167	34.845
27	2765.625	92.544	2836.458	58.990
28	2486.458	66.021	2384.375	96.268
29	2898.958	88.186	2581.250	162.860
30	2250.000	86.996	2239.583	179.445
31	2740.625	29.811	2606.250	80.344
32	2219.792	40.785	2183.333	117.607
33	2145.833	63.763	2138.542	73.243
34	2141.667	17.770	2034.375	12.500
35	2251.042	11.831	2198.958	113.938
36	2357.292	34.422	2164.583	31.458